

Long ties accelerate noisy threshold-based contagions

Dean Eckles^{a,*}, Elchanan Mossel^b, M. Amin Rahimian^{c,*} and Subhabrata Sen^d

^a Sloan School of Management, Massachusetts Institute of Technology

^b Department of Mathematics, Massachusetts Institute of Technology

^c Department of Industrial Engineering, University of Pittsburgh

^d Department of Statistics, Harvard University

* To whom correspondence should be addressed; email: eckles@mit.edu, rahimian@pitt.edu.

Network structure can affect when and how widely new ideas, products, and behaviors are adopted. In widely-used models of biological contagion, interventions that randomly rewire edges (on average making them “longer”) accelerate spread. However, there are other models relevant to social contagion, such as those motivated by myopic best-response in games with strategic complements, in which an individual’s behavior is described by a threshold number (θ) of adopting neighbors above which adoption occurs (i.e., complex contagions). Recent work has argued that highly clustered, rather than random, networks facilitate spread of these complex contagions. Here we show that minor modifications to this model reverse this result, thereby harmonizing qualitative facts about how network structure affects contagion. To model the trade-off between long and short ties, we analyze the rate of spread over networks that are the union of circular lattices and random graphs on n nodes. Allowing for noise in adoption decisions (i.e., adoptions below threshold) to occur with order $n^{-1/\theta}$ probability along at least some “short” cycle edges is enough to ensure that random rewiring accelerates the spread of a noisy threshold- θ contagion. This conclusion also holds under partial but frequent enough rewiring and when adoption decisions are reversible but infrequently so, as well as in high-dimensional lattice structures that facilitate faster-expanding contagions. Simulations illustrate the robustness of these results to several variations on this noisy best-response behavior. Hypothetical interventions that randomly rewire existing edges or add random edges (versus adding “short”, triad-closing edges) in hundreds of empirical social networks reduce time to spread. This revised conclusion suggests that those wanting to increase spread should induce formation of long ties, rather than triad-closing ties. More generally, this highlights the importance of noise in game-theoretic analyses of behavior.

How does network structure affect the spread of ideas, products, and behaviors? Social interactions among individuals facilitate a diverse range of contagions, and understanding the role of contact structure is central to the social and behavioral sciences. Decision-makers often rely on their knowledge of contagion in planning interventions that seed a behavior [1, 2, 3, 4, 5], prevent or reverse infection of nodes [6, 7, 8], or that attempt to modify network structure [9, 10, 11, 12]. Unfortunately, existing analyses of the two most widely used families of models (*simple and complex contagions*) have led to opposing conclusions (*weakness or strength of long ties*) about how network structure — in particular, clustering — affects spread of behavior; see Figure 1 insets.

Social contagions that are expected to be driven by incidental transfer of information are often modeled analogously to biological contagion of infectious disease. In such *simple contagion* models, a node has an independent (and typically identical) probability of being infected by each infected neighbor [13]; see Figure 1A. It is well known that such contagions spread more slowly in highly clustered networks than in more random networks [14, 15]. Related considerations lead to the “strength of weak ties” hypothesis by which “weak” (or more properly “long”) ties play critical roles in access to valuable information [16, 17, 18], such as in labor markets [19, 20]. On the other hand, adoptions which are costly, or occur because of normative social pressure or coordination, are often modeled as myopic best-responses in repeated graphical games of strategic complementarities (such as coordination games), whereby nodes’ utilities from adopting depend on the number of adopting neighbors [21, 22, 23, 24]. Threshold activation functions are the archetypal example of such *complex contagion* models [25, 26]. In their canonical form, a single parameter θ divides non-adoption from adoption such that adoption occurs if and only if the number of adopting neighbors reaches the threshold θ (Figure 1B); call this *deterministic θ -complex contagion*. Recent analyses of this deterministic model [26], or limits of noisy best responses as the noise level goes to zero ($q \rightarrow 0$ in Figure 1B) [27], have concluded that the spread of complex contagions is facilitated by more clustered networks, emphasizing the role of short ties in formation of wide bridges or complex paths [28], such that there is a “weakness of long ties” [26]. These lead to opposite recommendations about how to intervene on a network to facilitate (or slow) a social contagion.

Is such a deterministic model robust to modeling variations that may make it more consistent with both empirical evidence and widely-used random utility models of choice? Empirical studies of social contagion, including those that provide evidence for complex contagion, find substantial probability of adoption with a single adopting neighbor [1, 29, 30, 31], and empirical adoption rates with an additional adopter (beyond the first) increase by less than a factor of five (SI Figure S2), suggesting substantial nondeterminism or heterogeneity. More generally, rather than positing determinism, analyses of discrete choice problems typically hypothesize that individuals are random utility maximizers, thereby leading to positive choice probabilities specified by, e.g., probit or logit functions over the entire support (SI section S4.3). Here we show that allowing a small probability of below-threshold adoption (denoted by q in Figure 1B), even only via some short ties, reverses existing stylized facts about how network structure affects the spread of complex contagions, putting the emphasis back on the important structural role

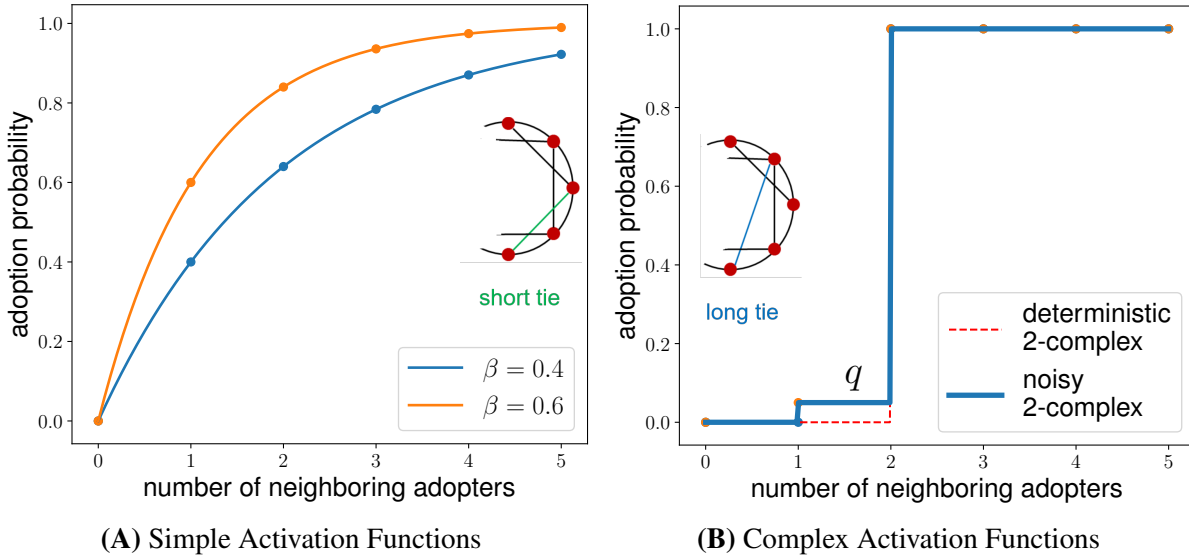


Figure 1: Activation functions for (A) simple contagion and (B) variations on complex contagion. In the case of a simple activation function (A), every edge has an independent probability β of transmitting infections (adoptions); subsequently, the probability of adoption with x adopters in the social neighborhood is given by $1 - (1 - \beta)^x$. In the case of a noisy threshold-based contagion model (B), there is a non-zero probability ($q > 0$) of adoptions below threshold. The inset figures illustrate rewiring (A) a short tie to get (B) a long tie, on a 4-regular circular lattice structure which we refer to as cycle-power-2 and denote by \mathcal{C}_2 . Rewiring a short tie speeds up the spread of simple contagions: *strength of the weak (or long) ties*. Recent studies have arrived at an opposite conclusion for complex contagion: *weakness of long ties*.

of long ties for complex contagions (see SI Figure S5). This harmonizes theoretical guidance about how network structure affects the spread of both simple and complex contagions.

Results

For our analytical results, we study the spread of θ -complex contagion starting from θ adjacent infected nodes in a variation on “small world” networks [14]. More specifically, we begin with 2-complex contagion from a pair of adjacent adopter nodes on rewired, circular, lattice networks. We use \mathcal{C}_k to denote a cycle-power- k graph which is defined as a circular lattice on n nodes where each node is connected to its $2k$ nearest neighbors on the cycle (Figure 2); the case $k = 1$ corresponds to an ordinary cycle (\mathcal{C}_1). In preliminary analysis (SI section S3), we show that the spread time of deterministic 2-complex contagion on \mathcal{C}_2 -union-random-graph is with high probability upper-bounded by $2n^{2/3}(\log \log n)^2$, which is asymptotically faster than the spread time on any cycle power graph (the latter being of order n). Hence, rewiring short

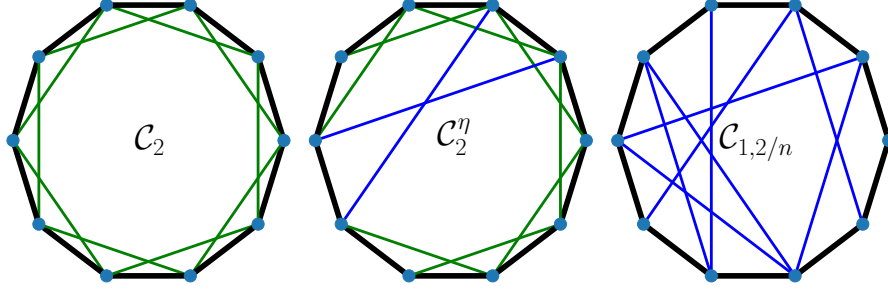


Figure 2: We consider the rewiring of a cycle-power-2 graph (\mathcal{C}_2 , left) as $\mathcal{C}_2 \setminus \mathcal{C}_1$ edges (short ties in green) are removed and replaced by random edges (long ties in blue), keeping the \mathcal{C}_1 edges (in black) fixed. Deterministic 2-complex contagion takes exactly $\lfloor n/2 \rfloor$ steps (i.e., $n/2 - 1$ for n even and $(n-1)/2$ for n odd) to spread over the entire \mathcal{C}_2 graph because starting from a pair of neighboring infected nodes at each step two new nodes are going to be infected, except for the last step in odd-sized networks where the contagion ends with the conversion of the single remaining node. Noisy 2-complex contagion spreads faster due to the additional possibility of passing infections through single, infected nodes, however, even if all nodes with infected neighbors become infected at every time step, it still takes $\lfloor n/4 \rfloor$ steps for contagion to spread across \mathcal{C}_2 entirely. On the other hand, a deterministic 2-complex contagion does not spread totally on the cycle-union-random-graph ($\mathcal{C}_{1,2/n}$ in the middle). In Theorem 1, we bound the spread time of noisy 2-complex contagion on $\mathcal{C}_{1,2/n}$ and show that when probability of adoptions below threshold is large enough, the noisy complex contagion spreads faster in $\mathcal{C}_{1,2/n}$ compared to \mathcal{C}_2 . In Theorem 3, we interpolate between \mathcal{C}_2 and $\mathcal{C}_{1,2/n}$ by rewiring the edges on $\mathcal{C}_2 \setminus \mathcal{C}_1$, keeping the average degree of the nodes constant (equal to four). Using η to denote the expected number of rewired edges (\mathcal{C}_2^η on the right), we show that for q and η large enough noisy 2-complex contagion spreads faster on \mathcal{C}_2^η than \mathcal{C}_2 . In Theorem 4, we study a variation of the noisy 2-complex contagion by allowing infected nodes to revert to the susceptible state with a probability δ . For this reversible, noisy, 2-complex contagion we again show a faster spread on $\mathcal{C}_{1,2/n}$ than \mathcal{C}_2 , for q large and δ small enough.

ties and replacing them with random, long ties speed up the spread of 2-complex contagion on a cycle power graph even without below-threshold adoptions (see SI Figures S3–S4). That preliminary result characterizes how long ties can speed up complex contagions, but only when the required short-tie structure for deterministic, 2-complex contagion (i.e., \mathcal{C}_2), is intact. Here we focus on what happens when \mathcal{C}_2 edges are replaced with random edges (i.e., *long ties*) so that a deterministic, 2-complex contagion would not spread on the rewired graph. Instead, we consider a *noisy* 2-complex contagion that allows for a non-zero (but vanishing as $n \rightarrow \infty$) probability of *simple* adoptions. We denote this probability of adoptions below threshold by q — or q_n to emphasize its dependence on the network size in analytical results. Formally, this implies that nodes that have only one infected neighbor get infected independently in each round with probability q_n .

Let $\mathcal{C}_{1,c/n} := \mathcal{C}_1 \cup \mathcal{G}_{n,c/n}$, where $\mathcal{G}_{n,c/n}$ is an Erdős–Rényi random graph with edge probability c/n for some fixed constant $c > 0$. In case of $\mathcal{C}_{1,2/n}$, the union graph has n nodes, each node has expected degree four ($4 - 2/n$, to be precise), and the set of edges is the union of edges in the two

graphs. Let $T_{\theta,q}(\mathcal{G})$ be the random variable representing the total spread time of noisy θ -complex contagion with simple adoption probability q over graph instance \mathcal{G} . The following theorem upper-bounds $T_{2,q}(\mathcal{C}_{1,2/n})$ by $(4\sqrt{n}/q_n)(\log \log n)^2$ implying that if $\sqrt{n}q_n \rightarrow \infty$, then noisy 2-complex contagion spreads faster on $\mathcal{C}_{1,2/n}$ than \mathcal{C}_2 : $T_{2,q}(\mathcal{C}_{1,2/n}) \ll T_{2,q}(\mathcal{C}_2)$ for $1/\sqrt{n} \ll q$. Throughout, we use \ll to indicate asymptotic dominance: $a_n \ll b_n$ iff $a_n/b_n \rightarrow 0$ as $n \rightarrow \infty$, and all our results hold with high probability (w.h.p.), i.e., with probability tending to one as $n \rightarrow \infty$. Note that (see Figure 2 caption): $\lfloor n/4 \rfloor \leq T_{2,q}(\mathcal{C}_2) \leq \lfloor n/2 \rfloor$.

Theorem 1. *Consider the noisy 2-complex contagion over $\mathcal{C}_{1,2/n}$ with simple adoption probability q . With high probability as $n \rightarrow \infty$, $T_{2,q}(\mathcal{C}_{1,2/n}) < \frac{4\sqrt{n}}{q}(\log \log n)^2$.*

The proof of Theorem 1 provides a clear intuition for how long ties accelerate noisy complex contagions (SI section S4). Recall our 2-complex contagions are initialized from two infected neighboring nodes on \mathcal{C}_1 . We upper-bound the spread time by breaking down the contagion into two sub-processes: (i) spreading along the cycle (\mathcal{C}_1) via rare, sub-threshold adoptions, and (ii) above-threshold adoption along the random, long ties. Initially, the infection spreads along the cycle. Once the infected nodes form long enough intervals, the infection spreads to far away points along pairs of random ties. The latter occurs when a susceptible node has at least two long ties connecting it to infected nodes. Our analysis (SI section S4) indicates that an infected interval of length $\sqrt{n} \log \log n$ is long enough to have a pair of random ties be incident to the same node across the cycle (see Figure S5), thus passing the 2-complex contagion with high probability as $n \rightarrow \infty$. This analysis (see SI Theorem 11) shows that the rate of spread over cycle-union-random-graph structures is determined by the time that it takes for the infected intervals along the cycle to grow long enough, to make the spread of complex contagion through their long ties a probable event.

This idea is reasonably general and can be applied to modeling variations where above-threshold adoption occurs with a probability ρ less than one or the adoption thresholds are greater than two ($\theta > 2$). In both cases the spread will be slowed down either to wait for above-threshold adoption to occur at the slower $1/\rho$ rate or for the intervals to grow longer to make a more stringent θ -complex adoption through θ random ties probable. These and other modeling variations are explored with extensive simulations in SI section S9; see Figures S15 to S18. In particular, for noisy θ -complex contagion we have (proved in SI Section S5):

Theorem 2. *Consider the noisy θ -complex contagion with simple adoption probability q over $\mathcal{C}_{1,c/n}$ for constant $c \geq \theta$. With high probability as $n \rightarrow \infty$, $T_{\theta,q}(\mathcal{C}_{1,c/n}) < \frac{4n^{1-1/\theta}}{q}(\log \log n)^2$.*

Starting with an infected interval of length θ , it takes $\lceil (n - \theta)/2 \rceil$ time steps for θ -complex contagion to spread on \mathcal{C}_θ entirely. In case of noisy θ -complex contagion, even if all simple contagion adoption attempts at every time step are successful, the total spread will take more than $\lceil (n - \theta)/(2\theta) \rceil$ steps: $T_{\theta,q}(\mathcal{C}_\theta) > (n - \theta)/(2\theta)$. Choosing $q \gg n^{-1/\theta}(\log \log n)^2$ will make $T_{\theta,q}(\mathcal{C}_{1,c/n}) \ll (n - \theta)/(2\theta) < T_{\theta,q}(\mathcal{C}_\theta)$; thence the requisite noise level for achieving a faster spread on the rewired lattice is $n^{-1/\theta}(\log \log n)^2$ which increases with increasing θ . With

heterogeneous thresholds, let us denote the vector of individual thresholds by $\bar{\theta} = (\theta_1, \dots, \theta_n)$ with $\theta_{\max} = \max\{\theta_i, i \in [n]\}$, and let $T_{\bar{\theta},q}(\mathcal{G})$ be the random variable measuring the total spread time of noisy “ $\bar{\theta}$ -complex contagion” with heterogeneous threshold vector $\bar{\theta}$ and simple adoption probability q over a (random) graph instance \mathcal{G} . Note that decreasing each individual’s threshold from θ_{\max} to θ_i for $i \in [n]$ can only speed up the spread, hence, $T_{\bar{\theta},q}(\mathcal{C}_{1,c/n}) \leq T_{\theta_{\max},q}(\mathcal{C}_{1,c/n})$ for any realization of random graphs and simple contagion infections (i.e., point-wise over the probability space). Subsequently, Theorem 2 is directly applicable to the case of heterogeneous thresholds after replacing θ with θ_{\max} : setting the simple adoption probability $q \gg n^{-1/\theta_{\max}}(\log \log n)^2$ is sufficient to ensure a faster noisy $\bar{\theta}$ -complex contagion spread over the rewired lattice because then $T_{\bar{\theta},q}(\mathcal{C}_{1,c/n}) \leq T_{\theta_{\max},q}(\mathcal{C}_{1,c/n}) \ll n$, with high probability as $n \rightarrow \infty$.

In what follows we investigate the robustness of our analytical findings in three respects: (i) when there are only some edges rewired (Theorem 3), (ii) when the adoptions are reversible (Theorem 4), and (iii) when contagions spread in high-dimensional structures (SI Section S8). Further robustness is revealed by simulations with other modeling variations and with empirical networks (SI Section S9).

Rewiring only some edges. We begin by interpolating continuously between \mathcal{C}_2 and the random graph $\mathcal{C}_{1,2/n}$. We track the evolution of the spreading time along the interpolation path, using a random graph model \mathcal{C}_2^η and study what happens as the edges in \mathcal{C}_2 but not in \mathcal{C}_1 (i.e. $\mathcal{C}_2 \setminus \mathcal{C}_1$) are rewired. In this context, η denotes the “expected” number of edges that are rewired to construct the random graph \mathcal{C}_2^η from \mathcal{C}_2 . Theorem 3 upper bounds the total spread time of noisy 2-complex contagion over \mathcal{C}_2^η for $\eta > \sqrt{n}$.

Theorem 3. *Consider a noisy 2-complex contagion over \mathcal{C}_2^η with simple adoption probability q . Let $\eta = n^\nu$ and $\frac{1}{2} < \nu < 1$, then with high probability as $n \rightarrow \infty$, $T_{2,q}(\mathcal{C}_2^\eta) < 4(\sqrt{n}/q + n^{3/2-\nu})(\log \log n)^2$.*

In Theorem 3, we parameterize $\eta = n^\nu$ and for $\nu \in (\frac{1}{2}, 1)$ we upper-bound the spread time of noisy 2-complex contagion by $n^{3/2-\nu} + \sqrt{n}/q$ (disregarding the logarithmic factors). For ν large enough ($\nu \rightarrow 1$) and $q \ll 1$, \sqrt{n}/q is the dominant term that fixes the spread time independently of ν , and we recover the $(4\sqrt{n}/q)(\log \log n)^2$ upper bound in Theorem 1. However, for $1/\sqrt{n} \ll q$ we can specify a range of ν for which increasing ν decreases the upper bound, with complex contagion spreading through the long ties. In particular, if $q = n^{-1/2+\nu'}$, then for $\frac{1}{2} < \nu < \frac{1}{2} + \nu'$ contagion spreads faster in \mathcal{C}_2^η compared to \mathcal{C}_2 . In comparison, the spread time on \mathcal{C}_2 is at least $\lfloor n/4 \rfloor$; see Figure 2 caption. Figure 3A shows the spreading time versus the rewiring parameters η for \mathcal{C}_2^η random graphs. It confirms that when the probability of adoptions below threshold (q) is large enough, the more we rewire $\mathcal{C}_2 \setminus \mathcal{C}_1$ edges, the faster the noisy 2-complex contagion. On the other hand, when q is very small, rewiring slows down the spread as it blocks the passage of fast 2-complex contagion along \mathcal{C}_2 . Our theoretical analysis in SI Section S6.1 shows that in the $\eta \ll \sqrt{n}$ regime, there are not enough long ties to initiate 2-complex contagion across the cycle and increased rewiring slows down the spread (see Theorem 24 in SI Section S6.1).

Reversible adoption. While prior work has examined “stochastic thresholds” via simulations [26, p. 724], that model importantly differs from our noisy threshold-based contagions as the activation function in that work (although allowing for sub-threshold adoptions) is reevaluated at every time step without regard for each nodes’ own prior adoption. That is, an infected node readily reverts back to being susceptible after reevaluation of its activation function, leading to a perfectly reversible, non-inertial process. This significantly diminishes the effect of sub-threshold adoptions because nodes that are activated below threshold are likely to be stochastically turned off when their activation function is reevaluated.

Indeed, allowing sub-threshold adoptions in a perfectly reversible complex contagion is not enough to reverse the conclusions about the weakness of long ties [26]: some inertia is critical to our conclusions. We note that many of the decisions theorized to be governed by threshold-based contagions have some inertia, often because they are costly or could be difficult to reverse (e.g., purchases). In the mechanism that we have identified for the spread of noisy 2-complex contagion on $\mathcal{C}_{1,2/n}$, it is critical to allow simple contagion to spread along an interval on \mathcal{C}_1 , until two random (long) ties are likely to be adjacent to the infected interval (Figure S5). Reversions at the interval boundaries can disrupt this interval growth mechanism and significantly slow down the spread of complex contagion through long ties. Notwithstanding, we can allow infected nodes to revert back to being “susceptible” with probability δ , and for small δ our conclusions hold. Note that in this model even with all nodes infected, a fraction δ of them are likely to revert to being susceptible. Therefore, it is useful to define $T_{2,q}^\delta(\mathcal{C}_{1,2/n})$ as the first time that $n(1 - \delta)$ nodes are infected starting from two neighboring infected nodes on the cycle under a reversible, noisy 2-complex contagion model with sub-threshold adoption probability q and reversion probability δ . Our following result provides an upper bound on $T_{2,q}^\delta(\mathcal{C}_{1,2/n})$, extending Theorem 1 to allow for a positive probability of reversions $\delta > 0$.

Theorem 4. *Consider a reversible, noisy 2-complex contagion over $\mathcal{C}_{1,2/n}$ with simple adoption probability q and reversion probability δ . If $\delta \ll 1/\sqrt{n}$, then $T_{2,q}^\delta(\mathcal{C}_{1,2/n}) < \frac{4\sqrt{n}}{q-\delta}(\log \log n)^2$, with high probability as $n \rightarrow \infty$.*

Of note, the spread time measured by $T_{2,q}^\delta(\mathcal{C}_{1,2/n})$ upper-bounds the faster model where each infected agent reevaluates its activation function with probability δ , rather than reverts to being susceptible. In the former case, we recover the stochastic threshold model of prior work [26] as $\delta \rightarrow 1$. Similarly, we can recover Theorem 1 by letting $\delta \rightarrow 0$. Figure 3B illustrates the effect of δ on the spread time with numerical simulations.

Higher-dimensional lattices. Contagion on circular lattices is limited to a single dimension. In higher dimensions, spread speeds up significantly as contagion expands simultaneously across multiple dimensions. Our analysis of noisy complex contagions on circular lattice such as \mathcal{C}_2 and $\mathcal{C}_{1,2/n}$ has natural extensions in d dimensions. In SI Section S8, we formalize this for $d = 2$ and show that contagion on a $\sqrt{n} \times \sqrt{n}$ square lattice with random, long-range ties can be upper bounded by $(36n^{1/4}/q)(\log \log n)^{3/2}$, which for $q \gg 1/n^{1/4}$ is strictly faster than the spread time on the square lattice with closed triads, the latter being of the order \sqrt{n} . Generally,

for $q \gg 1/n^{1/2d}$ the spread time on d -dimensional hypercube with random, long-range ties is strictly faster than $n^{1/d}$ which is the order of time that noisy 2-complex contagion takes to spread on the d -dimensional hypercube with closed diagonals (i.e., triad-closing ties).

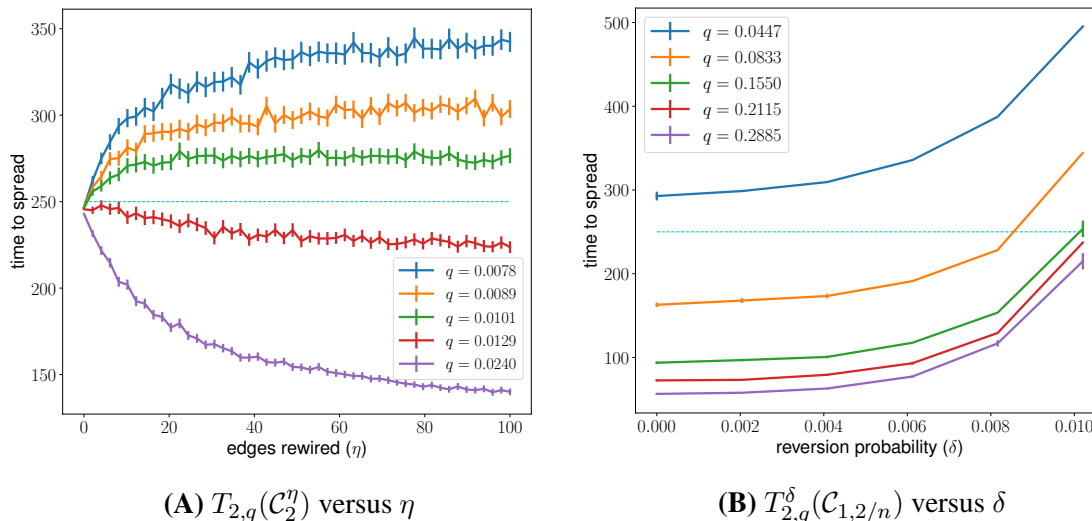


Figure 3: Spreading time of noisy complex contagion over rewired \mathcal{C}_2 graphs. In (A), we follow the same model as in Theorem 3: noisy 2-complex contagion with sub-threshold adoption probability q . In (B), we follow the reversible noisy 2-complex contagion model of Theorem 4 with reversion probability δ and sub-threshold adoption probability q . All networks have $n = 500$ nodes. The the spread time of 2-complex contagion on \mathcal{C}_2 is 250 which is marked by a dashed line. Each point is the average of 1000 random draws. The vertical bars indicate the 95% normal confidence intervals around the means.

Empirical networks

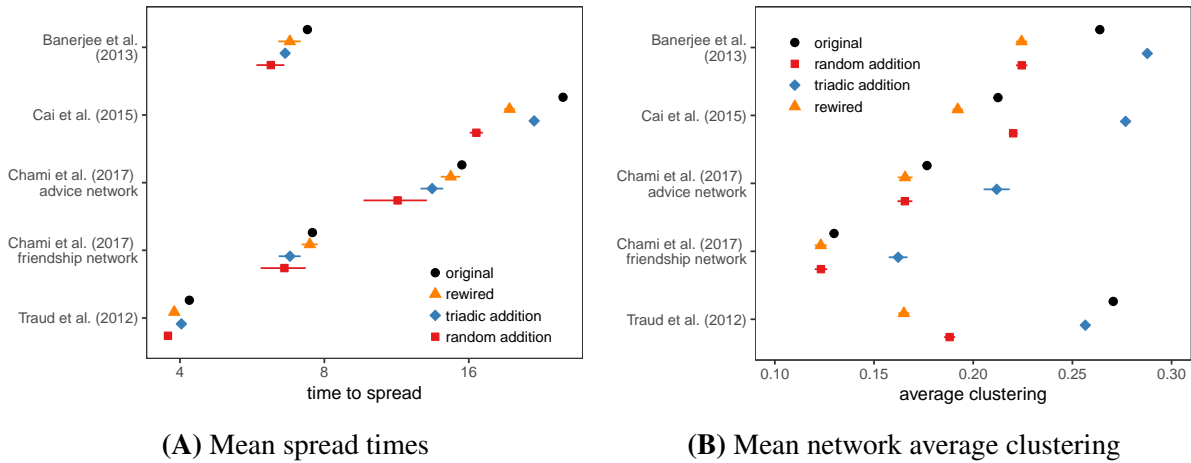
Our theoretical analysis of lattice structures with random, long-range ties is motivated by the well-documented, small-world phenomena in real social networks that simultaneously exhibit the high clustering of regular lattices and short average path length of random graphs [14]. The presence of long ties in real social networks could be due to life events [18] or through strategic efforts of network participants [32], and such ties are generally associated with positive economic outcomes. Social network platforms can also actively shape the network structure through link recommendations, e.g., LinkedIn’s “People You May Know” algorithm, with measurable consequences for individuals and groups [20]. In our simulation studies of contagions on empirical social networks, we test the effect of not only rewiring existing links but also adding either new random or new triad-closing edges to better inform interventions by platforms and others.

Our simulation results on empirical networks and with a broad class of contagion models support the robustness of our theoretical findings. We use five sets of empirical social networks;

see SI section S9, for a description of each. For each social network, contagion begins from two adjacent random seeds, and we measure the time to 90% spread under four conditions: (i) the original networks (no intervention), (ii) with 10% of edges rewired, (iii) with 10% added edges selected proportional to the number of triads they close, and (iv) with 10% new edges added randomly. For each intervention type, we simulate the spread times over the modified networks 500 times. In these simulations, a node adopts with certainty if it has at least two adopter neighbors. We fix the probability of adoption with a single adopter neighbor at $q = 0.05$.

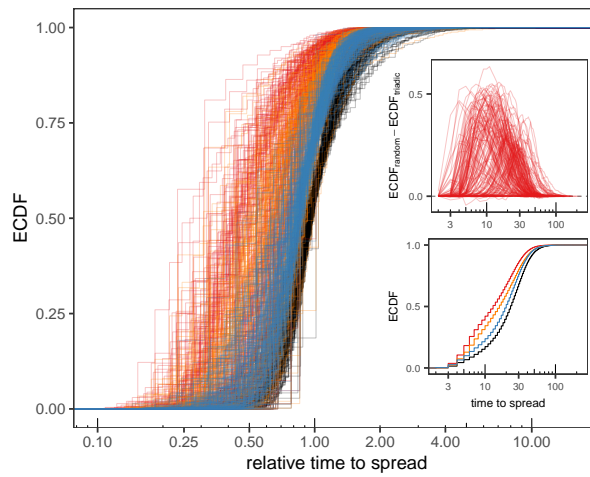
Across all five network datasets, random rewiring decreases mean time to spread (Figure 4A). Furthermore, adding random, rather than triad-closing, edges likewise reduces mean time to spread. To see the aggregate effect that the interventions have on the network structure, we plot the mean values of the network average clustering coefficients under the three interventions compared to the original networks in each dataset (Figure 4B). Random addition and rewiring generally decrease the average clustering compared to the original networks. One would expect that triad-closing edge additions should lead to the highest average clustering among the four conditions; however, addition of triad-closing edges can also introduce new open triangles in the vicinity of the added edge. In the case of the Traud et al. (2012) dataset we see a decrease in average clustering with triadic addition. This can point to the existence many broker nodes who connect otherwise disconnected regions of the network. Triadic additions in the neighborhood of the broker nodes will close some triangles while generating many open ones between the newly connected network regions. We further examine spreading times for each network in the largest set — households in 175 villages in rural China [33] — in Figure 4C, where we observe a corresponding shift in the distribution of spreading times.

These results with empirical networks are robust to a number of variations, including the intervention size (SI Figure S18) and the percentage of total spread (SI Figure S14). In SI section S9, we present a variation of this model where the probability of adoptions above threshold (called ρ) is less than one ($\rho = 0.5, q = 0.025$), as well as a case with very small simple adoption probability ($\rho = 1, q = 0.001$). In another variation, infected nodes transition to an inactive state (with probability $\gamma = 0.5$), in which they are no longer infectious, although they are still counted as being adopters. In yet another variation, we consider a fractional threshold model with relative thresholds set to $\theta^* = 0.5$. Results are qualitatively similar for other threshold values ($\theta = 2, 3, 4, 5$; SI Figure S15) and heterogeneous thresholds, drawn at random from different distributions (SI Figure S16). Simulation results in all cases reveal the same direction for the effect of interventions, although the effect sizes vary.



(A) Mean spread times

(B) Mean network average clustering



(C) Distributions of spread times

Figure 4: (A) Mean time to spread in each set of empirical networks. Each point averages over all networks in that set. Error bars are 95% confidence intervals for the difference from the original network computed by treating each network as a single observation. (B) The effect that each intervention type has on the network average clustering coefficients. The confidence intervals indicate the the difference from the original network computed by treating each network as a single observation. (C) Distribution of time to spread for each of the 175 networks of Chinese households in Cai et al. [33]. For each village, we plot the empirical cumulative distribution function (ECDF) of the spreading times in the original village (black) and under rewiring (orange), as well as random (red) and triad-closing (blue) edge additions. Hence, the main figure overlays $4 \times 175 = 700$ curves, corresponding to the ECDFs of the 500 spreading time samples computed for each village under the four conditions. Time to spread is normalized by the mean time to spread in the original network. Compared with closing triads, adding random edges consistently speeds up spread, as illustrated by the positive difference in ECDFs (upper inset). The positive difference in each case implies stochastic dominance: the spreading time over the village network with 10% added triad-closing edges dominates (is slower than) the spreading time over the network with the 10% new edges added randomly. The distributions of time to spread averaging over all 175 networks (lower inset) illustrate that both rewiring and random additions speed up the contagion.

Discussion

Our simulations indicate that in many real social networks rewiring the edges causes these contagions to spread faster. Moreover, these contagions spread faster when new edges are added uniformly at random rather than with probability proportional to the number of open triads that they close. The latter suggests that it is advantageous to introduce new ties that close fewer triads. This is true even if the decisions to adopt heavily rely on local reinforcement from the neighboring adopters, e.g., with $\rho = 1$ and $q = 0.001$.

Contrary to the ideas surrounding the “weakness of long ties” [26, 31, 27], we find that interventions that introduce long ties via random rewiring or adding random ties accelerate the spread of complex contagions. In common versions of such contagions, there is at least a small probability for adoption to occur even when there is only a single adopter in the social neighborhood. This is enough to change the landscape of results, thereby leading to the conclusion that long ties accelerate these contagions — just as they do for simple contagions.

Our results indicate that introducing long ties is more effective for accelerating the spread of social contagion — whether simple and complex. Thus, we propose a more unified recommendation for structural interventions aimed at increasing spread: adding long ties. This conclusion is consistent with empirical studies that identify structural diversity as a correlate of increased adoption [34] and document the prevalence of long ties with high information-exchange bandwidth [35].

Interventions in social networks are often unable to directly form arbitrary relationships; rather, they typically consist in some encouragement to interaction. For example, individuals can be randomly assigned to groups, but only some endogenously form friendships, with substantial consequence for the success of such interventions [11]. While there can be non-compliance in edge formation, our simulations suggest that even if one can induce triad-closing edges to form at a greater rate, focusing on forming long ties could still be more effective. In the networks of households in rural China [33], we observe that even with 25% additional short, triad-closing ties, spread is slower than with only 10% additional long, random ties (SI Figure S21A). Nonetheless, our results do not address the decision to form a tie. Rather, we clarify the effect that the introduction of new ties has on the speed of spread. We propose the confluence of these two decisions — whether to form a tie, perhaps in response to an intervention, and whether to adopt a behavior given its adoption by network neighbors — as a topic for further study.

A central theme of our work is that deterministic models based on complex contagion are unrealistically constrained and various sources of uncertainty across social networks (observable or unobservable) cause actions in the real world to be significantly stochastic. Capturing the full complexity of network contexts for social contagion, including tie formation tendencies of the agents (homophilous or heterophilous) and timing of their actions, opens up many avenues for future research into the role of network structure. Individuals may show differential preferences for observations that originate from within or outside their communities and structurally-correlated distribution of thresholds can significantly influence which type of so-

cial ties are more conducive to contagion. In other contexts individuals may be sensitive to adoptions beyond the local neighborhoods that are coded by pairwise network interactions, leading to a rich variety of contagions across higher-order structures such as hyperedges and simplices [36, 37]. In yet other contexts, temporally-nuanced behaviours such as forgetting or burstiness [38] may favor special structures, e.g., those that facilitate simultaneous or closely-timed adoptions. We speculate that empirically-grounded theories of social contagion in complex networks can explain rich classes of behaviors and provide a firm foundation for stylized facts about the role of social ties in broad contexts, informing robust interventions that facilitate diffusion of innovations and adoption of new technologies in social networks.

Methods

Rewiring circular lattices, $\mathcal{C}_{1,2/n}$ and \mathcal{C}_2^η . We use $\mathcal{C}_{1,2/n}$ and \mathcal{C}_2^η to denote graph instances that can be generated by randomly rewiring a cycle-power-2 graph on n nodes, keeping the expected degrees of the nodes (asymptotically) fixed at four (Figure 2). We construct $\mathcal{C}_{1,2/n}$ by taking the union of an Erdős–Rényi random graph with edge probability $2/n$ and a cycle \mathcal{C}_1 . The graph instances of \mathcal{C}_2^η are meant to continuously interpolate between \mathcal{C}_2 , corresponding to $\eta = 0$, and $\mathcal{C}_{1,2/n}$, corresponding to $\eta \rightarrow \infty$. Formally, we define two random graph processes \mathcal{D}_η and \mathcal{G}_η that are coupled through the common index η . We construct \mathcal{C}_2^η as a union graph, $\mathcal{C}_2^\eta := \mathcal{C}_1 \cup \mathcal{G}_\eta \cup \mathcal{D}_\eta$. The coupling between \mathcal{D}_η and \mathcal{G}_η is achieved as follows. To each pair of nodes, i and j , we associate independent exponential random variables X_{ij} with mean n^2 and Y_{ij} with mean $2n$. Graph \mathcal{G}_η is comprised of all edges $\{i, j\}$ for which $X_{ij} < \eta$. Therefore, \mathcal{G}_η is distributed as Erdős–Rényi with edge probability $\mathbb{P}\{X_{ij} > \eta\} = 1 - e^{-\eta/n^2}$. On the other hand, \mathcal{D}_η is comprised of all edges belonging to $\mathcal{C}_2 \setminus \mathcal{C}_1$ for which $Y_{i,j} > \eta$. Therefore, each edge of $\mathcal{C}_2 \setminus \mathcal{C}_1$ is missing from \mathcal{D}_η with probability $1 - e^{-\eta/2n}$, independently of others. In the $\eta \ll n$ regime, the expected degree of nodes in \mathcal{C}_2^η is asymptotically fixed at four, which is the degree of nodes in \mathcal{C}_2 . Motivated by this observation, we refer to \mathcal{C}_2^η as the “ η -rewired \mathcal{C}_2 ” random graph.

Spreading times T_2 , $T_{2,q}$, and $T_{2,q}^\delta$. Let \mathcal{X}_n be any graph on n nodes that includes \mathcal{C}_1 as a subgraph (e.g., $\mathcal{C}_{1,2/n}$ or \mathcal{C}_2^η). We use $T_2(\mathcal{X}_n)$, $T_{2,q}(\mathcal{X}_n)$, and $T_{2,q}^\delta(\mathcal{X}_n)$ to denote the random variables measuring the spread times of contagions on \mathcal{X}_n under specific models starting from an infected pair of neighboring nodes on \mathcal{C}_1 : T_2 for deterministic 2-complex contagion, $T_{2,q}$ for noisy 2-complex contagion with simple contagion probability q , and $T_{2,q}^\delta$ for reversible, noisy 2-complex contagion with simple contagion probability q and reversion probability δ . $T_2(\mathcal{X}_n)$ and $T_{2,q}(\mathcal{X}_n)$ measure the time until the entire graph \mathcal{X}_n is infected. Deterministic 2-complex contagion may not spread to the entire \mathcal{X}_n , in which case we set $T_2(\mathcal{X}_n) = \infty$. $T_{2,q}^\delta(\mathcal{X}_n)$ measures the first time until $n(1 - \delta)$ nodes in \mathcal{X}_n are infected. Our main results in Theorems 1-4 bound these random variables with high probability as $n \rightarrow \infty$.

Agent-based simulations. We implement an agent-based model with transitions between susceptible and infected states according to an activation function that determines the type of contagion, e.g., simple, deterministic complex, or noisy complex; see SI Figure S13 for a block diagram of state transitions. Activation functions for different models of contagion are characterized by different parameters, e.g., the independent transmission probabilities (β) for the simple contagion activation functions in Figure 1A, or the threshold value (θ) and sub-threshold adoption probability (q) for the complex contagion activation functions in Figure 1B. In addition to the transitions that we investigate in our theoretical analysis (e.g., reversion from infected to susceptible with probability δ), our simulations include transition probabilities between active and inactive infected states, to model situations that adopter agents transition into an “inactive infected” state where they do not influence their neighbors but remain adopters.

Empirical networks data. The empirical network data for our simulation studies are derived from publicly available data [8, 33, 39, 40]. The Cai et al. [33] data is comprised of 175 social networks of Chinese farm villages that are collected in the study of farmers being encouraged to sign up for a weather insurance product. The friendship and health advice network data are collected by Chami et al. [8] from 17 rural villages in Uganda. The Banerjee et al. [39] data contains the interconnection data for multi-dimensional social relations in 77 villages in southern India. Traud et al. [40] data contains the Facebook friendship networks at U.S. colleges and universities; we use the 40 smallest networks, for which such simulations are more computationally practical. The village networks in the first three sets have as few as tens of nodes but have typically hundreds of nodes. A typical Facebook college network has thousands of nodes. SI Table S1 summarizes the statistics for each set of networks.

Data availability

The simulations on empirical networks use publicly available data [8, 33, 39, 40].

Code availability

Code for reported simulations can be accessed from <https://github.com/aminrahimian/social-contagion/wiki>.

Acknowledgements

Authors are listed alphabetically. Mossel was partially supported by NSF grant CCF 1665252, DOD ONR grant N00014-17-1-2598, and NSF grant DMS-1737944. Rahimian acknowledges support from Pitt Momentum Funds and a Pitt Cyber Accelerator grant. This research was supported in part by the University of Pittsburgh Center for Research Computing, RRID:SCR_022735, through the resources provided. Specifically, this work used the H2P cluster, which is supported by NSF award number OAC-2117681. During his postdoctoral work at MIT, Rahimian was supported by an Amazon Research Award to Eckles. We thank Carlos Hurtado, Yixuan Long and Clinton S. Reid for research assistance. We thank Sinan Aral, Stephen Morris, and David G. Rand for helpful comments. We also thank James Moody, two other anonymous referees, and editors at Nature Human Behaviour for their helpful feedback in revising the manuscript.

Potential competing interests

Meta (which operates Facebook) has sponsored a conference co-organized by Eckles and has funded some of his other research. Rahimian has served on the advisory committee of a vaccine confidence fund created by Meta and Merck, and some of his research has been also funded by Meta.

References

- [1] J. Leskovec, L. A. Adamic, B. A. Huberman, The dynamics of viral marketing, *ACM Transactions on the Web (TWEB)* **1**, 5 (2007).
- [2] D. Kempe, J. Kleinberg, É. Tardos, Maximizing the spread of influence through a social network, *Proceedings of the ninth ACM SIGKDD international conference on Knowledge discovery and data mining* (ACM, 2003), pp. 137–146.
- [3] O. Hinz, B. Skiera, C. Barrot, J. U. Becker, Seeding strategies for viral marketing: An empirical comparison, *Journal of Marketing* **75**, 55 (2011).
- [4] B. Libai, E. Muller, R. Peres, Decomposing the value of word-of-mouth seeding programs: Acceleration versus expansion, *Journal of Marketing Research* **50**, 161 (2013).
- [5] L. Beaman, A. BenYishay, J. Magruder, A. M. Mobarak, Can network theory-based targeting increase technology adoption?, *American Economic Review* **111**, 1918 (2021).
- [6] R. Cohen, S. Havlin, D. Ben-Avraham, Efficient immunization strategies for computer networks and populations, *Physical Review Letters* **91**, 247901 (2003).
- [7] V. M. Preciado, M. Zargham, C. Enyioha, A. Jadbabaie, G. J. Pappas, Optimal resource allocation for network protection against spreading processes, *IEEE Transactions on Control of Network Systems* **1**, 99 (2014).
- [8] G. F. Chami, S. E. Ahnert, N. B. Kabatereine, E. M. Tukahebwa, Social network fragmentation and community health, *Proceedings of the National Academy of Sciences* **114**, E7425 (2017).
- [9] V. Chaoji, S. Ranu, R. Rastogi, R. Bhatt, Recommendations to boost content spread in social networks, *Proceedings of the 21st international conference on World Wide Web* (ACM, 2012), pp. 529–538.
- [10] T. W. Valente, Network interventions, *Science* **337**, 49 (2012).
- [11] S. E. Carrell, B. I. Sacerdote, J. E. West, From natural variation to optimal policy? The importance of endogenous peer group formation, *Econometrica* **81**, 855 (2013).
- [12] D. A. Cerdeiro, M. Dziubiński, S. Goyal, Individual security, contagion, and network design, *Journal of Economic Theory* **170**, 182 (2017).
- [13] P. S. Dodds, D. J. Watts, A generalized model of social and biological contagion, *Journal of Theoretical Biology* **232**, 587 (2005).
- [14] D. J. Watts, S. H. Strogatz, Collective dynamics of ‘small-world’ networks, *Nature* **393**, 440 (1998).

- [15] L. Hébert-Dufresne, P.-A. Noël, V. Marceau, A. Allard, L. J. Dubé, Propagation dynamics on networks featuring complex topologies, *Physical Review E* **82**, 036115 (2010).
- [16] M. S. Granovetter, The strength of weak ties, *American Journal of Sociology* **78**, 1360 (1973).
- [17] S. Aral, M. Van Alstyne, The diversity–bandwidth trade-off, *American Journal of Sociology* **117**, 90 (2011).
- [18] E. Jahani, S. P. Fraiberger, M. Bailey, D. Eckles, Long ties, disruptive life events, and economic prosperity, *Proceedings of the National Academy of Sciences* **120**, e2211062120 (2023).
- [19] L. K. Gee, J. J. Jones, C. J. Fariss, M. Burke, J. H. Fowler, The paradox of weak ties in 55 countries, *Journal of Economic Behavior & Organization* **133**, 362 (2017).
- [20] K. Rajkumar, G. Saint-Jacques, I. Bojinov, E. Brynjolfsson, S. Aral, A causal test of the strength of weak ties, *Science* **377**, 1304 (2022).
- [21] A. Galeotti, S. Goyal, M. O. Jackson, F. Vega-Redondo, L. Yariv, Network games, *The Review of Economic Studies* **77**, 218 (2010).
- [22] L. E. Blume, The statistical mechanics of strategic interaction, *Games and Economic Behavior* **5**, 387 (1993).
- [23] S. Morris, Contagion, *The Review of Economic Studies* **67**, 57 (2000).
- [24] H. P. Young, The dynamics of social innovation, *Proceedings of the National Academy of Sciences* **108**, 21285 (2011).
- [25] M. Granovetter, Threshold models of collective behavior, *American Journal of Sociology* **83**, 1420 (1978).
- [26] D. Centola, M. Macy, Complex contagions and the weakness of long ties, *American Journal of Sociology* **113**, 702 (2007).
- [27] A. Montanari, A. Saberi, The spread of innovations in social networks, *Proceedings of the National Academy of Sciences* **107**, 20196 (2010).
- [28] D. Guilbeault, D. Centola, Topological measures for identifying and predicting the spread of complex contagions, *Nature Communications* **12**, 1 (2021).
- [29] E. Bakshy, I. Rosenn, C. Marlow, L. Adamic, The role of social networks in information diffusion, *Proceedings of the 21st international conference on World Wide Web* (ACM, 2012), pp. 519–528.

- [30] E. Bakshy, D. Eckles, R. Yan, I. Rosenn, Social influence in social advertising: Evidence from field experiments, *Proceedings of the 13th ACM conference on electronic commerce* (ACM, 2012), pp. 146–161.
- [31] D. Centola, The spread of behavior in an online social network experiment, *Science* **329**, 1194 (2010).
- [32] M. O. Jackson, B. W. Rogers, The economics of small worlds, *Journal of the European Economic Association* **3**, 617 (2005).
- [33] J. Cai, A. De Janvry, E. Sadoulet, Social networks and the decision to insure, *American Economic Journal: Applied Economics* **7**, 81 (2015).
- [34] J. Ugander, L. Backstrom, C. Marlow, J. Kleinberg, Structural diversity in social contagion, *Proceedings of the National Academy of Sciences* **109**, 5962 (2012).
- [35] P. S. Park, J. E. Blumenstock, M. W. Macy, The strength of long-range ties in population-scale social networks, *Science* **362**, 1410 (2018).
- [36] I. Iacopini, G. Petri, A. Barrat, V. Latora, Simplicial models of social contagion, *Nature communications* **10**, 2485 (2019).
- [37] G. Ferraz de Arruda, G. Petri, P. M. Rodriguez, Y. Moreno, Multistability, intermittency, and hybrid transitions in social contagion models on hypergraphs, *Nature Communications* **14**, 1375 (2023).
- [38] M. Akbarpour, M. O. Jackson, Diffusion in networks and the virtue of burstiness, *Proceedings of the National Academy of Sciences* **115**, E6996 (2018).
- [39] A. Banerjee, A. G. Chandrasekhar, E. Duflo, M. O. Jackson, The diffusion of microfinance, *Science* **341**, 1236498 (2013).
- [40] A. L. Traud, P. J. Mucha, M. A. Porter, Social structure of Facebook networks, *Physica A: Statistical Mechanics and its Applications* **391**, 4165 (2012).

References

Supplementary Information

This Supplementary Information is organized in eight sections. We give an overview of the mathematical notation in Section S1. In Section S2 we provide a review of the related literature and give additional context for our work. In Section S3 we present a preliminary result (Theorem 5) that tightens the known bounds on the spreading time of deterministic 2-complex contagion on cycle union random graphs. Sections S4 to S9 parallel the results in the main text. In Sections S4, S6 and S7, we provide proofs and additional discussions surrounding Theorems 1, 3, and 4. In Section S9, we expand on our study of empirical networks and present additional simulation results under various contagion models that deviate from those considered in the main text. These additional results support the robustness of our main claims against modeling variations. Supplementary references are listed in Section S10.

Contents

S1 Notation	S2
S2 Additional related work	S3
S2.1 Adoption probabilities by the number of adopting peers in real data	S4
S3 Deterministic 2-complex contagion on $\mathcal{C}_{2,c/n}$	S6
S3.1 Lower bound on $T_2(\mathcal{C}_{2,c/n})$	S7
S3.2 Upper bound on $T_2(\mathcal{C}_{2,c/n})$	S10
S4 Noisy 2-complex contagion on $\mathcal{C}_{1,2/n}$	S13
S4.1 Lower bound on $\bar{T}_{2,q}(\mathcal{C}_{1,2/n})$	S15
S4.2 Upper bound on $\bar{T}_{2,q}(\mathcal{C}_{1,2/n})$	S16
S4.3 Adoption probabilities under logit and probit activation functions	S21
S5 Noisy θ-complex contagion	S24
S6 Noisy 2-complex contagion on \mathcal{C}_2^η	S27
S6.1 Lower bound on $\bar{T}_{2,q}(\mathcal{C}_2^\eta)$ for $\eta = o(\sqrt{n})$	S29
S6.2 Lower bound on $\bar{T}_{2,q}(\mathcal{C}_2^\eta)$ for $\eta = n^\nu, 1/2 < \nu < 1$	S30
S6.3 Upper bound on $\bar{T}_{2,q}(\mathcal{C}_2^\eta)$ for $\eta = n^\nu, 1/2 < \nu < 1$	S31
S6.4 Simulations with simple contagion adoptions only along \mathcal{C}_1 edges	S33
S7 Reversible noisy 2-complex contagion on $\mathcal{C}_{1,2/n}$	S35
S8 Noisy complex contagions in higher dimensions	S37
S9 Simulations with empirical networks data	S39
S10 References	S58

S1 Notation

For convenience of the reader, we collect some notation here that is used throughout. For positive integer n , we use $[n]$ to denote the set $\{1, \dots, n\}$. For sequences of real numbers, we use the usual Bachman-Landau notation $O(\cdot)$, $o(\cdot)$ and $\Theta(\cdot)$. When $f(n) = o(h(n))$, we also, equivalently, write $h(n) = \omega(f(n))$, $h(n) \gg f(n)$, or $f(n) \ll h(n)$. We use $f(n) = \Omega(g(n))$ to signify that $g(n) = O(f(n))$. We sometimes describe the asymptotic orders up to a logarithmic factor and use $O^*(f(n))$ to mean $O(f(n) \log^\alpha(n))$ for some fixed α .

We study noisy 2-complex contagions as stochastic processes on random graph models and use $\mathbb{P}(\cdot)$ and $\mathbb{E}(\cdot)$ to denote the associated probability measure and its expectation operator. For a sequence of non-negative real numbers $\{a_n : n \geq 1\}$ and a sequence of random variables $\{X_n : n \geq 1\}$, we say that $X_n = o(a_n)$ if $X_n/a_n \xrightarrow{\mathbb{P}} 0$ as $n \rightarrow \infty$. Similarly, we declare $X_n = O(a_n)$ if there exists a universal constant $C > 0$ such that $\mathbb{P}(|X_n|/a_n \leq C) \rightarrow 1$ as $n \rightarrow \infty$. Finally, say that $X_n = \Theta(a_n)$ if there exist universal constants $0 < c < C < \infty$ such that $\mathbb{P}(ca_n < X_n < Ca_n) \rightarrow 1$ as $n \rightarrow \infty$. For two random variables X, Y , we set $X \preceq Y$ if X is stochastically dominated by Y . A sequence of events $\{A_n\}$ occurs with high probability as $n \rightarrow \infty$ (referred to as w.h.p.) if $\mathbb{P}(A_n^c) \rightarrow 0$ as $n \rightarrow \infty$ where A_n^c is the complement of A_n . We end the notations by a list of the main symbols we use:

Table S1: A reference list of the main symbols used in this paper.

Symbol	Meaning
$\mathcal{G}_{n,c/n}$	Erdős-Rényi random graph on n nodes with edge probability c/n
\mathcal{C}_k	cycle-power- k (cycle with edges between k nearest neighbors)
$\mathcal{C}_{k,c/n}$	cycle-power- k union $\mathcal{G}_{n,c/n}$
\mathcal{C}_2^η	η -rewired \mathcal{C}_2
\mathcal{Z}_2	square lattice with edges in four directions (\boxplus)
\mathcal{Z}_4	square lattice with closed diagonals (edges in eight directions, \boxtimes)
$\mathcal{Z}_{2,c/n}$	$\sqrt{n} \times \sqrt{n}$ square lattice \mathcal{Z}_2 union $\mathcal{G}_{n,c/n}$
$T_\theta(\mathcal{G})$	spread time* of deterministic θ -complex contagion on graph** \mathcal{G}
$T_{\theta,q}(\mathcal{G})$	spread time* of noisy θ -complex contagion on graph** \mathcal{G} with sub-threshold adoption probability q
$\bar{T}_{\theta,q}(\mathcal{C}_{k,c/n})$	spread time* of noisy θ -complex contagion on $\mathcal{C}_{k,c/n}$ with sub-threshold adoption probability q only along \mathcal{C}_1 edges
$\bar{T}_{2,q}(\mathcal{C}_2^\eta)$	spread time* of noisy 2-complex contagion on \mathcal{C}_2^η with sub-threshold adoption probability q only along \mathcal{C}_1 edges
$T_{2,q}^\delta(\mathcal{C}_{1,c/n})$	spread time* of noisy 2-complex contagion on $\mathcal{C}_{1,c/n}$ with sub-threshold adoption probability q and reversion probability δ

* Spread times are measured starting from two neighboring infected nodes until the entire network is infected.

** Graph models that we study are circular lattices (\mathcal{C}_k), square lattices (\mathcal{Z}_2 and \mathcal{Z}_4), and their randomized variations ($\mathcal{C}_{k,c/n}$, \mathcal{C}_2^η , and $\mathcal{Z}_{2,c/n}$).

S2 Additional related work

Our results fall in the general category of work that addresses how network structure affects social contagions [1, 2, 3]. This question has been studied by researchers in many fields, including applied probability [4, 5], computer science [6, 7, 8, 9], physics [10], economics [11], organization science [12], and sociology [13].

Janson et al. [4] study the threshold spreading process (known in applied probability as bootstrap percolation) using a mean-field approximation. They use a random graph model that is the union of lattice with random (long) edges. The lattice structure provides for local clustering, while the random (long) edges decrease the network diameter. Both these features (high clustering and a small diameter) are observed in real network data and are the basis for the Watts–Strogatz small-world random graph model [14], where the edges of a cycle-power- k graph (denoted by \mathcal{C}_k , see Figure S1) are rewired and replaced by random long ties. The Watts–Strogatz model is suitable for studying the effect of network structure and interventions that modify local clustering. It is often useful to consider the closely related and more analytically amenable Newman–Watts model [15] in which random edges are added on top of \mathcal{C}_k . Our first result (Section S3) establishes the rate of spread over \mathcal{C}_2 union random graphs with fixed expected degree, and tightens the existing upper and lower bounds for rate of spread over the Newman–Watts random graphs [6]. Our second and third results (Sections S4 and S6) allow us to provide a more refined picture for cases with partial rewiring of the cycle structure (\mathcal{C}_k). The spread of threshold processes have been also analyzed in a variety of other random graph models, including random regular graphs, power-law and configuration models [7, 8, 9, 16, 17, 18]. In other related work [19, 20], researchers analyze how the network structure affects the equilibria of coordination games, where agents best respond to the fraction of their adopting neighbors. The concept of cohesiveness proposed by Morris [19] is useful for characterizing the final adopter set. Accordingly, highly cohesive (and clustered) groups with many internal edges are difficult to penetrate, impeding the spread of fractional threshold models.

We are interested in noisy models of complex contagion which allow for a non-zero probability of adoption below threshold. Focusing on the canonical case of 2-complex contagion¹, we denote the probability of (simple) adoptions with a single neighboring adopter by q_n , where n is the network size. Our characterization is in terms of time to global spread. We show that having $q_n = \omega(1/\sqrt{n})$ is enough to make contagion spread faster over the rewired graph; thus changing the landscape of results leading to weakness of long ties for complex contagions. Our theoretical analyses and simulation results indicate that long ties accelerate noisy complex (i.e., threshold-based) contagions.

¹In a d -regular graph, 2-complex contagion corresponds to a fractional threshold model [21, 19] with fixed (relative) thresholds set to $2/d$. Using an absolute threshold allows us to isolate the effect of structural interventions irrespective of the initial seed sets. For example, introduction of a new edge has a monotone increasing influence on the spreading rate in an absolute threshold model; whereas, if thresholds are specified with respect to the ratio of adopters in each neighborhood, then depending on the size and location of adopters one can place the new edges carefully to impede the spread.

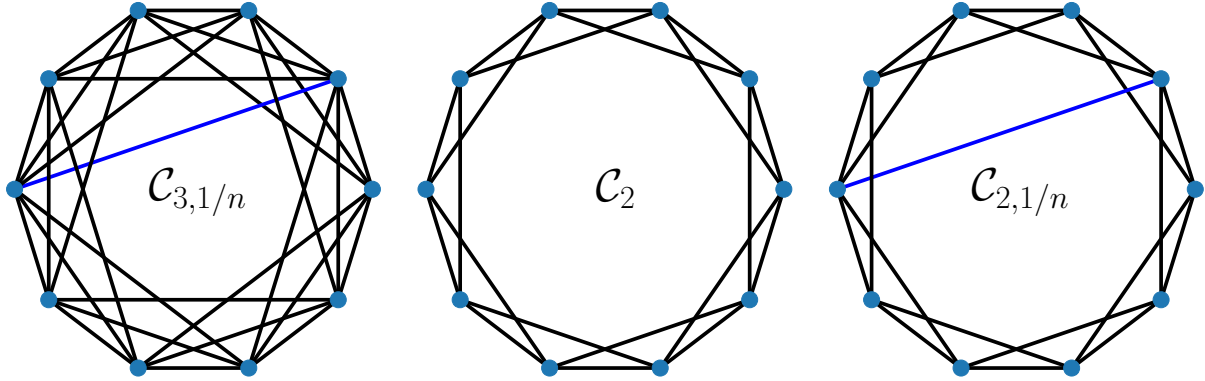


Figure S1: Unions of cycle-powers and random graphs. The cycle edge are colored black and random (long) edges are colored blue. The cycle-power- k graph, denoted by \mathcal{C}_k , is constructed by connecting each node on an n -cycle to all nodes within its k -hop distance (i.e., the $2k$ nearest neighbors), where the hop distance is measured on the cycle \mathcal{C}_1 . The cycle-power- k union random graph is denoted by $\mathcal{C}_{k,p_n} := \mathcal{C}_k \cup \mathcal{G}_{n,p_n}$, where \mathcal{G}_{n,p_n} is the Erdős–Rényi random graph model with edge probability p_n . The union graph, \mathcal{C}_{k,p_n} , has n nodes and the set of edges is the union of edges in the two graphs.

S2.1 Adoption probabilities by the number of adopting peers in real data

We use a number of prior empirical studies to report on the relative rates of adoptions when there are k and $k - 1$ adopting neighbors: $p(k)/p(k - 1)$, for integers $k \geq 2$. We find that the reported ratios are less than five, consistently, across a multitude of studies (Figure S2); thus, there is evidence against homogeneous deterministic thresholds for adoption.

Aral et al. [22] aim to distinguish how much of the clustering in the observed patterns of adoption of a mobile phone application can be explained by contagion as opposed to homophily. The adoption patterns demonstrate significant clustering in terms of both network location of the adopters as well as the time at which neighboring nodes become adopters. However, the correlated outcomes can be attributed to both contagion and homophily: On the one hand, the linked nodes influence each other in their decisions to adopt; and on the other hand, they simply have greater likelihoods of displaying correlated outcomes as a consequence of their similar attributes. Using a dynamic matched sample estimation framework², Aral et al. [22] show that previous methods over-estimate peer influence in a study of the global instant messaging network of 27.4 million users, using data on the day-by-day adoption of a mobile service ap-

²They consider four different treatment levels corresponding to having one, two, three, or four adopter friends and estimate the treatment probabilities at different levels as a function of observable and latent node characteristics using logistic regression. They use the estimated treatment probabilities to create a dynamic matched sample of treated and untreated nodes over time: Every treated node (having one or more friends who are adopters) is matched with an untreated node (having fewer number of adopter friends) whose likelihoods of being treated (propensity scores) are closest.

plication called Yahoo Go mobile. In Fig. 3B (right inset) of [22], Aral et al. [22] report the adoption ratios among the matched pairs versus the number of adopter friends. We have extracted and plotted these ratios in Figure S2.

Bakshy et al. [23] present their results from a large-scale field experiment about sharing URLs on Facebook with 253 million subjects. The experiment randomizes whether or not individuals are exposed via Facebook to information about their friends' sharing behavior. The authors find that additional exposure has an increasing causal effect on the propensity to share. We extracted the probability of sharing versus the number of sharing friends on the Facebook News Feed from their Fig. 4(a). This is the observational association, as the experiment only randomizes exposure or non-exposure. We have plotted the ratio of probabilities for different values of k in Figure S2.

In a controlled study to test for effects of complex contagion, Centola [24] randomizes subjects between two network conditions: a clustered lattice consisting entirely of short ties, and a random regular graph with very few triangle (short ties). The node degrees in both conditions are fixed and the same. The author studies the spread of a health-related behavior (registering for a health forum website) in an online community in which users were informed about the activities of their assigned neighbors ("health buddies") through email invitations to adopt the same behavior. The faster spread over the clustered lattice has been interpreted as evidence of complex contagion. In Figure S2, we have extracted the values reported in Figure 3 of [24], where up to three additional social signals significantly increases the probability of adoption.

Mørnsted et al. [25] present the results of a non-randomized field experiment conducted on the Twitter social network. They test the adoption of new hashtags using a network of Twitter bots ("botnet") with a large number of followers. The large user base who follow multiple bots are exposed to coordinated interventions by the bots to test the effects of multiple exposures. They observe that their proposed model of complex contagion is a better fit to the observed adoption rates than an alternative simple contagion model. We have extracted the percentage of retweets versus the total number of unique exposures from Figure 3A of [25] and plotted the results in Figure S2.

Ugander et al. [26] use e-mail invitations for joining Facebook to study the growth of Facebook's user base. In a corpus of 54 million such email invitations, they analyze the probability of accepting an invitation as a function of the structure of the contact neighborhoods. They observe that adoption probabilities are better explained by the number of connected components in the contact neighborhoods; thus highlighting the effect of structural diversity in determining the conversion decisions. In Figure S2, we have plotted the ratios of the aggregate conversion rates for each neighborhood size. This data, extracted from a supplementary figure provided by the authors, is partially presented in their Figure 1.

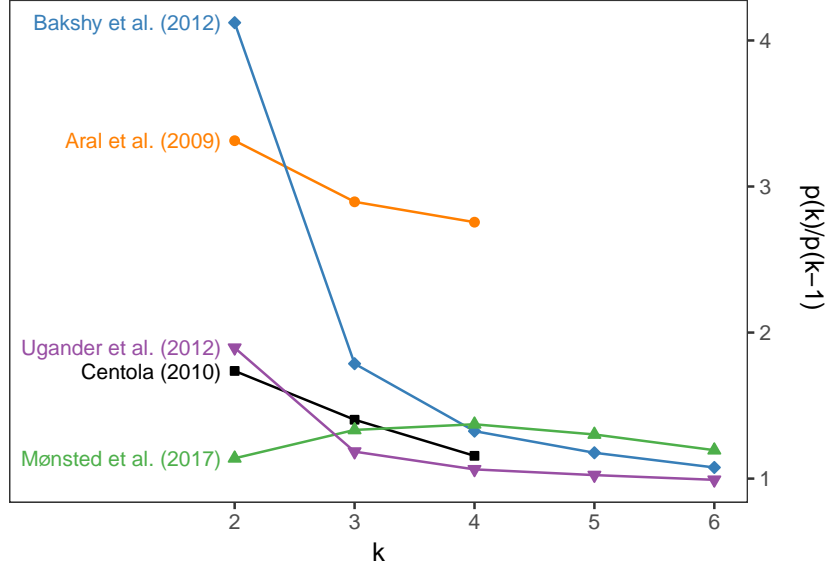


Figure S2: Empirical adoption rate ratios. These are ratios of observed rates of adoption when there are k and $k - 1$ adopting neighbors: $p(k)/p(k - 1)$, for integers $k \geq 2$. Of note, given the decreasing ratios in all but one study (Mønsted et al. [25]), we could only find evidence of a minimally complex contagion (threshold at most 2), with substantial level of sub-threshold adoption. Lee, Lazer and Riedl provide causal evidence of social reinforcement from a country-scale randomized controlled network experiment, where consumers are randomly encouraged to share coupons, either alone or in pairs, as part of a viral marketing campaign for a mobile data product in a large Asian country. In their Figure A4, they reproduce the above plot and place their own estimates for $p(k)/p(k - 1)$ when $k = 2$ from the measurements of adoptions in their randomized controlled experiments. Their reported estimates are in the 2.28 to 2.90 range [27].

S3 Deterministic 2-complex contagion on $\mathcal{C}_{2,c/n}$

In this section we provide the asymptotic rate of deterministic 2-complex contagion over $\mathcal{C}_{2,c/n}$ for $c > 0$; see Theorem 5 below. However, before focusing on proving Theorem 5, it worth considering the rate of spread on $\mathcal{C}_{2+c/2}$ lattice which has the same average degree as $\mathcal{C}_{2,c/n}$, when c is a positive, even integer. Starting from two neighboring nodes, deterministic 2-complex contagion spreads on $\mathcal{C}_{2+c/2}$ by growing an interval around the initially infected nodes. Every time c new nodes on both sides of the interval are infected and deterministic 2-complex contagion spreads to the entire graph in $T_2(\mathcal{C}_{2+c/2}) = \lceil (n/2 - 1)/c \rceil = \Theta(n)$ time steps (using $\lceil \cdot \rceil$ for the smallest integer greater than or equal to). Our analysis below establishes that with high probability $T_2(\mathcal{C}_{2,c/n}) \in O^*(n^{2/3})$, which is significantly faster than $\Theta(n)$ for any $c > 0$.

In fact, we show that the spreading time is w.h.p. greater than any $o(n^{2/3})$, thus essentially fixing the asymptotic order of the spreading time at $n^{2/3}$ (up to logarithmic factors). On the other hand, deterministic 2-complex contagion almost surely fails to spread totally on $\mathcal{C}_{1,c/n}$ as $n \rightarrow \infty$; hence, $T_2(\mathcal{C}_{1,c/n}) = \infty$. We can change the latter significantly by allowing for a small probability (q) of adoptions below threshold in SI Section S4; see Theorem 11.

Theorem 5 (Complex contagion over $\mathcal{C}_{2,c/n}$). *Fix $c > 0$ and consider the deterministic 2-complex contagion over $\mathcal{C}_{2,c/n}$. For any $\varepsilon > 0$, with high probability, the total spreading time, $T_2(\mathcal{C}_{2,c/n})$, can be upper and lower bounded as follows:*

$$n^{2/3-\varepsilon} < T_2(\mathcal{C}_{2,c/n}) < 2n^{2/3}(\log \log n)^2.$$

Prior work [6] bounds the spreading time of deterministic 2-complex contagion in the related Newman–Watts random graph model [28] by $O(\sqrt[5]{n^4 \log n})$ and $\Omega(\sqrt{n/\log n})$. Our results suggest that the order of the spreading time is more precisely characterized as $O^*(n^{2/3})$ and $\Omega(n^{2/3-\varepsilon})$ for $\varepsilon > 0$ fixed, arbitrarily small.

S3.1 Lower bound on $T_2(\mathcal{C}_{2,c/n})$

Theorem 6 (Upper-Bounding the number of infected nodes in $o(n^{2/3})$ steps). *Let I_t denote the number of infected nodes at time t . For $t = o(n^{2/3})$, $I_t = o(n^{2/3})$.*

Proof. Let \mathcal{I}_t be the set of all infected nodes at time t and let \mathcal{B}_t denote the interval of length $2t$ from the deterministic growth of the two neighboring initial seeds. Note that the nodes in \mathcal{B}_t are always infected due to two-complex contagion along \mathcal{C}_2 ; hence, $B_t = |\mathcal{B}_t| = 2t = T$. We define $\mathcal{I}_t^0 = \mathcal{B}_t$ and note that $\mathcal{I}_t^0 \subset \mathcal{I}_t$. However, other nodes might be infected due to complex contagion along the edges of $\mathcal{G}_{n,c/n}$. To control these secondary infections, we introduce an algorithm which proceeds in rounds. These rounds are indexed by τ and they build up the infected set $\{\mathcal{I}_t^\tau : \tau \geq 1\}$ by exposing new random edges connecting infected nodes, identified at the current round, to “healthy” nodes. The analysis below tracks the growth of the infected set over iterations, and establishes that for $t = o(n^{2/3})$, the algorithm terminates after two rounds with high probability. Further, the additional infected nodes gained are $o(n^{2/3})$ in number, and all isolated. Thus they do not give rise to secondary infections along \mathcal{C}_2 via deterministic 2-complex contagion.

Let us introduce the sequential algorithm formally before we proceed further. For notational convenience, let $\{\mathcal{S}_t^\tau : \tau \geq 1\}$ denote nodes with exactly one neighbor in \mathcal{I}_t^τ and call them “susceptible” nodes. Further, let \mathcal{H}_t^τ denote nodes that have no neighbors in \mathcal{I}_t^τ and call them “healthy” nodes. Moreover, we denote the nodes that are added to the infected set at round τ by $\mathcal{A}_t^\tau = \mathcal{I}_t^\tau \setminus \mathcal{I}_t^{\tau-1}$. Finally, for $v \in [n]$ and $C \subset [n]$, $\mathcal{N}_C(v)$ will denote the number of neighbors of v in the set C .

Algorithm 1 Edge Revelation

- 1: Initialize: $\mathcal{I}_t^{-1} = \emptyset, \mathcal{I}_t^0 = \mathcal{B}_t, \mathcal{A}_t^0 = \mathcal{B}_t, \mathcal{S}_t^0 = \emptyset, \mathcal{H}_t^0 = [n] \setminus (\mathcal{I}_t^0 \cup \mathcal{S}_t^0)$.
 - 2: **for** $\tau \geq 1$ **do** \triangleright reveal all the long ties that are incident to $\mathcal{A}_t^{\tau-1}$ and update the sets using the revealed edges:
 - 3: $\bar{\mathcal{S}}_t^\tau = \{v \in \mathcal{S}_t^{\tau-1} : \mathcal{N}_{\mathcal{I}_t^{\tau-1} \setminus \mathcal{I}_t^{\tau-2}}(v) \geq 1\}$. \triangleright nodes that are susceptible at round $\tau - 1$ and join the infected at round τ .
 - 4: $\bar{\mathcal{H}}_t^\tau = \{v \in \mathcal{H}_t^{\tau-1} : \mathcal{N}_{\mathcal{I}_t^{\tau-1} \setminus \mathcal{I}_t^{\tau-2}}(v) \geq 2\}$. \triangleright nodes that are healthy at round $\tau - 1$ and join the infected at round τ .
 - 5: $\hat{\mathcal{H}}_t^\tau = \{v \in \mathcal{H}_t^{\tau-1} : \mathcal{N}_{\mathcal{I}_t^{\tau-1}}(v) = 1\} = \{v \in \mathcal{H}_t^{\tau-1} : \mathcal{N}_{\mathcal{I}_t^{\tau-1} \setminus \mathcal{I}_t^{\tau-2}}(v) = 1\}$. \triangleright healthy nodes at round $\tau - 1$ that join the susceptible set at round τ .
 - 6: $\mathcal{A}_t^\tau = \bar{\mathcal{S}}_t^\tau \cup \bar{\mathcal{H}}_t^\tau$. \triangleright nodes that become infected in step τ .
 - 7: $\mathcal{I}_t^\tau = \mathcal{I}_t^{\tau-1} \cup \mathcal{A}_t^\tau$. \triangleright adding the nodes that become infected in step τ .
 - 8: $\mathcal{S}_t^\tau = \bar{\mathcal{S}}_t^\tau \cup \hat{\mathcal{H}}_t^\tau \setminus \bar{\mathcal{S}}_t^\tau$. \triangleright updating the set of susceptible nodes for the next step.
 - 9: $\mathcal{H}_t^\tau = \bar{\mathcal{H}}_t^\tau \setminus (\bar{\mathcal{H}}_t^\tau \cup \hat{\mathcal{H}}_t^\tau)$. \triangleright updating the set of healthy nodes for the next step.
 - 10: **end for**
-

Recall that for notational convenience, we use roman fonts to refer to sizes of sets introduced in Algorithm 1 — for example, $H_t^0 = |\mathcal{H}_t^0|$, $B_t = |\mathcal{B}_t|$ and so on. We will refer to the natural filtration associated with the sequential procedure in Algorithm 1 as $\{\mathcal{F}_\tau : \tau \geq 1\}$.

To track the evolution of the infected and susceptible nodes over the subsequent iterations of Algorithm 1, we make the following elementary observation. For any sequence $a_n = o(n)$, on the event $\{A_t^{\tau-1} \leq a_n\}$, we have, using Taylor expansion for the binomial probabilities:

$$\begin{aligned} \mathbb{P}[\text{Bin}(A_t^{\tau-1}, c/n) \geq 1 \mid \mathcal{F}_{\tau-1}] &= 1 - (1 - \frac{c}{n})^{A_t^{\tau-1}} = 1 - \left(1 - A_t^{\tau-1} \frac{c}{n} + O\left(\frac{(cA_t^{\tau-1})^2}{n^2}\right)\right) \\ &= (1 + o(1))A_t^{\tau-1} \frac{c}{n}. \end{aligned}$$

Similarly, on the event $\{A_t^{\tau-1} \leq a_n\}$,

$$\begin{aligned} \mathbb{P}[\text{Bin}(A_t^{\tau-1}, c/n) \geq 2 \mid \mathcal{F}_{\tau-1}] &= 1 - (1 - \frac{c}{n})^{A_t^{\tau-1}} - \frac{c}{n} A_t^{\tau-1} (1 - \frac{c}{n})^{A_t^{\tau-1}-1} \\ &= 1 - \left(1 - A_t^{\tau-1} \frac{c}{n} + \frac{c^2}{2n^2} (A_t^{\tau-1})(A_t^{\tau-1} - 1) + o\left(\frac{(cA_t^{\tau-1})^2}{n^2}\right)\right) \\ &\quad - \frac{c}{n} A_t^{\tau-1} \left(1 - (A_t^{\tau-1} - 1) \frac{c}{n} + O\left(\frac{(cA_t^{\tau-1})^2}{n^2}\right)\right) \\ &= (1 + o(1)) \left(\frac{(cA_t^{\tau-1})^2}{2n^2}\right). \end{aligned}$$

The algorithm terminates at the first step $\tau \geq 1$, such that $\bar{\mathcal{S}}_t^\tau \cup \bar{\mathcal{H}}_t^\tau = \emptyset$. Upon termination

at τ , we have that $\mathcal{I}_t^\tau = \mathcal{I}_t$. We show that when $t = o(n^{2/3})$, then with high probability this algorithm terminates in $\tau = 2$; moreover, $I_t = I_t^{\tau=2} = o(n^{2/3})$ w.h.p.

We analyze the rounds of the algorithm sequentially. We start with $\tau = 0$, and note that $I_t^0 = B_t = 2t = T = o(n^{2/3})$. For $\tau = 1$, we get:

$$\begin{aligned}\hat{H}_t^1 &= \text{Bin}(H_t^0, \mathbb{P}[\text{Bin}(A_t^0, c/n) = 1]), \\ \bar{H}_t^1 &= \text{Bin}(2, \mathbb{P}[\text{Bin}(A_t^0, c/n) = 1]) + \text{Bin}(H_t^0, \mathbb{P}[\text{Bin}(A_t^0, c/n) \geq 2]), \\ \bar{S}_t^1 &= \text{Bin}(S_t^0, \mathbb{P}[\text{Bin}(A_t^0, c/n) \geq 1]) = 0.\end{aligned}$$

Direct computation yields $\mathbb{E}[\hat{H}_t^1] = o(n^{2/3})$ and $\mathbb{E}[\bar{H}_t^1] = o(n^{1/3})$. Using Markov inequality, this immediately implies that $\hat{H}_t^1 = o(n^{2/3})$ and $\bar{H}_t^1 = o(n^{1/3})$. This, in turn implies that

$$\begin{aligned}S_t^1 &= S_t^0 - \bar{S}_t^1 + \hat{H}_t^1 = T = o(n^{2/3}), \quad H_t^1 = H_t^0 - \bar{H}_t^1 - \hat{H}_t^1 = \Theta(n), \\ A_t^1 &= \bar{H}_t^1 = o(n^{1/3}), \quad I_t^1 = I_t^0 + A_t^1 = o(n^{2/3}).\end{aligned}$$

We next analyze the next round of the Edge Revelation algorithm. For $\tau = 2$, we have

$$\begin{aligned}\hat{H}_t^2 &= \text{Bin}(H_t^1, \mathbb{P}[\text{Bin}(A_t^1, c/n) = 1]), \\ \bar{H}_t^2 &= \text{Bin}(H_t^1, \mathbb{P}[\text{Bin}(A_t^1, c/n) \geq 2]), \\ \bar{S}_t^2 &= \text{Bin}(S_t^1, \mathbb{P}[\text{Bin}(A_t^1, c/n) \geq 1]).\end{aligned}$$

For any $\varepsilon > 0$, we have, for $\xi_1 > 0$

$$\mathbb{P}[\hat{H}_t^2 > \varepsilon n^{1/3}] \leq \mathbb{P}[\hat{H}_t^2 > \varepsilon n^{1/3}, A_t^1 < \xi_1 n^{1/3}] + o(1) \leq \frac{\xi_1 c}{\varepsilon} + o(1),$$

where the last inequality follows using Markov inequality, conditioned on \mathcal{F}_1 . We note that as $\xi_1 > 0$ is arbitrary, $\hat{H}_t^2 = o(n^{1/3})$. A similar analysis reveals that $\bar{H}_t^2 = o(1)$ and $\bar{S}_t^2 = o(1)$. Armed with these observations, we immediately conclude that

$$\begin{aligned}S_t^2 &\leq 4A_t^1 + S_t^1 - \bar{S}_t^2 + \hat{H}_t^2 = o(n^{2/3}), \quad H_t^2 = H_t^1 - \bar{H}_t^2 - \hat{H}_t^2 = \Theta(n), \\ A_t^2 &= \bar{S}_t^2 + \bar{H}_t^2 = o(1), \quad I_t^2 = I_t^1 + A_t^2 = o(n^{2/3}).\end{aligned}\tag{S.1}$$

The upper bound in (S.1) is due to the $4A_t^1$ term which accounts for the four neighbors of an additionally infected node (outside of \mathcal{B}_t) on the \mathcal{C}_2 . The validity of this recursion hinges crucially on the observation that with high probability, two nodes that are infected at round 2 (belonging to \mathcal{A}_t^2) are at least distance two apart on \mathcal{C}_2 . We state this assertion formally in the lemma below, and complete the proof assuming this lemma. We defer its proof to the end of the section.

Lemma 7. *With high probability as $n \rightarrow \infty$, no two infected nodes outside \mathcal{B}_t are neighbors on \mathcal{C}_2 .*

Note that after $\tau = 2$ steps the algorithm terminates with high probability, as there are no additional infected nodes identified. This completes the proof. \square

Finally, we turn to the proof of Lemma 7.

Proof of Lemma 7: Note that two neighboring nodes are infected in the first two rounds of the Edge Revelation algorithm provided there exist two nodes at distance at most two on \mathcal{C}_2 such that at least one is infected and the other node becomes susceptible. There are $\Theta(n)$ such pairs, and the probability of such an event is $\mathbb{P}(\text{Bin}(A_t^1, c/n) \geq 1)\mathbb{P}(\text{Bin}(A_t^1, c/n) \geq 2)$. The required result follows upon computing the expected number of such neighboring pairs on \mathcal{C}_2 . \square

S3.2 Upper bound on $T_2(\mathcal{C}_{2,c/n})$

Theorem 8. *With high probability as $n \rightarrow \infty$, $T_2(\mathcal{C}_{2,c/n}) \leq n^{2/3}(\log \log n)^2(1 + o(1))$.*

Proof of Theorem 8. We devise an algorithm to lower bound the initial growth of the set of infected nodes. Let us consider a sequence $a_n \rightarrow \infty$ as $n \rightarrow \infty$, to be specified later. Next, we divide the cycle into consecutive intervals of length $L_n = n^{2/3}a_n(\log \log n)^2$. Call an interval *active* if two neighboring nodes (an adjacent pair) within that interval are infected. Initially, declare the interval containing the original seed nodes as an active interval. Starting with the initial seed nodes, after $n^{2/3}a_n$ steps the length of the original interval grows to $2n^{2/3}a_n$. In general, after $n^{2/3}a_n$ time steps the length of infected segments in each active interval will be at least $n^{2/3}a_n$ due to the deterministic growth along the cycle. By revealing the edges of $\mathcal{G}_{n,c/n}$ that are incident to the newly infected nodes at the end of each epoch of length $n^{2/3}a_n$, we can identify new active intervals that will, in turn, grow and activate other intervals. Formally, we consider the following algorithm to undercount the number of infected nodes. Denote by \mathcal{X}_τ the set of active intervals after τ epochs of length $n^{2/3}a_n$ each, and let $X_\tau = |\mathcal{X}_\tau|$ be the number of such intervals.

Algorithm 2 Interval Growth

Input: Random graph model $\mathcal{C}_{2,c/n}$ and interval length $L_n = n^{2/3}a_n(\log \log n)^2$.

- 1: **Initialize:** Set $N_n = n/L = n^{1/3}/(a_n(\log \log n)^2)$. Divide the cycle into N_n intervals of length L_n each, and label them by $[N_n]$; let the initial seed nodes be contained in the interval that is labeled one: $\mathcal{X}_0 = \{1\}$.
 - 2: **for** $\tau \geq 1$ **do**
 - 3: Infect $n^{2/3}a_n$ new nodes along the cycle in each of the active intervals. Add edges independently with probability c/n , connecting the newly infected nodes to the healthy nodes.
 - 4: Update the set of active intervals by adding all intervals that have two adjacent infected nodes due to the edge exposure operation in the previous step: $\mathcal{X}_\tau \leftarrow \mathcal{X}_{\tau-1}$.
 - 5: **end for**
-

The following lemma derives a lower bound on the number of active intervals after $O(\log \log n)$ steps.

Lemma 9 (Initial Growth of the intervals). *For any $C > 0$, there exists a sequence $t_n := t_n(C) = o(\log \log n)$ such that for*

$$\tau_n = \frac{1}{\log 3} \left(\log \log n + t_n \right),$$

with high probability as $n \rightarrow \infty$, $X_{\tau_n} \geq Cn^{1/9}(\log n)^{1/3}$.

An extra $n^{2/3}$ steps beyond the τ_n -th epoch ensures that each activated interval has at least $n^{2/3}$ infected nodes. The next Lemma shows that this is enough to guarantee that the whole graph will be infected in $(\tau_n a_n + 2)n^{2/3} + 2$ time.

Lemma 10 (End Regime). *Let T_n be the first time that deterministic 2-complex contagion infects $Cn^{7/9}(\log n)^{1/3}$ nodes, where $C > 2/c$ is a universal constant. Then with high probability, all nodes are infected by time $T_n + n^{2/3} + 2$.*

This concludes the proof. □

It remains to prove Lemma 9 and Lemma 10. We first turn to the proof of Lemma 9.

Proof of Lemma 9. Let us denote the natural filtration associated with the growth process outlined in Algorithm 2 by $\{\mathcal{F}_\tau : \tau \geq 1\}$. Note that at the end of $\tau - 1$ steps, we have $X_{\tau-1}$ infected intervals, and thus $N - X_{\tau-1}$ non-active intervals. Each non-active interval of length L has at least $\frac{1}{2}L$ mutually disjoint adjacent pairs, and the interval is activated if any one of these adjacent pairs is infected in the next step of Algorithm 2 introduced above. The independence of the added edges naturally implies that given $\mathcal{F}_{\tau-1}$, we have:

$$X_\tau = X_{\tau-1} + \text{Bin}(N - X_{\tau-1}, p_\tau),$$

where p_τ is the conditional probability that an interval is activated by the edge exposure operation in Algorithm 2. Given $\mathcal{F}_{\tau-1}$ we can lower bound p_τ as follows. Each non-active interval has at least $\frac{1}{2}L$ disjoint adjacent pairs of neighboring nodes, and thus if the edge exposure infects a node and creates at least one infected edge for one of its cycle neighbors, the interval is activated due to complex contagion along the cycle (Figure S3B). Thus we have,

$$p_\tau \geq \mathbb{P} \left[\text{Bin} \left(\frac{1}{2}L, \mathbb{P} \left[\text{Bin} \left(X_{\tau-1} n^{2/3} a_n, \frac{c}{n} \right) \geq 2 \right] \mathbb{P} \left[\text{Bin} \left(X_{\tau-1} n^{2/3} a_n, \frac{c}{n} \right) \geq 1 \right] \right) \geq 1 \right].$$

Set $\xi_n \rightarrow 0$ as $n \rightarrow \infty$. Consider a choice of τ_n satisfying the conditions of Lemma 9. On the event that $X_{\tau_n-1} > \varepsilon N$ for some $\varepsilon > 0$, the claim holds automatically. Thus we have, on the event $\{X_{\tau_n-1} \leq N\xi_n\}$

$$\mathbb{E} \left[X_{\tau_n} - X_{\tau_n-1} \right] \geq \frac{1}{4} X_{\tau_n-1}^3 (a_n c)^3.$$

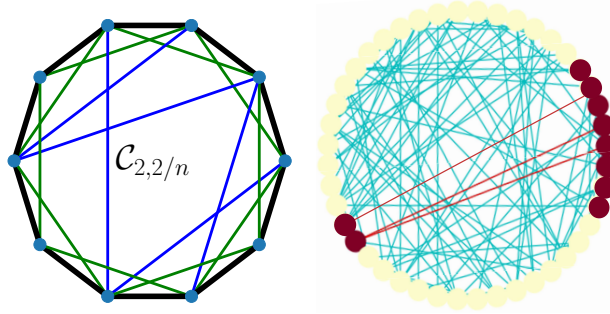


Figure S3: Spread of minimally complex contagions through wide bridges. In Theorem 5, we show that $T_2(\mathcal{C}_{2,c/n}) \in O^*(n^{2/3})$ w.h.p., which is asymptotically faster than $T_2(\mathcal{C}_{2+c/2}) \in \Theta(n)$. Our result emphasizes the intuitive understanding that rewiring accelerates the spread of complex contagion, as long as the essential short tie structure (\mathcal{C}_2) that facilitates local reinforcements remains intact. On the right, we have reproduced a version of figure 2 of [13]. In [13], Centola and Macy argue that for minimally complex (2-complex) contagions on a ring lattice, a bridge of size three is required to pass complex contagion from one neighborhood of the ring lattice to another [13, equation 4]. We complement their argument by showing that bridges of size three made up of random, long ties are formed with high probability as $n \rightarrow \infty$ and they determine the speed of complex contagion on $\mathcal{C}_{2,c/n}$. Indeed, an interval of length $n^{2/3} \log \log n$ is large enough to produce a pair of neighboring activated nodes through three long ties, as shown in the figure, and this random configuration occurs with high probability as $n \rightarrow \infty$.

Using Bernstein's inequality (lower tail bound), we have, for some universal constant $c_0 > 0$ with probability at least $1 - 2 \exp(-c_0 a_n^3)$

$$X_\tau \geq X_{\tau-1}^3 \left(\frac{c a_n}{2} \right)^3.$$

Let us choose $\tau_n = \frac{\log \log n + t_n}{\log 3}$ for some sequence $t_n = t_n(C) = o(\log \log n)$. Then using union bound, the probability that we do not have the desired growth in the number of infected intervals in at least one of the rounds may be upper bounded by $\tau_n \exp(-c_0 a_n^3)$. We note that if we choose $a_n = \log \log n$, the probability of this bad event is $o(1)$. Moreover, on the good event, we have, $X_{\tau_n} \geq \left(\frac{c a_n}{2} \right)^{3\tau_n}$. With $\tau_n = (\log \log n + t_n) / \log 3$, we can choose t_n appropriately such that $X_{\tau_n} \geq C n^{1/9} (\log n)^{1/3}$. Finally, note that in $\Theta(\log \log n)$ rounds, we grow to length $n^{2/3} a_n \log \log n$ on the first interval, which is $o(L)$, thus indicating that the growth in infected nodes is sustained throughout the first τ rounds. This establishes the desired lower bound on the number of activated intervals in the first τ rounds. □

Finally, we prove Lemma 10.

Proof of Lemma 10. Fix any node x in the graph, and consider the interval \mathcal{L}_x along the \mathcal{C}_2 cycle with center at x and of length $n^{2/3}$. We say that the interval \mathcal{L}_x contains a *susceptible pair* if it contains two neighboring nodes on \mathcal{C}_2 , at least one of which is infected, and the other (possibly uninfected) has at least one additional infected neighbor. We note that if an interval contains a susceptible pair at time T_n , x will be infected by time $T_n + 2 + n^{2/3}$ due to complex contagion along the cycle. Thus without loss of generality, consider x such that \mathcal{L}_x does not contain a susceptible pair at time T_n . Let A_x denote the event that \mathcal{L}_x contains a susceptible pair at time $T_n + 1$. For any fixed x , \mathcal{L}_x has at least $\frac{1}{2}n^{2/3}$ disjoint pairs of adjacent nodes. Each such pair is susceptible if at least one node is infected and the other has an infected neighbor. Denoting the number of infected nodes at T_n as I_{T_n} , we observe that a fixed pair becomes susceptible by time $T_n + 1$ with probability at least $\mathbb{P}[\text{Bin}(I_{T_n}, \frac{c}{n}) \geq 2] \mathbb{P}[\text{Bin}(I_{T_n}, \frac{c}{n}) \geq 1]$. The probability of the complement is thus at most $(1 - \mathbb{P}[\text{Bin}(I_{T_n}, \frac{c}{n}) \geq 2] \mathbb{P}[\text{Bin}(I_{T_n}, \frac{c}{n}) \geq 1])$. Using independence of the adjacent pairs in \mathcal{L}_x , we have,

$$\begin{aligned} \mathbb{P}(A_x^c) &\leq \left(1 - \mathbb{P}\left[\text{Bin}\left(Cn^{7/9}(\log n)^{1/3}, \frac{c}{n}\right) \geq 2\right] \mathbb{P}\left[\text{Bin}\left(Cn^{7/9}(\log n)^{1/3}, \frac{c}{n}\right) \geq 1\right]\right)^{\frac{1}{2}n^{2/3}} \\ &= o\left(\frac{1}{n}\right), \end{aligned}$$

for $C > 1$ satisfying $Cc > 2$. Finally, a union bound over the nodes x with no adjacent infected pair in \mathcal{L}_x immediately implies that with high probability, every node has an infected adjacent pair within distance $n^{2/3}$ by time $T_n + 1$. Thus we can guarantee that all nodes will be infected by time $T_n + n^{2/3} + 2$, establishing the desired result. \square

Figure S4 shows the time that it takes for the contagion to spread over $\mathcal{C}_{k,(D-2k)/n}$ graphs. Setting $p_n = (D - 2k)/n$ in \mathcal{C}_{k,p_n} ensures that the expected degree of each node is kept fixed at D . Thus by varying k , we can study the spreading rate of contagion as the cycle edges are rewired and replaced by (random) long ties. In Figure S4, the expected degree is fixed at $D = 15$. Simulation results show that rewiring the cycle edges and replacing them with random long ties speeds up the spread of contagion. However, this trend is not carried through all the way until $k = 2$. Note that if we rewire the cycle edges beyond \mathcal{C}_2 , complex contagion may not spread to the entire graph. In the following section, we consider a noisy 2-complex contagion model whereby with a vanishing probability ($q_n \rightarrow 0$) of sub-threshold adoptions the contagion spreads totally even as the \mathcal{C}_2 edges are rewired.

S4 Noisy 2-complex contagion on $\mathcal{C}_{1,2/n}$

In this section we prove the upper-bound in Theorem 1. We begin by noting that $T_2(\mathcal{C}_2) = \lceil n/2 \rceil - 1 \ll T_2(\mathcal{C}_{1,2/n}) = \infty$ because deterministic 2-complex contagion does not spread to the entire $\mathcal{C}_{1,2/n}$. However, we are interested in comparing the diffusion speeds between $\mathcal{C}_{1,2/n}$ and \mathcal{C}_2 under the noisy 2-complex contagion, i.e., $T_{2,q}(\mathcal{C}_{1,2/n})$ and $T_{2,q}(\mathcal{C}_2)$. Inclusion of sub-threshold adoptions cannot speed up the spread time over \mathcal{C}_2 beyond the $\lfloor n/4 \rfloor$ lower bound;

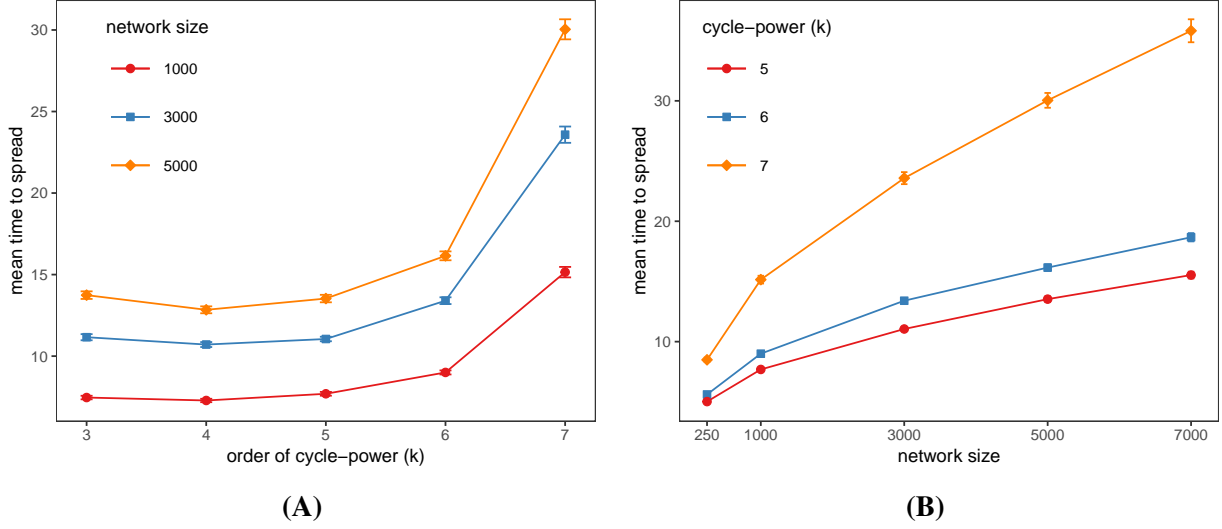


Figure S4: Spreading time of deterministic 2-complex contagion over \mathcal{C}_k union random graphs. We consider \mathcal{C}_{k,p_n} random graphs with $p_n = (15 - 2k)/n$ such that the expected degree of each node is fixed at $D = 15$ as we vary k . The spreading model is the deterministic 2-complex contagion (with no simple/sub-threshold adoptions, as in Theorem 5). Each point is the average of 100 random draws. The vertical bars indicate the 95% normal confidence intervals around the means.

see Figure 2 caption: $T_{2,q}(\mathcal{C}_2) > \lfloor n/4 \rfloor$. To upper-bound $T_{2,q}(\mathcal{C}_{1,2/n})$, we consider an auxiliary model where we have simple contagion adoptions only along the \mathcal{C}_1 edges, i.e., contagion can spread with probability q_n along \mathcal{C}_1 in addition to deterministic 2-complex contagion. Let $\bar{T}_{2,q}(\mathcal{C}_{1,2/n})$ denote the random variable measuring the total spread time under this variation of noisy 2-complex contagion where adoptions below threshold are blocked except on \mathcal{C}_1 edges. Note that $T_{2,q}(\mathcal{C}_{1,2/n}) \leq \bar{T}_{2,q}(\mathcal{C}_{1,2/n})$ every where, hence, it suffices to show the upper bound in Theorem 1 for $\bar{T}_{2,q}(\mathcal{C}_{1,2/n})$. In fact, we prove both a lower and an upper bound which match each other except for logarithmic factors.

Theorem 11. Consider the noisy 2-complex contagion over $\mathcal{C}_{1,2/n}$ and allow for simple contagion adoptions to occur with probability q along \mathcal{C}_1 edges. For any $\varepsilon > 0$, with high probability, the time to total spread can be upper and lower bounded as follows:

$$\frac{\sqrt{n}}{qn^\varepsilon} < \bar{T}_{2,q}(\mathcal{C}_{1,2/n}) < \frac{4\sqrt{n}}{q}(\log \log n)^2.$$

We conclude that for large enough q_n , contagion spreads faster in $\mathcal{C}_{1,2/n}$. Hence, when there is a high enough (but vanishing with increasing n) probability of simple contagion adoptions along the cycle edges, the rewiring of even \mathcal{C}_2 edges will speed up the spread of noisy complex contagions.

S4.1 Lower bound on $\bar{T}_{2,q}(\mathcal{C}_{1,2/n})$

Throughout the subsequent discussion, we denote by I_t the number of infected nodes by time t .

Theorem 12 (Upper-bounding the number of infected nodes in $o(\sqrt{n}/q_n)$ steps). *For $t = o(\sqrt{n}/q_n)$, with high probability as $n \rightarrow \infty$, $I_t = o(\sqrt{n})$.*

Proof of Theorem 12. Let \mathcal{B}_t be the largest interval on \mathcal{C}_1 containing the initial seed nodes and the neighboring nodes infected by simple contagion along the cycle in time t . Denoting the size of this set by B_t , note that B_t is increasing in t , $B_0 = 2$ and $B_t \rightarrow n$ with probability one as $t \rightarrow \infty$. The proof of Theorem 12 is complete given the following lemma.

Lemma 13 (Initial Simple Contagion Phase). *For $t = o(\sqrt{n}/q_n)$, with high probability as $n \rightarrow \infty$, $B_t = o(\sqrt{n})$ and none of the nodes outside \mathcal{B}_t are infected.*

We prove the preceding assertion in the rest of this subsection. □

To prove Lemma 13, we will utilize the following lower tail bound on negative binomial random variables.

Lemma 14 (Lower Tail Bounds for Geometric Variables). *Let $\mathbf{g}_i, i = 1, \dots, n$ be a sequence of i.i.d. geometric variables with mean $1/\hat{q}_n$, $\hat{x} = \hat{q}_n t$ and consider $\mathbf{G}(\hat{x}) := \sum_{i=1}^{\lfloor \hat{x} \rfloor} \mathbf{g}_i$. If $t\hat{q}_n \rightarrow \infty$ as $n \rightarrow \infty$, then $\mathbf{G}(\hat{x}) > t/2$ with high probability.*

Proof of Lemma 14. Let Y_1, Y_2, \dots be a sequence of i.i.d. Bernoulli variables with success probability \hat{q}_n . Then $\mathbf{G}(\hat{x})$ has the same (negative binomial) distribution as the smallest j such that exactly $\lfloor \hat{x} \rfloor$ of Y_1, \dots, Y_j are one (see, e.g., [29]). In particular, $\mathbf{G}(\hat{x}) < t/2$ if, and only if, $\sum_{i=1}^{\lfloor t/2 \rfloor} Y_i > \hat{x} = \hat{q}_n t$. We can bound the probability of the latter event by a simple application of Markov inequality for the sum of i.i.d. Bernoulli variables:

$$\mathbb{P} \left\{ \sum_{i=1}^{\lfloor t/2 \rfloor} Y_i > \hat{q}_n t \right\} \leq \frac{\mathbb{E} \left\{ \left(\sum_{i=1}^{\lfloor t/2 \rfloor} Y_i \right)^2 \right\}}{\hat{q}_n^2 t^2} = \frac{(t/2)\hat{q}_n}{\hat{q}_n^2 t^2} = \frac{1}{2t\hat{q}_n} = o(1).$$

Hence, $\mathbb{P}\{\mathbf{G}(\hat{x}) \geq t/2\} \rightarrow 1$ as $n \rightarrow \infty$, completing the proof. □

Armed with Lemma 14, we can now establish Lemma 13.

Proof of Lemma 13. Let $t = o(\sqrt{n}/q_n)$ and consider the spread of simple contagion along the \mathcal{C}_1 edges up to time t . Starting from two adjacent seeds, the time for the simple contagion to spread to either neighboring node is a geometric random variable with mean $1/q_n$. In particular, the time that it takes until the first of the two nodes (at either sides of the two adjacent initial seeds) gets infected is the minimum of two i.i.d. geometric mean $1/q_n$ variables, which is another geometric variable with success probability $\hat{q}_n = 1 - (1 - q_n)^2 = (2 + o(1))q_n$. To upper-bound the number of simple infections up to time $t = o(\sqrt{n}/q_n)$ we can consider a sped up infection process whereby whenever the first of the two nodes at either side of the infected

interval is infected we force the second one to be infected as well. Denote the infected interval that results from this sped-up simple infection process by $\hat{\mathcal{B}}_t$, set $\hat{B}_t = |\hat{\mathcal{B}}_t|$ and observe that $B_t < \hat{B}_t$ for all t . First, we show that $\hat{B}_t = o(\sqrt{n})$ for $t = o(\sqrt{n}/q_n)$. To this end, let $\mathbf{g}_i, i = 1, \dots, n$ be a sequence of i.i.d. geometric variables with mean $1/\hat{q}_n$, and $\mathbf{x}^* := \sup\{x : \sum_{i=1}^x \mathbf{g}_i < t\}$. The random variable \mathbf{x}^* measures the growth of $\hat{\mathcal{B}}_t$ at both ends until time t ; hence, $\hat{B}_t = 2 + 2\mathbf{x}^*$. Let $\hat{x} = 2\hat{q}_n t$ and consider $\mathbf{G}(\hat{x}) := \sum_{i=1}^{\lfloor \hat{x} \rfloor} \mathbf{g}_i$. Lemma 14 implies that $\mathbf{G}(\hat{x}) > t$ with high probability whenever $tq_n \rightarrow \infty$ as $n \rightarrow \infty$. Thus $B_t < \hat{B}_t = 2 + 2\mathbf{x}^* < 2 + 2\hat{x} = 2 + 4t\hat{q}_n = o(\sqrt{n})$ with high probability when $t\hat{q}_n = \omega(1)$. The case $t\hat{q}_n = O(1)$ follows from the monotonicity of B_t . So far we have shown that, in $t = o(\sqrt{n}/q_n)$ steps, with high probability simple contagion spreads to at most $o(\sqrt{n})$ nodes belonging to \mathcal{B}_t . This implies that there exists a sequence $a_n = o(\sqrt{n})$ such that $\mathbb{P}(B_t < a_n) = 1 - o(1)$. Now, conditional on $\{B_t < a_n\}$, note that for contagion to spread to some node outside of \mathcal{B}_t , there has to be at least one node outside of \mathcal{B}_t that has at least two long ties to the nodes inside \mathcal{B}_t . Therefore

$$\begin{aligned} & \mathbb{P}\{\text{Some node outside } \mathcal{B}_t \text{ is infected}\} \\ & \leq \mathbb{P}\{\text{Some nodes outside } \mathcal{B}_t \text{ has two long-tie to the nodes inside}\} \\ & \leq \mathbb{P}\{\text{Bin}(n - B_t, \mathbb{P}[\text{Bin}(B_t, 2/n) \geq 2]) \geq 1\} = O\left((n - B_t) \frac{4B_t^2}{n^2}\right) = o(1). \end{aligned}$$

Hence for $t = o(\sqrt{n}/q_n)$, with high probability all infected nodes belong to \mathcal{B}_t , and $\mathcal{I}_t = \mathcal{B}_t$. This completes the proof. \square

S4.2 Upper bound on $\bar{T}_{2,q}(\mathcal{C}_{1,2/n})$

The next result derives an upper bound on the infection time of all nodes in the graph. Some aspects of the proof are similar to that of Theorem 8.

Theorem 15. *With high probability as $n \rightarrow \infty$, $\bar{T}_{2,q}(\mathcal{C}_{1,2/n}) \leq 3(\sqrt{n}/q_n)(\log \log n)^2(1 + o(1))$.*

Proof of Theorem 15. As in the proof of Theorem 8, we devise an algorithm to lower bound the initial growth of the set of infected nodes. Next, we divide the cycle into consecutive intervals of length $L_n = \sqrt{n}(\log \log n)^3$. Call an interval *active* if it contains an infected node. Initially, declare the interval containing the original seed nodes, an active interval. Starting with the initial seed nodes, after $E_n = (2\sqrt{n}/q_n) \log \log n$ steps the length of the original interval grows to at least $\sqrt{n} \log \log n$ with high probability. In general, with high probability as $n \rightarrow \infty$, over the first $O(\log \log n)$ iterations of this algorithm, after each epoch with $E_n = (2\sqrt{n}/q_n) \log \log n$ time steps, the length of the infected segments in each active interval will grow at least $\sqrt{n} \log \log n$ due to the simple contagion along the cycle. By revealing the edges of $\mathcal{G}_{n,2/n}$ that are incident to the newly infected nodes at the end of each E_n -step epoch, we can identify new active intervals that will, in turn, grow and activate other intervals. Formally, we consider the following algorithm to undercount the number of infected nodes. Denote by X_τ the number of active intervals after τ epochs of length E_n each.

Algorithm 3 Super-Exponential Activation Growth

Input: Random graph model $\mathcal{C}_{1,2/n}$.

- 1: Initialize: Set $N_n = \sqrt{n}/(\log \log n)^3$. Divide the cycle into N_n intervals of length $L_n = \sqrt{n}(\log \log n)^3$ each, and label them by $[N_n] = \{1, 2, \dots, N_n\}$; let the initial seed nodes be contained in the interval that is labeled one: $\mathcal{X}_0 = \{1\}$.
 - 2: **for** $\tau \geq 1$ **do**
 - 3: Wait for an epoch of length $E_n = 2(\sqrt{n}/q_n) \log \log n$, and track the growth of infected nodes along \mathcal{C}_1 by simple contagion during this epoch.
 - 4: Add edges independently with probability $2/n$ connecting the newly infected nodes to the uninfected nodes.
 - 5: Update the set of active intervals by adding all intervals that have new infected nodes in them: $\mathcal{X}_\tau \leftarrow \mathcal{X}_{\tau-1}$.
 - 6: **end for**
-

We first establish that for the first $O(\log \log n)$ rounds of the preceding algorithm, at least $\sqrt{n} \log \log n$ new nodes are infected over each $E_n = (2\sqrt{n}/q_n) \log \log n$ epoch.

Lemma 16. *Fix $\tau_n = \frac{1}{\log 2}(1 + o(1)) \log \log n$. With high probability as $n \rightarrow \infty$, every active interval gains at least $\sqrt{n} \log \log n$ new infected nodes over each of the first τ_n epochs of length $E_n = (2\sqrt{n}/q_n) \log \log n$.*

The next lemma derives a lower bound on the number of active intervals after $O(\log \log n)$ steps.

Lemma 17 (Initial Growth of the Intervals). *For any $C > 0$, there exists a sequence $t_n := t_n(C) = o(\log \log n)$ such that for*

$$\tau_n = \frac{1}{\log 2} \left(\log \log n + t_n \right),$$

with high probability as $n \rightarrow \infty$, $X_{\tau_n} \geq Cn^{1/4} \sqrt{\log n}$.

By Lemmas 16 and 17, for $C > 1$ we can choose $\tau_n(C) = (\log \log n / \log 2)(1 + o(1))$ to get at least $X_{\tau_n} \sqrt{n} \log \log n \geq Cn^{3/4} (\log n)^{1/2} (\log \log n)$ infected nodes, with high probability as $n \rightarrow \infty$, in time $T_n = \tau_n E_n = (2/\log 2)(1 + o(1)) \sqrt{n} (\log \log n)^2 / q_n < (3\sqrt{n}/q_n) (\log \log n)^2$. Finally, the next result states that with high probability, the contagion process spreads to the whole graph in time $T_n + 1 + 2\sqrt{n}/q_n$, completing the proof.

Lemma 18 (End Regime). *Let T_n be the first time that at least $Cn^{3/4} \sqrt{\log n}$ nodes are infected, where $C > 1$ is a universal constant. Then with high probability, all nodes are infected by time $T_n + 1 + 2\sqrt{n}/q_n$.*

We turn to the proofs of Lemmas 16 to 18 in the remainder of this subsection. □

Proof of Lemma 16. We begin with the observation that the waiting time for an activated interval to gain at least $\sqrt{n} \log \log n$ new nodes via simple contagion is a sum of $\sqrt{n} \log \log n$ i.i.d. Geometric random variables, each with mean $1/q_n$. Let $\{\mathbf{g}_1, \mathbf{g}_2, \dots\}$ be a sequence of i.i.d. Geometric random variables with mean $1/q_n$. Thus during an epoch of length $E_n = (2\sqrt{n}/q_n) \log \log n$, an activated interval fails to gain at least $\sqrt{n} \log \log n$ new infected nodes via simple contagion along the circle if $\sum_{i=1}^{\sqrt{n} \log \log n} \mathbf{g}_i > 2\sqrt{n} \log \log n / q_n$. Next consider the following Chernoff bound on the upper tail of the sum of i.i.d. geometric random variables [29, Theorem 1.14]):

$$\mathbb{P}\left[\mathbf{G}(m) > (1 + \delta)\mathbb{E}[\mathbf{G}(m)]\right] \leq \exp\left(-\frac{\delta^2(m-1)}{2(1+\delta)}\right), \quad (\text{S.2})$$

where $\mathbf{G}(m) := \sum_{i=1}^m \mathbf{g}_i$. Replacing $\delta = 1$ and $m = \sqrt{n} \log \log n$ in (S.2) yields:

$$\mathbb{P}\left[\mathbf{G}(\sqrt{n} \log \log n) > E_n\right] \leq \exp\left(-\frac{\sqrt{n} \log \log n - 1}{4}\right).$$

Note that at each epoch, there are at most $N = \sqrt{n}/(\log \log n)^3 < \sqrt{n}$ active intervals. Thus a direct union bound argument over $O(\log \log n)$ rounds of the algorithm establishes that with high probability, each activated interval gains the desired number of infected nodes at each epoch. It is implicit in the calculation above that the infection of new nodes is sustained as long as an active interval is not exhausted (does not run out of nodes). To show this sustained growth, we need to upper-bound the number of new active nodes that an interval gains during each epoch of length E_n . Note that an interval gains more than $M\sqrt{n} \log \log n$ nodes in an epoch of length E_n if, and only if, $\mathbf{G}(M\sqrt{n} \log \log n) < E_n$. An upper bound on the lower tail probability of the sum of geometric variables help us ensure the latter event is unlikely and the simple contagion growth of the intervals can be sustained during the first τ_n intervals. We use the following upper bound on the lower tail probability of the sum of m' i.i.d. geometric variables with mean $1/q_n$ [30, Theorem 3.1]:

$$\mathbb{P}\left[\mathbf{G}(m') \leq \lambda \mathbb{E}[\mathbf{G}(m')]\right] \leq \exp\left(-q_n \mathbb{E}[\mathbf{G}(m')](\lambda - 1 - \log \lambda)\right), 0 < \lambda < 1. \quad (\text{S.3})$$

To upper bound the probability that an active interval gains more than $M\sqrt{n} \log \log n$ new infected nodes over an epoch of length E_n , we set

$$\begin{aligned} m' &= M\sqrt{n} \log \log n, \\ \mathbb{E}[\mathbf{G}(m')] &= (M/q_n)\sqrt{n} \log \log n, \\ \lambda &= E_n/\mathbb{E}[\mathbf{G}(m')] = 2/M, \end{aligned}$$

in (S.3) to obtains:

$$\mathbb{P}\left[\mathbf{G}(M\sqrt{n} \log \log n) \leq E_n\right] \leq \exp\left(- (M\sqrt{n} \log \log n)(2/M - 1 - \log(2/M))\right).$$

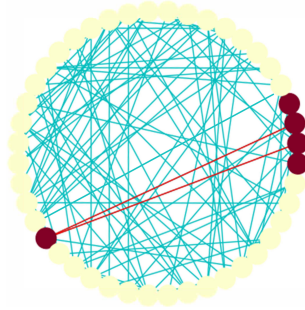


Figure S5: Strength of long ties for the spread of noisy complex contagion when there are no redundant ties ($\mathcal{C}_{1,2/n}$ and \mathcal{C}_2). Centola and Macy propose the *weakness* of long ties for propagating complex contagions by pointing out that if there are no “redundant” ties along the local structure of the ring (e.g., when spreading deterministic 2-complex contagion on \mathcal{C}_2), then every short tie that is removed and replaced by a random, long tie creates a break along the ring [13, pages 716-717]. Here, we propose a counter-argument for the *strength* of long ties in propagating *noisy* complex contagions even when there are no redundant ties along the ring lattice (comparing the rate of spread of noisy 2-complex contagion over $\mathcal{C}_{1,2/n}$ and \mathcal{C}_2). We show that a pair of long ties are likely to form a bridge, as shown in the figure, to pass the complex contagion across $\mathcal{C}_{1,2/n}$ while contagion propagates slowly, locally along the ring. The local growth of contagion along the ring is slow because we assume only a small probability (q) of adoptions below threshold so that the expected wait time for the contagion to pass through each link along the ring ($1/q$) is large. We show that an active interval of length $\sqrt{n} \log \log n$ on $\mathcal{C}_{1,2/n}$ is large enough to produce a pair of long ties that are incident to same node across the circle to pass the complex contagion with high probability as $n \rightarrow \infty$. Subsequently, the spread time of noisy 2-complex contagion along $\mathcal{C}_{1,2/n}$ can, with high probability, be upper-bounded as $O(\frac{\sqrt{n}}{q_n} (\log \log n)^2)$ which for $q_n = \omega(1/\sqrt{n})$ is $o(n)$, which is strictly faster than the at least $\lfloor n/4 \rfloor$ time that it takes for the noisy 2-complex contagion to spread on \mathcal{C}_2 ; see also Figure 2 caption.

Thus for $M > 1$ sufficiently large, by union bound over the $N_n = \sqrt{n}/(\log \log n)^3$ intervals in $\tau_n = (1/\log 2) \log \log n(1 + o(1))$ epochs of length E_n each, we can guarantee that in each epoch, no active interval gains more than $M\sqrt{n} \log \log n$ many new nodes by simple infection. Hence, no active interval is exhausted in the first $\tau_n = (1/\log 2) \log \log n(1 + o(1))$ rounds with high probability as $n \rightarrow \infty$ since $L_n = \sqrt{n}(\log \log n)^3 \gg \tau_n M\sqrt{n} \log \log n$. This completes the proof. \square

Given Lemma 16, we can now prove Lemma 17.

Proof of Lemma 17. Let us use $\{\mathcal{F}_\tau : \tau \geq 1\}$ to denote the natural filtration associated with Algorithm 3. Note that at the end of $\tau - 1$ steps, we have $X_{\tau-1}$ active intervals, and thus $N - X_{\tau-1}$ non-active intervals. Each non-active interval is activated if at least one of its nodes

has two infected neighbors in Algorithm 3 described above (Figure S5). The independence of the added edges implies that given $\mathcal{F}_{\tau-1}$, we have,

$$X_\tau = X_{\tau-1} + \text{Bin}(N - X_{\tau-1}, p_\tau), \quad (\text{S.4})$$

where p_τ is the conditional probability (given $\mathcal{F}_{\tau-1}$) that an interval is activated by the edge exposure operation in Algorithm 3. Let \mathcal{E} denote the “good” event that each active interval has gained at least $\sqrt{n} \log \log n$ new infected nodes during each epoch of length $2\sqrt{n} \log \log n / q_n$ up to the τ^{th} round. Observe that Lemma 16 implies that $\mathbb{P}(\mathcal{E}) = 1 - o(1)$. Now, given $\mathcal{F}_{\tau-1}$, we can lower bound p_τ on the event \mathcal{E} as follows:

$$\begin{aligned} p_\tau &\geq \mathbb{P}\left[\text{Bin}\left(L, \mathbb{P}\left[\text{Bin}\left(X_{\tau-1}\sqrt{n} \log \log n, \frac{2}{n}\right) \geq 2\right]\right) \geq 1\right] \\ &\geq 2LX_{\tau-1}^2 \frac{(\log \log n)^2}{n}. \end{aligned} \quad (\text{S.5})$$

On the event that $X_{\tau-1} > \varepsilon N_n$ for some $\varepsilon > 0$, the claim is automatically satisfied: $X_{\tau_n} > \varepsilon N_n = \varepsilon \sqrt{n} / (\log \log n)^3 \gg Cn^{1/4} (\log n)^{1/2}$, as $n \rightarrow \infty$. Thus we shift attention to the event that $X_{\tau-1} \leq N_n \varepsilon_n$ where $\varepsilon_n \rightarrow 0$ as $n \rightarrow \infty$. Taking expectations of both sides in (S.4) and applying the lower bound in (S.5), on the event $\{X_{\tau-1} \leq N \varepsilon_n\} \cap \mathcal{E}$, we have:

$$\mathbb{E}[X_\tau - X_{\tau-1}] \geq X_{\tau-1}^2 (\log \log n)^2.$$

Note from (S.4) that X_τ can be expressed as sum of independent binomial random variables. Using Bernstein’s inequality, for some universal constant $c_0 > 0$ with probability at least $1 - 2 \exp(-c_0 (\log \log n)^2)$, we have:

$$X_\tau \geq X_{\tau-1}^2 \left(\frac{\log \log n}{2}\right)^2. \quad (\text{S.6})$$

Let us choose $\tau_n = \frac{\log \log n + t_n}{\log 2}$ for some sequence $t_n = t_n(C) = o(\log \log n)$. Then using union bound, the probability that we do not have the desired growth in the number of infected intervals in at least one of the rounds may be upper bounded by $\tau_n \exp(-c_0 (\log \log n)^2)$. We note that the probability of this bad event is $o(1)$. Moreover, on the complement of this event, we have, $X_{\tau_n} \geq \left(\frac{\log \log n}{2}\right)^{2\tau}$. We choose t_n appropriately such that $X_{\tau_n} \geq Cn^{1/4} \sqrt{\log n}$. This establishes the desired lower bound on the number of infected nodes in the first τ rounds. \square

Finally we establish Lemma 18.

Proof of Lemma 18. For a node x , let \mathcal{L}_x denote the interval of length \sqrt{n} on the cycle centered at x . We will show that with high probability, for each x , \mathcal{L}_x contains at least one infected node by time $T_n + 1$. This implies that with high probability, all nodes will be infected by time $T_n + 1 + 2\sqrt{n}/q_n$ due to simple contagion along the cycle. This last assertion follows using

upper tail concentration for a sum of geometric random variables and union bound, exactly as described in the proof of Lemma 16. Thus we will omit this step in the subsequent argument.

By time T_n , we have at least $Cn^{3/4}\sqrt{\log n}$ infected nodes. Let A_x denote the event that none of the nodes in \mathcal{L}_x are infected by time $T_n + 1$. If any of these infected nodes fall in \mathcal{L}_x then we are done. If not, then for any fixed x , \mathcal{L}_x has \sqrt{n} nodes; and the probability that each such node has less than two infected neighbors is at most $\mathbb{P}\left[\text{Bin}(Cn^{3/4}\sqrt{\log n}, \frac{2}{n}) < 2\right]$. Using independence of the edges in $\mathcal{G}_{n,2/n}$, the probability of the event A_x that none of the nodes in \mathcal{L}_x is infected by time $T_n + 1$ is upper-bounded as follows:

$$\begin{aligned}\mathbb{P}(A_x) &\leq \mathbb{P}\left[\text{Bin}(Cn^{3/4}\sqrt{\log n}, \frac{2}{n}) < 2\right]^{\sqrt{n}} \\ &\leq \left(1 - \mathbb{P}\left[\text{Bin}(Cn^{3/4}\sqrt{\log n}, \frac{2}{n}) = 2\right]\right)^{\sqrt{n}} \\ &\leq n^{-C^2}.\end{aligned}\tag{S.7}$$

Finally, a union bound over all nodes on the cycle completes the proof, as $n \cdot n^{-C^2} \rightarrow 0$ with $n \rightarrow \infty$ for $C > 1$. \square

S4.3 Adoption probabilities under logit and probit activation functions

Here we derive the corresponding conditions on the parameters of the logit and probit functions to ensure that $q = \omega(1/\sqrt{n})$ under these classes of activation functions (Figure S6).

Consider a probit activation function such that the probability of adoptions when the number of infected neighbors is x is given by:

$$\Phi_{\theta, \sigma_n}(x) = \int_{-\infty}^{\frac{x-\theta}{\sigma_n}} \frac{1}{\sqrt{2\pi}} e^{-t^2/2} dt$$

We are interested in the asymptotic regime $\sigma_n \rightarrow 0$ as $n \rightarrow \infty$. We choose $\theta = 1.5$ to ensure a high probability of adoption with two infected neighbors and a low (but non-zero) adoption probability with only one infected neighbor (Figure S6). There is no adoption when there are no infections in the agent's neighborhood. The probability of adoptions below threshold is given by:

$$\hat{q}_n = \Phi_{1.5, \sigma_n}(1) = \int_{-\infty}^{-\frac{1}{2\sigma_n}} \frac{1}{\sqrt{2\pi}} e^{-t^2/2} dt = \int_{\frac{1}{2\sigma_n}}^{+\infty} \frac{1}{\sqrt{2\pi}} e^{-t^2/2} dt$$

Using the Gaussian tail bounds for $x > 0$,

$$\frac{1}{\sqrt{2\pi}} \frac{x}{x^2 + 1} e^{-x^2/2} \leq \int_x^{\infty} \frac{1}{\sqrt{2\pi}} e^{-t^2/2} dt \leq \int_x^{\infty} \frac{t}{x} \frac{1}{\sqrt{2\pi}} e^{-t^2/2} dt = \frac{e^{-x^2/2}}{x\sqrt{2\pi}},$$

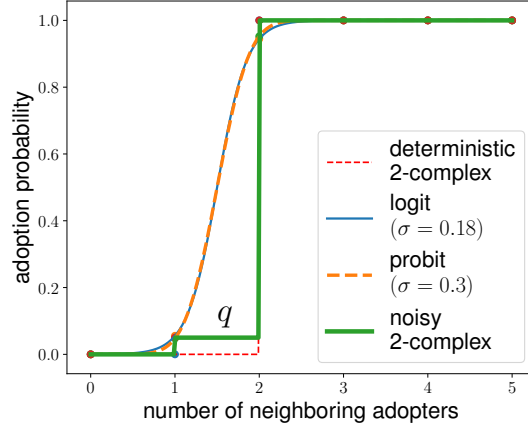


Figure S6: Probit and Logit Activation Functions. A noisy threshold-based contagion model allows for a non-zero probability ($q > 0$) of adoptions below threshold. In a probit activation function the probability of adoption with x adopters in the social neighborhood is equal to $\Phi_{\theta,\sigma}(x)$, where $\Phi_{\theta,\sigma}(\cdot)$ is the normal CDF with mean θ and standard deviation σ . The logit activation function is given by $\Psi_{\theta,\sigma}(x) = (1 + e^{(\theta-x)/\sigma})^{-1}$. Both functions describe a noisy threshold response that converges to a deterministic threshold θ as $\sigma \rightarrow 0$.

we get

$$\frac{e^{-1/8\sigma_n^2}}{\sqrt{2\pi}} \left(\frac{2\sigma_n}{1 + 4\sigma_n^2} \right) \leq \hat{q}_n \leq 2\sigma_n \frac{e^{-1/8\sigma_n^2}}{\sqrt{2\pi}},$$

Hence,

$$\hat{q}_n = \Theta \left(2\sigma_n e^{-1/8\sigma_n^2} \right),$$

In particular, taking $\sigma_n = 1/\sqrt{8 \log n^\alpha}$ yields that

$$\hat{q}_n = \Theta \left(\frac{n^{-\alpha}}{\sqrt{2 \log n^\alpha}} \right),$$

Hence, $\hat{q}_n = o(n^{-1/2})$ for $\alpha \geq 1/2$ and $\hat{q}_n = \omega(n^{-1/2})$ for $\alpha < 1/2$.

We can repeat the same calculations when the activation functions are specified by a logistic function:

$$\Psi_{\theta,\sigma_n}(x) = \frac{1}{1 + e^{(1/\sigma_n)(\theta-x)}}.$$

The probability of adoptions below threshold for logistic activation functions is given by:

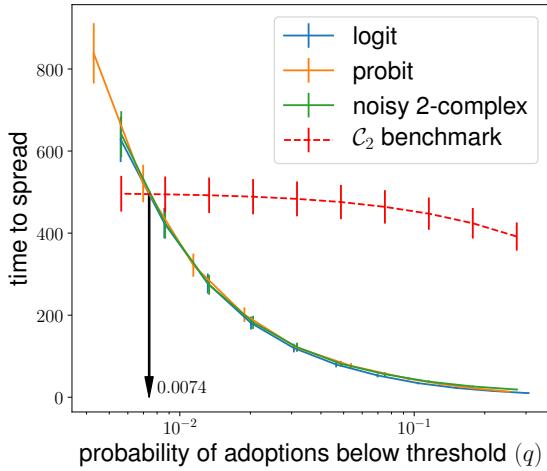
$$\tilde{q}_n = \Psi_{1.5, \sigma_n}(1) = \frac{1}{1 + e^{(1/2)\sigma_n}} = \Theta(e^{-1/2\sigma_n}).$$

for $\sigma_n \rightarrow 0$ as $n \rightarrow \infty$. Choosing $\sigma_n = \frac{1}{2\log(n^\alpha)}$ yields $\tilde{q}_n = \Theta(n^\alpha)$: $\tilde{q}_n = o(n^{-1/2})$ for $\alpha > 1/2$ and $\tilde{q}_n = \omega(n^{-1/2})$ for $\alpha < 1/2$.

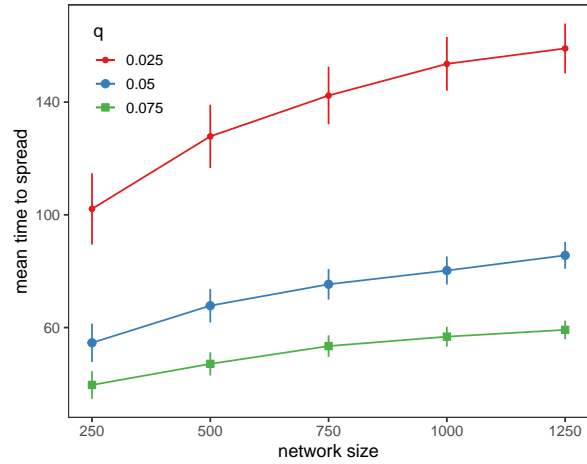
Note that $\Phi_{\theta, \sigma}(0) > 0$ and $\Psi_{\theta, \sigma}(0) > 0$; hence, the logit and probit activation functions allow for a small probability of "spontaneous" adoptions even when there are no infected neighboring nodes.

Theorems 6 and 8 characterize the time needed for all nodes to be infected by deterministic 2-complex contagion on $\mathcal{C}_{2,2/n}$. In comparison, pure complex 2-contagion on \mathcal{C}_4 requires $\Theta(n)$ time to infect all nodes, although the average degree is the same in the two cases. One could naturally envision obtaining $\mathcal{C}_{2,2/n}$ by a "rewiring" of the edges in \mathcal{C}_4 , and thus from a network intervention viewpoint, the result strongly suggests the usefulness of increasing long ties to speed up the deterministic complex contagion procedure. However, any further rewiring destroys the 2-core necessary for the spread of deterministic 2-complex contagion, and thus will actually stall the infection procedure. Theorems 12 and 15 amend this picture to conclude that in presence of a small probability of adoption below threshold (i.e., noisy 2-complex contagion), the inclusion of long ties significantly speeds up the adoption procedure even when the \mathcal{C}_2 edges are replaced.

In Figure S7A we present the simulation results for the spreading time of complex contagion over $\mathcal{C}_{1,2/n}$, with $n = 1000$, for various values of simple contagion probability q . We use three activation functions: logit, probit, and modified threshold with non-zero probability (q) of adoptions below threshold. Indeed, logit and probit functions even allow for spontaneous adoptions (when there are no infected neighbors). Moreover, the probability of adoptions above threshold in case of logit and probit functions is high but less than one (Figure S6). The simulation results show that spread of contagion over $\mathcal{C}_{1,1/n}$ is faster than \mathcal{C}_2 when adoptions below threshold happen with probabilities greater than 0.0074. This is consistent with the predictions of Theorem 1, whereby for $\sqrt{n}q \rightarrow \infty$ the time to spread is $O^*(\sqrt{n}/q) = o(n)$ which is strictly faster than the $\lfloor n/4 \rfloor$ minimum required time for noisy 2-complex contagion to spread over \mathcal{C}_2 ; see Figure 2 caption. In the next section, we adopt a more dynamical viewpoint, and interpolate between \mathcal{C}_2 and $\mathcal{C}_{1,2/n}$.



(A) Spread times versus sub-threshold adoption



(B) Spread time versus network size

Figure S7: Noisy complex contagion spread times versus sub-threshold adoption probabilities (q) and network size (n). (A) The spread time of noisy complex contagion on $\mathcal{C}_{1,2/n}$, $n = 1000$ with different activation functions versus sub-threshold adoption probability (q). The \mathcal{C}_2 benchmark, $T_{2,q}(\mathcal{C}_2)$, is close to $n/2 = 500$ when $q \rightarrow 0$ and decreases slowly as q increases. (B) The spread time of noisy complex contagions on $\mathcal{C}_{1,2/n}$ versus network size (n) for three different values of sub-threshold adoption probability (q). Each point on the plots in figures A and B is the average of 500 random draws. The vertical bars indicate the 95% normal confidence intervals around the means.

S5 Noisy θ -complex contagion

We now briefly consider the general case of noisy θ -complex contagion with sub-threshold adoption probability q to establish Theorem 2 of the main text, i.e., to prove that $T_{\theta,q}(\mathcal{C}_{1,c/n}) < \frac{4n^{1-1/\theta}}{q} (\log \log n)^2$, with high probability as $n \rightarrow \infty$ for $c \geq \theta$ and integers $\theta \geq 2$. We will instead upper bound $\bar{T}_{\theta,q}(\mathcal{C}_{1,c/n})$ which restricts sub-threshold adoptions to the \mathcal{C}_1 edges and is thus strictly slower than $T_{\theta,q}(\mathcal{C}_{1,2/n})$: $T_{\theta,q}(\mathcal{C}_{1,c/n}) \leq \bar{T}_{\theta,q}(\mathcal{C}_{1,c/n})$, everywhere. We will repeat the proof steps in Section S4.2 and adapt them to the general threshold θ case.

The arguments leading to the proof of Theorem 15 remain true for $\theta > 2$ by increasing the epoch length from $E_n = (2\sqrt{n}/q_n) \log \log n$ for noisy 2-complex contagion to $E_{n,\theta} = (2n^{1-1/\theta}/q_n) \log \log n$ for general θ -complex contagion. The reason is that after each epoch of length $E_{n,\theta}$ an active interval will gain at least $\ell_{n,\theta} := n^{1-1/\theta} \log \log n$ new infected nodes through simple contagion with high probability (using concentration bounds on the sum of i.i.d. geometric random variable as in Lemma 16). These $\ell_{n,\theta}$ many new active nodes are enough to generate a new infected node at a random location on the cycle through θ -complex contagion with high probability because $\mathbb{P}[\text{Bin}(\ell_{n,\theta}, c/n) \geq \theta] \gg 1/n$. Similarly, interval length L_n in Algorithm 3 need to be increased to $L_{n,\theta} = n^{1-1/\theta} (\log \log n)^3$. This length provides enough nodes within each interval to ensure that with high probability none of the

$N_{n,\theta} = n/L_{n,\theta} = \sqrt[\theta]{n}/(\log \log n)^3$ intervals are exhausted by (i.e., ran out of nodes for) simple contagion growth as we iterate through the epochs of Algorithm 3; $\tau = 1, 2, \dots, \tau_{n,\theta}$. In the sequel, we choose $\tau_{n,\theta} = \frac{1}{\log \theta}(1 + o(1)) \log \log n$ to ensure enough intervals are activated during the super-exponential growth phase of Algorithm 3 so that we can later repeat an end-regime analysis similar to Lemma 18 in Section S4.2 (see Lemma 21 below).

The geometric wait times to gain $\ell_{n,\theta}$ new nodes during each epoch of length $E_{n,\theta}$ via simple contagion in Lemma 16 remains true with minor modifications: using $m = \ell_{n,\theta}$ in (S.2) and $m' = M\ell_{n,\theta}$ in (S.3) with $E_{n,\theta}$ instead of E_n all the steps in the proof of Lemma 16 remains valid. In particular, with high probability as $n \rightarrow \infty$, every activated interval gains at least $\ell_{n,\theta}$ — and no more than $M\ell_{n,\theta} \ll L_{n,\theta}$ — new infected nodes over each of the first $\tau_{n,\theta}$ epochs of length $E_{n,\theta}$ in Algorithm 3. We thus obtain the following variation of Lemma 16 in the general threshold θ case:

Lemma 19. *Fix $\tau_{n,\theta} = \frac{1}{\log \theta}(1 + o(1)) \log \log n$. With high probability as $n \rightarrow \infty$, every active interval gains at least $\ell_{n,\theta}$ new infected nodes over each of the first $\tau_{n,\theta}$ epochs of length $E_{n,\theta}$ in Algorithm 3.*

We now proceed to establish the super-exponential growth rate of the number of activated intervals (X_τ) during the initial $\tau_{n,\theta}$ iterations of Algorithm 3 with $L_{n,\theta}$, $E_{n,\theta}$ and $N_{n,\theta} = n/L_{n,\theta} = \sqrt[\theta]{n}/(\log \log n)^3$ replacing L_n , E_n and N_n in the general threshold θ case; and in step 5, each non-active interval is activated if at least one of its nodes has θ infected neighbors. The super exponential growth dynamics can be described similarly to (S.4):

$$X_\tau = X_{\tau-1} + \text{Bin}(N_{n,\theta} - X_{\tau-1}, p_{\tau,\theta}), \tau = 1, \dots, \tau_{n,\theta} \quad (\text{S.8})$$

but the lower bound in (S.5) should be modified as follows:

$$\begin{aligned} p_{\tau,\theta} &\geq \mathbb{P}\left[\text{Bin}\left(L_{n,\theta}, \mathbb{P}\left[\text{Bin}\left(X_{\tau-1}\ell_{n,\theta}, \frac{c}{n}\right) \geq \theta\right]\right) \geq 1\right] \\ &\geq c^\theta L_{n,\theta} X_{\tau-1}^\theta \frac{(\log \log n)^\theta}{n(\theta!)} (1 - o(1)) \\ &\geq \left(\frac{c}{\theta}\right)^\theta L_{n,\theta} X_{\tau-1}^\theta \frac{(\log \log n)^\theta}{n} \\ &\geq L_{n,\theta} X_{\tau-1}^\theta \frac{(\log \log n)^\theta}{n}, \end{aligned} \quad (\text{S.9})$$

for θ fixed, $c \geq \theta$, and using the fact that each active interval gains at least $\ell_{n,\theta}$ new infected nodes during the first $\tau_{n,\theta}$ epochs of Algorithm 3 with high probability as $n \rightarrow \infty$ (Lemma 19). We now use the growth dynamics in (S.8) and (S.9) to conclude that $X_{\tau_{n,\theta}} \geq Cn^{1/\theta^2} \sqrt[\theta]{\log n}$ with high probability as $n \rightarrow \infty$, for $\tau_{n,\theta} = (\log \log n + t_n)/\log \theta$ with an appropriate choice of $t_n := t_n(C, \theta) = o(\log \log n)$ given $C > 1$. If $X_{\tau-1} > \varepsilon N_{n,\theta}$ for some $\varepsilon > 0$, then the claim is automatically satisfied: $X_{\tau_{n,\theta}} \geq X_{\tau-1} > \varepsilon N_{n,\theta} = \varepsilon n^{1/\theta}/(\log \log n)^3 \gg Cn^{1/\theta^2} \sqrt[\theta]{\log n}$ as $n \rightarrow \infty$. Thus we shift attention to the case that $X_{\tau-1} \leq N_{n,\theta} \varepsilon_n$ where $\varepsilon_n \rightarrow 0$ as $n \rightarrow \infty$.

By taking expectations of both sides in (S.8), applying the lower bound in (S.9), and using $N_{n,\theta} - X_{\tau-1} = N_{n,\theta}(1 - o(1))$, we obtain:

$$\begin{aligned} \mathbb{E}[X_\tau - X_{\tau-1}] &\geq (N_{n,\theta} - X_{\tau-1})p_{\tau,\theta} \\ &= N_{n,\theta}L_{n,\theta}X_{\tau-1}^\theta \frac{(\log \log n)^\theta}{n}(1 - o(1)) \\ &= X_{\tau-1}^\theta (\log \log n)^\theta (1 - o(1)), \end{aligned}$$

as $n \rightarrow \infty$. The dynamics in (S.8) also implies that X_τ grows as a sum of independent binomial random variables whose deviations can be bounded by Bernstein's inequality:

$$X_\tau \geq X_{\tau-1}^\theta \left(\frac{\log \log n}{2} \right)^\theta, \quad (\text{S.10})$$

for some universal constant $c_0 > 0$ with probability at least $1 - 2 \exp(-c_0(\log \log n)^\theta)$. Using union bound, we can further upper-bound the probability that (S.10) is violated during any of the first $\tau_{n,\theta} = O(\log \log n)$ epochs by $\tau_{n,\theta} \exp(-c_0(\log \log n)^\theta) \rightarrow 0$ as $n \rightarrow \infty$. Moreover, on the complement of this event, we have the super-exponential activation growth: $X_\tau \geq (\log \log n/2)^{\theta^\tau} \gg \theta^{\theta^\tau}$ as $n \rightarrow \infty$. Choosing $\tau_{n,\theta} = \frac{\log \log n + t_n}{\log \theta} = O(\log \log n)$ with

$$\begin{aligned} t_n = t_n(C, \theta) &= \log \log(\sqrt[\theta]{\log n}) + \log(1/\theta^2) + \log \log C - 3 \log \log \theta \\ &= \log \log \log n - 3 \log \theta + \log \log C - 3 \log \log \theta \\ &= o(\log \log n), \end{aligned}$$

yields: $X_{\tau_n} \geq Cn^{1/\theta^2} \sqrt[\theta]{\log n}$, establishing the following variation of Lemma 17 for the initial growth of the intervals during the first $\tau_{n,\theta}$ epochs of noisy θ -complex contagion on $\mathcal{C}_{1,c/n}$:

Lemma 20. *Given $C > 1$, we can choose a sequence $t_n := t_n(C, \theta) = o(\log \log n)$ such that for $\tau_{n,\theta} = (\log \log n + t_n)/\log \theta$, with high probability as $n \rightarrow \infty$, $X_{\tau_n} \geq Cn^{1/\theta^2} \sqrt[\theta]{\log n}$.*

Finally, we can repeat the end regime analysis of Lemma 18 and adapt it to the case of noisy θ -complex contagion: Let $T_{n,\theta}$ be the first time that at least $Cn^{1-1/\theta+1/\theta^2} \sqrt[\theta]{\log n}$ nodes are infected. We can prove that by time $T_{n,\theta} + 1 + 2n^{1-1/\theta}/q_n$ all nodes on the cycle will be infected, with high probability as $n \rightarrow \infty$. We follow the proof steps of Lemma 18. For a node x , let $\mathcal{L}_{x,\theta}$ denote the interval of length $n^{1-1/\theta}$ centered at x on the cycle. We show that with high probability, for each x , $\mathcal{L}_{x,\theta}$ contains at least one infected node by time $T_{n,\theta} + 1$, and hence with high probability, all nodes will be infected by time $T_{n,\theta} + 1 + 2n^{1-1/\theta}/q_n$ due to simple contagion along $\mathcal{L}_{x,\theta}$ — the $(2n^{1-1/\theta}/q_n)$ upper bound on the simple contagion time to infect the entire $\mathcal{L}_{x,\theta}$ interval is by Chernoff bound on the upper tail of the sum of i.i.d. geometric random variables in (S.2), similar to Lemmas 16 and 19. Hence, if there is already an infected node on $\mathcal{L}_{x,\theta}$ for all x , then the proof is complete by the simple contagion noted above. If there is an x with no infections within its $\mathcal{L}_{x,\theta}$ interval at time $T_{n,\theta}$, then $Cn^{1-1/\theta+1/\theta^2} \sqrt[\theta]{\log n}$ infected nodes

that lie outside of $\mathcal{L}_{x,\theta}$ — by assumption at time $T_{n,\theta}$ — are numerous enough to infect at least one of the $n^{1-1/\theta}$ nodes on $\mathcal{L}_{x,\theta}$ with high probability at time $T_{n,\theta} + 1$ by θ -complex contagion. To show this we bound the probability of the complement event, denoted by $A_{x,\theta}$, that every node on $\mathcal{L}_{x,\theta}$ has less than θ neighbors among the $Cn^{1-1/\theta+1/\theta^2} \sqrt[\theta]{\log n}$ infected nodes. Using independence of the random graph connections ($\mathcal{G}_{n,c/n}$) we have:

$$\begin{aligned} \mathbb{P}(A_{x,\theta}) &\leq \left(\mathbb{P} \left[\text{Bin} \left(Cn^{1-1/\theta+1/\theta^2} \sqrt[\theta]{\log n}, \frac{c}{n} \right) < \theta \right] \right)^{n^{1-1/\theta}} \\ &\leq \left(1 - \mathbb{P} \left[\text{Bin} \left(Cn^{1-1/\theta+1/\theta^2} \sqrt[\theta]{\log n}, \frac{c}{n} \right) = \theta \right] \right)^{n^{1-1/\theta}} \\ &\leq \left(1 - C^\theta n^{1/\theta-1} \log n \right)^{n^{1-1/\theta}} \leq n^{-C^\theta}, \end{aligned}$$

for $n \rightarrow \infty$ and $c \geq \theta$. A union bound over all x on the cycle shows that with high probability as $n \rightarrow \infty$, every $\mathcal{L}_{x,\theta}$ interval will include at least one infected node by time $T_{n,\theta} + 1$; and therefor, the entire cycle will be infected by time $T_{n,\theta} + 1 + 2n^{1-1/\theta}/q_n$. Hence, we have the following characterization of the end regime for noisy θ -complex contagion on $\mathcal{C}_{1,c/n}$:

Lemma 21. *Given $C > 1$ if T_n is the first time that at least $Cn^{1-1/\theta+1/\theta^2} \sqrt[\theta]{\log n}$ nodes are infected, then with high probability all nodes are infected by time $T_{n,\theta} + 1 + 2n^{1-1/\theta}/q_n$.*

The super exponential growth in the number of active intervals during the first $\tau_{n,\theta}$ epochs of Algorithm 3 ensures that $\ell_{n,\theta} Cn^{1/\theta^2} \sqrt[\theta]{\log n} = Cn^{1-1/\theta+1/\theta^2} \sqrt[\theta]{\log n} \log \log n$ nodes are infected by time $T_{n,\theta} = \tau_{n,\theta} E_{n,\theta} = 2 \frac{n^{1-1/\theta}}{q_n \log \theta} (1 + o(1)) (\log \log n)^2$ per Lemmas 19 and 20. Subsequently, Lemma 21 implies that all nodes will be infected by time $T_{n,\theta} + 1 + 2n^{1-1/\theta}/q_n < 4 \frac{n^{1-1/\theta}}{q_n} (\log \log n)^2$, establishing Theorem 2 of the main text.

S6 Noisy 2-complex contagion on \mathcal{C}_2^η

The goal of this section is to prove Theorem 3, upper-bounding the spread time of noisy 2-complex contagion on \mathcal{C}_2^η . The latter is an interpolation model between \mathcal{C}_2 and $\mathcal{C}_{1,2/n}$. Formally, \mathcal{C}_2^η is constructed as follows. Consider two random graph processes $\{\mathcal{D}_\eta, \eta \geq 0\}$ and $\{\mathcal{G}_\eta, \eta \geq 0\}$ that are coupled through the common index $\eta \geq 0$. For any fixed $\eta > 0$, the graph processes are distributed as follows.

1. Let $\{X_{ij} : 1 \leq i < j \leq n\}$ be i.i.d. Exponential random variables with rate $1/n^2$. Construct \mathcal{G}_η with node set $[n]$, and for any $i < j$, we add an edge connecting the two nodes if $\{X_{ij} < \eta\}$. Therefore, the random graph \mathcal{G}_η is Erdős-Rényi with edge probability $\mathbb{P}\{X_{ij} < \eta\} = 1 - e^{-\eta/n^2}$.
2. Associate with every edge i, j in $\mathcal{C}_2 \setminus \mathcal{C}_1$ an independent exponential variable Y_{ij} with mean $2n$. Retain edge i, j in $\mathcal{D}_\eta \subset \mathcal{C}_2 \setminus \mathcal{C}_1$ if $Y_{i,j} > \eta$. Thus the probability that the cycle edge i, j is removed is $1 - e^{-\eta/2n}$.

We study the spread of contagion on the interpolated graph $\mathcal{C}_2^\eta := \mathcal{C}_1 \cup \mathcal{G}_\eta \cup \mathcal{D}_\eta$ in the regime $\eta = o(n)$. Note that for $\eta = o(n)$, the expected degree of a node in \mathcal{C}_2^η is

$$\begin{aligned} 2 + (n-3)(1 - e^{-\eta/n^2}) + 2e^{-\eta/n} &= 2 + (n-3) \left(\frac{\eta}{n^2} + o\left(\frac{\eta}{n^2}\right) \right) + 2 \left(1 - \frac{\eta}{2n} + o(\eta/n) \right) \\ &= 4 + o(\eta/n). \end{aligned}$$

Hence, for $\eta = o(n)$ the expected average degree in \mathcal{C}_2^η remain fixed and equal to four, which is the degree of nodes in \mathcal{C}_2 . In this formulation, η is asymptotically twice the expected number of edges that are rewired to construct \mathcal{C}_2^η from \mathcal{C}_2 .

As in Section S4, we upper-bound $\bar{T}_{2,q}(\mathcal{C}_2^\eta)$ by analyzing an auxiliary random variable $\bar{T}_{2,q}(\mathcal{C}_2^\eta)$ that measures the total spread time after blocking all sub-threshold adoptions along the non- \mathcal{C}_1 edges, thus ensuring $T_{2,q}(\mathcal{C}_2^\eta) \leq \bar{T}_{2,q}(\mathcal{C}_2^\eta)$ everywhere. Our findings indicate that initially rewiring slows down the infection process when η is small, whereas after a point, provided q_n is large enough, contagion speeds up with increasing η . For the subsequent analysis, we parametrize $\eta = n^\nu$ and analyze $\bar{T}_{2,q}(\mathcal{C}_2^\eta)$ in two regimes.

- (i) For $\nu \in (0, \frac{1}{2})$ we show that the spreading slows down with increasing ν . Hence, rewiring is detrimental to the spread of contagion. In this regime, it is unlikely that two random edges land on the same “faraway” node. Therefore, complex contagion cannot yet reliably spread through the long ties when $\nu < 1/2$. Under such circumstances, the rewiring only slows down the spread, since it introduces new break points for the spread of complex contagion along the (short) cycle edges. A formal statement is provided in Theorem 24 below.
- (ii) For $1/2 < \nu < 1$ we show that contagion takes $O^*(n^{3/2}/\eta + \sqrt{n}/q_n)$ time to spread. For η large enough, \sqrt{n}/q_n is the dominant term that fixes the spreading speed. Moreover, for $q_n \gg 1/\sqrt{n}$ we can specify a range of η for which increasing η increases the speed, with complex contagion spreading through the long-ties. In particular, if $q_n = n^{-1/2+\epsilon}$, then for $1/2 < \nu < 1/2 + \epsilon$, contagion spreads faster for larger values of η (see Theorem 27 below).

Theorem 22 (Noisy 2-complex contagion over \mathcal{C}_2^η with simple contagion q only along \mathcal{C}_1). *Let $\nu \in (0, 1)$, and consider $\eta = n^\nu$:*

- (i) *If $0 < \nu < \frac{1}{2}$, then, with high probability as $n \rightarrow \infty$:*

$$\frac{n}{2} + \frac{\eta}{4q} < \bar{T}_{2,q}(\mathcal{C}_2^\eta).$$

- (ii) *If $\frac{1}{2} < \nu < 1$, then, for any $\epsilon > 0$, with high probability as $n \rightarrow \infty$:*

$$n^{1/2-\epsilon}/q_n + n^{3/2-\nu-\epsilon} < \bar{T}_{2,q}(\mathcal{C}_2^\eta) < 4(\sqrt{n}/q + n^{3/2-\nu})(\log \log n)^2.$$

S6.1 Lower bound on $\bar{T}_{2,q}(\mathcal{C}_2^\eta)$ for $\eta = o(\sqrt{n})$

We establish a lower bound on the speed of contagion for $\nu \in (0, \frac{1}{2})$ in this section. We need the following preliminary lemmas. For any graph G , let $\deg_{\min}(G)$ denote the minimum degree in G .

Lemma 23 (Unlikely occurrence of complex contagions). *For $\eta = o(\sqrt{n})$, $\mathbb{P}(\deg_{\min}(\mathcal{G}_\eta) \geq 2) = o(1)$.*

Proof of Lemma 23. Note that for any node $i \in [n]$, its degree in the induced subgraph is distributed as $\text{Bin}(n, 1 - e^{-\eta/n^2})$. Thus the probability that a fixed node has degree at least two is

$$\mathbb{P}(\text{Bin}(n, 1 - \exp(-\eta/n^2)) \geq 2) = O\left(\frac{\eta^2}{n^2}\right).$$

Thus the expected number of nodes with degree at least two in the subgraph induced by G_η is $O(\eta^2/n) = o(1)$. This concludes the proof. \square

Armed with this lemma, we can now provide a lower bound on the time to contagion in this regime.

Theorem 24. *If $\eta = o(\sqrt{n})$, then $\bar{T}_{2,q}(\mathcal{C}_2^\eta) \geq \frac{n}{2} + \frac{\eta}{4q_n}$, with high probability as $n \rightarrow \infty$.*

Proof of Theorem 24. Fix $\nu \in (0, \frac{1}{2})$. First, note that the number of edges deleted in $\mathcal{C}_2 \setminus \mathcal{C}_1$ is distributed as $\text{Bin}(n, 1 - \exp(-\frac{\eta}{2n}))$. We denote this number as M_η . Next, observe that Lemma 23 implies that with high probability, none of the nodes may be infected by complex contagion, and the infection has to spread along the cycle. To pass each missing edge in $\mathcal{C}_2 \setminus \mathcal{C}_1$, one incurs an independent $\text{Geo}(q_n)$ waiting time. Setting τ as the time for contagion, we have,

$$\mathbb{P}\left(\tau < \frac{n}{2} + \frac{\eta}{4q_n}\right) \leq \mathbb{P}\left(\sum_{i=1}^{M_\eta} \tau_i - M_\eta < \frac{\eta}{4q_n}\right) \leq \mathbb{P}\left(\sum_{i=1}^{M_\eta} \tau_i < \frac{\eta}{4q_n}(1 + o(1))\right) + o(1),$$

where $\{\tau_i : i \geq 1\}$ are i.i.d. $\text{Geo}(q_n)$ random variables and the second inequality follows since $\mathbb{E}[M_\eta] = \eta/2 = o(\eta/q_n)$. By direct computation

$$\begin{aligned} \mathbb{E}\left[\sum_{i=1}^{M_\eta} \tau_i\right] &= \mathbb{E}[M_\eta]\mathbb{E}[\tau_i] = \frac{\eta}{2q_n}(1 + o(1)). \\ \text{Var}\left[\sum_{i=1}^{M_\eta} \tau_i\right] &= \frac{1}{q_n^2}\text{Var}(M_\eta) + \frac{1 - q_n}{q_n^2}\mathbb{E}[M_\eta] = O\left(\frac{\eta}{q_n^2}\right). \end{aligned}$$

Finally, using Chebyshev's inequality, we have,

$$\mathbb{P}\left(\sum_{i=1}^{M_\eta} \tau_i < \frac{\eta}{4q_n}(1 + o(1))\right) \leq 4 \frac{\text{Var}\left[\sum_{i=1}^{M_\eta} \tau_i\right]}{\mathbb{E}^2\left[\sum_{i=1}^{M_\eta} \tau_i\right]} = O\left(\frac{1}{\eta}\right) = o(1).$$

This completes the proof. \square

Theorem 24 establishes that for $\eta = o(\sqrt{n})$, the infection spread is slowed down due to the missing edges along the cycle.

S6.2 Lower bound on $\bar{T}_{2,q}(\mathcal{C}_2^\eta)$ for $\eta = n^\nu$, $1/2 < \nu < 1$

Let us fix $\nu \in (\frac{1}{2}, 1)$. Let us first concentrate on the spread of infection along the cycle via simple or complex contagion. We initialize the process by infecting two adjacent nodes. The infection spreads via 2-complex contagion until a \mathcal{C}_2 edge is missing, at which point there is a geometric waiting time (with mean $1/q_n$) for simple contagion to pass through the \mathcal{C}_1 edge. Thus to control how many nodes are infected over certain time periods, one needs a good control on the number of missing \mathcal{C}_2 edges in any sub-interval of the cycle. The following lemma provides this necessary control.

Lemma 25. *Consider an interval \mathcal{I} of length L on the cycle. Let $\mathcal{N}(\mathcal{I})$ denote the number of missing \mathcal{C}_2 edges on this segment. For $\lambda \in (0, 1)$*

$$\mathbb{P}\left[|\mathcal{N}(\mathcal{I}) - \mathbb{E}[\mathcal{N}(\mathcal{I})]| > \lambda \mathbb{E}[\mathcal{N}(\mathcal{I})]\right] \leq 2 \exp\left(-\frac{\lambda^2}{3} \mathbb{E}[\mathcal{N}(\mathcal{I})]\right).$$

Proof of Lemma 25. We observe that for any fixed interval \mathcal{I} of length L , the number of missing cycle edges $\mathcal{N}(\mathcal{I}) \sim \text{Bin}(L, 1 - \exp(-\eta/2n))$. The thesis follows by a direct application of Chernoff inequality for Binomial random variable. \square

Given Lemma 25, we can turn to deriving a lower bound on the spreading time for the infection on the cycle.

Theorem 26. *Fix $t = o(\sqrt{n}/q_n + n^{3/2-\nu})$. With high probability as $n \rightarrow \infty$, the number of infected nodes is $o(n^{3/2-\nu})$. Consequently, for any $\varepsilon > 0$ and $1/2 < \nu < 1$, $\bar{T}_{2,q}(\mathcal{C}_2^\eta) > n^{1/2-\varepsilon}/q_n + n^{3/2-\nu-\varepsilon}$, w.h.p. as $n \rightarrow \infty$.*

Proof of Theorem 26. Fix $t = o(\sqrt{n}/q_n + n^{3/2-\nu})$. For any $\varepsilon > 0$, consider an interval of length $L = \varepsilon n^{3/2-\nu}$ centered at the seed nodes. Denote this interval as \mathcal{I} and let $\mathcal{N}(\mathcal{I})$ denote the number of missing cycle edges in this interval. Recalling $\eta = n^\nu$, we observe that $\mathcal{N}(\mathcal{I}) \sim \text{Bin}(L, 1 - \exp(-\eta/2n))$ and thus $\mathbb{E}[\mathcal{N}(\mathcal{I})] = L \frac{\eta}{2n} (1 + o(1)) = \varepsilon \sqrt{n}/2 (1 + o(1))$. Thus, by Lemma 25 we have:

$$\mathbb{P}\left[\mathcal{N}(\mathcal{I}) > \frac{1}{2} \mathbb{E}[\mathcal{N}(\mathcal{I})]\right] \geq 1 - 2 \exp\left(-\frac{\varepsilon}{24} \sqrt{n} (1 + o(1))\right).$$

Hence, with high probability as $n \rightarrow \infty$, $\mathcal{N}(\mathcal{I}) > \varepsilon \sqrt{n}/4$. Note that the waiting time for the simple contagion along the cycle edges to cover the interval \mathcal{I} is distributed as $\sum_{i=1}^{\mathcal{N}(\mathcal{I})} g_i$, where $\{g_i : i \geq 1\}$ are i.i.d. geometric random variables with mean $1/q_n$. For $\nu > 0$ small enough, using [30, Theorem 3.1], we have,

$$\mathbb{P}\left[\sum_{i=1}^{\mathcal{N}(\mathcal{I})} g_i < \nu \frac{\mathcal{N}(\mathcal{I})}{q_n} \mid \mathcal{N}(\mathcal{I})\right] \leq \exp\left(-\frac{\nu}{2} \mathcal{N}(\mathcal{I})\right).$$

Thus with high probability as $n \rightarrow \infty$, for simple contagion along the cycle to cover \mathcal{I} , the waiting time to cross the single edges is at least $\varepsilon\nu\sqrt{n}/4q_n$. Further, Lemma 25 implies that the number of missing \mathcal{C}_2 edges is $O(\sqrt{n} \log n)$ with high probability. As a consequence, with high probability for $\nu < 1$, there are $\varepsilon n^{3/2-\nu} - \mathcal{N}(\mathcal{I}) = \varepsilon n^{3/2-\nu}(1 - o(1)) = \Theta_\varepsilon(n^{3/2-\nu})$ locations on the cycle with no missing \mathcal{C}_2 edges where 2-complex contagion spreads in $\Theta_\varepsilon(n^{3/2-\nu})$ time. Thus in time $t = o(\sqrt{n}/q_n + n^{3/2-\nu})$, with high probability as $n \rightarrow \infty$, contagion along the cycle covers only a subset of the nodes in \mathcal{I} .

Finally, to complete the proof, we show that with high probability as $n \rightarrow \infty$, no nodes outside of \mathcal{I} are infected by 2-complex contagion along the long ties. To this end, note that a node outside of \mathcal{I} is infected if it has at least two edges to the infected nodes in \mathcal{I} . The probability of infection of each node outside \mathcal{I} is thus upper bounded by $\mathbb{P}[\text{Bin}(L, 1 - \exp(-\eta/n^2)) \geq 2]$.

Thus the expected number of infected nodes is at most $n\mathbb{P}[\text{Bin}(L, 1 - \exp(-\eta/n^2)) \geq 2] = O(\varepsilon^2)$. The claim follows using Markov inequality, once we note that $\varepsilon > 0$ is arbitrary. \square

S6.3 Upper bound on $\bar{T}_{2,q}(\mathcal{C}_2^\eta)$ for $\eta = n^\nu, 1/2 < \nu < 1$

The next theorem derives an upper bound to the spreading time for the infection in the regime $\frac{1}{2} < \nu < 1$.

Theorem 27 (High probability upper bound on the spreading time). *Fix $\nu \in (\frac{1}{2}, 1)$. Then with high probability as $n \rightarrow \infty$, all nodes are infected by time $3(\sqrt{n}/q_n + n^{3/2-\nu})(\log \log n)^2(1 + o(1))$. Consequently, $\bar{T}_{2,q}(\mathcal{C}_2^\eta) < 4(\sqrt{n}/q_n + n^{3/2-\nu})(\log \log n)^2$, w.h.p. as $n \rightarrow \infty$.*

Proof of Theorem 27. The proof is similar to that of Theorem 15 and thus we only sketch the proof, focusing on the differences. The proof again proceeds in two stages. In the first stage, we lower bound the growth of infected nodes in the original process and establish that $\Theta(n^{5/4-\nu/2}\sqrt{\log n})$ nodes are infected in $O((n^{3/2-\nu} + \sqrt{n}/q_n) \log \log n)$ steps. An independent argument, in the second stage, establishes that all nodes are infected in $O(n^{3/2-\nu} + \sqrt{n}/q_n)$ additional time. Formally, we establish the following results.

Lemma 28. *For any fixed $\nu \in (\frac{1}{2}, 1)$ and $C > 1$, there exists a sequence $t_n := t_n(C, \nu) = o(\log \log n)$ such that with high probability as $n \rightarrow \infty$, the infection spreads to $Cn^{5/4-\nu/2}\sqrt{\log n}$ nodes in at most $3(n^{3/2-\nu} + \sqrt{n}/q_n) \log \log n(\log \log n + t_n)$ steps.*

Lemma 29. *Let T_n be the first time when the contagion infects $Cn^{5/4-\nu/2}\sqrt{\log n}$ nodes, where $C > 1$ is a universal constant. Then with high probability, all nodes are infected by time $T_n + 2(\frac{\sqrt{n}}{q_n} + n^{3/2-\nu})$.*

The proof follows. \square

Proof of Lemma 28. As before, we divide the node set $[n]$ into N equal intervals of length $L = n^{3/2-\nu}(\log \log n)^3$ each. We call an interval *active* if it contains at least one infected node. At time zero, we call the interval containing the original infected nodes active. We will

undercount the original growth of infected nodes by a more tractable growth process. To this end, we look at the infection process at epochs of size $(n^{3/2-\nu} + \sqrt{n}/q_n) \log \log n$, and index the epochs by $\tau \geq 1$. During each epoch, the active intervals gain new infected nodes due to infections (simple and complex contagions) along the cycle edges. At the end of an epoch, we expose the long range random edges. This in turn, leads to new active intervals, and provides a lower bound on the growth of infected nodes in the original process. We denote the natural filtration associated with the undercounting process as \mathcal{F}_τ , and let X_τ denote the number of active intervals after τ epochs. In each epoch, with high probability, an infected node further infects its neighbor within $2 \log n/q_n$ time. Once we have two neighboring infected nodes, infection spreads along the cycle via simple and complex contagion. Consider the one-sided interval of length $\frac{1}{2}n^{3/2-\nu} \log \log n$ on any active interval (to one side if the infected segment on the active interval). Lemma 25 implies that with (exponentially) high probability, the maximum number of missing cycle edges is $\frac{1}{2}\sqrt{n} \log \log n$. The total weight time to cross these missing edges is $\sqrt{n} \log \log n/q_n$, with (exponentially) high probability. Union bound provides that, with high probability, the contagion process along the cycle infects at least $\frac{1}{2}n^{3/2-\nu} \log \log n$ new nodes in each active interval in each epoch of size $(n^{3/2-\nu} + \sqrt{n}/q_n) \log \log n$. Note that given $\mathcal{F}_{\tau-1}$,

$$X_\tau - X_{\tau-1} = \text{Bin}(N - X_{\tau-1}, p_\tau).$$

where p_τ is the conditional probability of activation of a susceptible interval (i.e., an interval with no active nodes) due to the edge-exposure step at this round. We can lower bound this probability as

$$p_\tau \geq \mathbb{P}\left[\text{Bin}\left(L, \mathbb{P}\left[\text{Bin}\left(\frac{X_{\tau-1}}{2}n^{3/2-\nu} \log \log n, 1 - \exp(-\eta/n^2)\right) \geq 2\right]\right) \geq 1\right].$$

Thus conditional on $\mathcal{F}_{\tau-1}$, we have the lower bound

$$\mathbb{E}[X_\tau - X_{\tau-1}] \geq (N - X_{\tau-1})L\left(\frac{X_{\tau-1}}{2}n^{3/2-\nu} \log \log n\left(\frac{\eta}{n^2}\right)\right)^2 \geq \frac{1}{8}X_{\tau-1}^2(\log \log n)^2$$

Using Bernstein inequality, we can guarantee that this growth is sustained over the first $O(\log \log n)$ epochs leading to $X_{\tau_n} > Cn^{\nu/2-1/4}\sqrt{\log n}$, for $\tau_n = (\log \log n + t_n)/\log 2$ and appropriate choice of $t_n = t_n(C, \nu) = o(\log \log n)$, exactly as outlined in the proof of Lemma 17. The proof now follows using the same arguments as outlined in the proof of Lemma 17. \square

Proof of Lemma 29. Fix a node x and let \mathcal{L}_x be the interval of length $L = n^{3/2-\nu}$ centered at x . The probability that any fixed node in this interval has at least two infected neighbors is at least $\mathbb{P}[\text{Bin}(Cn^{5/4-\nu/2}\sqrt{\log n}, 1 - \exp(-\eta/n^2)) \geq 2]$. Using independence of the edges, the probability that no nodes in the interval have at least two infected neighbors is at most $(1 - \mathbb{P}[\text{Bin}(Cn^{5/4-\nu/2}\sqrt{\log n}, 1 - \exp(-\eta/n^2)) \geq 2])^{n^{3/2-\nu}}$. Denoting this event as A_x , simple computations implies that,

$$\mathbb{P}(A_x) \leq n^{-C},$$

for $C > 1$. By a union bound, with high probability, each node has at least one infected node in the interval of length L surrounding it. With exponentially high probability, an infected node further infects its neighbor within $2 \log n/q_n$ time. Using union bound (over n choices of x), in $2(\log n)/q_n$ additional time, every interval \mathcal{L}_x will have two neighboring infected nodes and infection spreads throughout the \mathcal{L}_x intervals via simple and complex contagion. Next note that using Lemma 25 and a union bound over x , the maximum number of missing $\mathcal{C}_2 \setminus \mathcal{C}_1$ edges in any interval \mathcal{L}_x is at most \sqrt{n} . Further, an application of [29, Theorem 1.14] and union bound (over x) implies that the total passage time across the missing edges in any interval \mathcal{L}_x is at most $2\sqrt{n}/q_n$. Finally, complex contagion covers the remaining part of each interval in less than $n^{3/2-\nu}$ steps. Thus with high probability, the entire graph is infected by time $T_n + 2(\sqrt{n}/q_n + n^{3/2-\nu})$. \square

S6.4 Simulations with simple contagion adoptions only along \mathcal{C}_1 edges

Figure S8 is a redone of the simulation results presented in Figure 3A of the main text, but limiting simple contagion to \mathcal{C}_1 edges. Both figures reveal the same kind of qualitative behavior in that, rewiring accelerates the spread for large enough values of q . Moreover, comparisons of the two figures reveal interesting consequences of the handicap assumption that we impose on the model in Figure S8, by allowing simple contagion adoptions only along the \mathcal{C}_1 edges. Figure S8 confirms the theoretical predictions of Theorem 22 about an initial slow down followed by the speeding up of the contagion process as more cycle edges are rewired. However, the initial slow down phase that is predicted by Theorem 24 and observed in Figure S8 is not present in Figure 3A, where we allow all edges to have simple contagion probability q . Indeed, the slow down for $\eta \ll \sqrt{n}$ is a consequence of the handicap that we impose on our model: allowing simple contagion only along the \mathcal{C}_1 edges. Under this restriction, long ties can facilitate the spread only if two of them are likely to fall on the same faraway node (Figure S5). If the number of rewired edges is too few (i.e., $\eta \ll \sqrt{n}$), then the probability that two edges from an infected “island” land on the same faraway node is very small. Limiting simple contagion adoptions to only \mathcal{C}_1 edges (as in Figure S8) will only make our claim stronger: random rewiring accelerates noisy threshold-based contagions even after limiting sub-threshold adoptions to the sort ties.

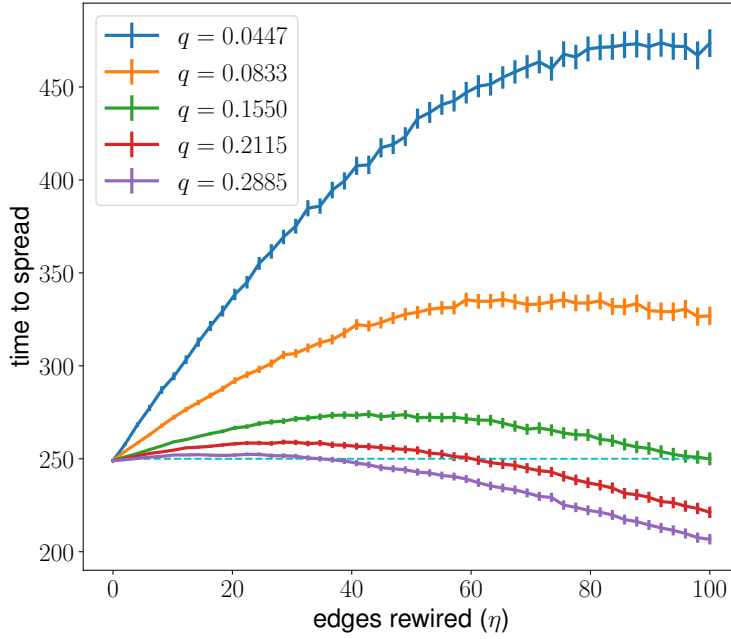


Figure S8: Spreading time of complex contagion over \mathcal{C}_2^η random graphs with $n = 500$, allowing for simple contagion with probability q only along the \mathcal{C}_1 edges — compare with Figure 3A. Not only the spread is accelerated for much smaller values of q in Figure 3A compared to Figure S8, but also the initial slow down phase is not present in Figure 3A when q is large. To the contrary, for all values of q and η small enough in Figure S8, contagion slows down with increasing η , consistent with the lower bound in Theorem 24. Each point is the average of 1000 random draws and the error bars show the 95% normal confidence intervals around the means. The spread of 2-complex contagion on \mathcal{C}_2 with $n = 500$ takes 250 time steps which is marked with a dashed line as a baseline.

S7 Reversible noisy 2–complex contagion on $\mathcal{C}_{1,2/n}$

First note that introduction of $\delta > 0$ to the contagion can only slow down the spread; therefore, the lower bounds that we have derived on the spread times with $\delta = 0$, continue to remain valid for $\delta > 0$ as well. Here we prove the the upper bound in Theorem 4 by repeating the steps in Subsection S4.2 and adapting the proofs of Lemmas 16, 17, and 18 to the $\delta > 0$ case.

Consider the rate of growth of simple contagion along \mathcal{C}_1 , captured by Lemma 16 in Subsection S4.2. Let us refer to the two infected nodes at either ends of an infected interval as boundary infected nodes. We refer to all other infected nodes that are not boundary as internal infected nodes. Recall that in Lemma 16 an interval grows longer as a boundary node infects its \mathcal{C}_1 -neighbor with probability q . Next consider a boundary infected node, denoted by ν at time t , and its susceptible neighbor on \mathcal{C}_1 , denoted by u . Under the reversible noisy 2–complex contagion model, if u is infected by simple contagion and ν reverts to being susceptible, then, with two infected neighbors at time $t + 1$, node ν will be re-infected through 2–complex contagion. However, if ν reverts back to being susceptible without infecting u then the length of the infected interval decreases by one. Moreover, if both ν and its $k - 1$ consecutive, internal neighbors on the cycle revert back to being susceptible (irrespective of the status of u), then, the length of the infected interval decreases by k . To avoid the latter cases, let us assume that $\delta^2 \ll 1/n$ so that simultaneous reversion of consecutive nodes on the cycle becomes unlikely (happens with zero probability as $n \rightarrow \infty$). Building on this observation, the length of the infected interval at time t under the reversible noisy 2–complex contagion can be lower-bounded by the following asymmetric, lazy random walk where $Y_0 = 0$ and for $t \geq 0$ we have:

$$Y_{t+1} = Y_t + \begin{cases} 1, & \text{with probability } q, \\ 0, & \text{with probability } 1 - q - \delta, \\ -1, & \text{with probability } \delta, \end{cases} \quad (\text{S.11})$$

Hence, we can upper-bound the time until the infected interval increases by k by the random walk hitting time: $T_k := \inf\{t : Y_t = k\}$. Note that $\mathbb{E}(T_k)$ satisfies the following recursion:

$$\mathbb{E}(T_k) = 1 + q\mathbb{E}(T_{k-1}) + \delta\mathbb{E}(T_{k+1}) + (1 - q - \delta)\mathbb{E}(T_k),$$

with the boundary condition $\mathbb{E}(T_0) = 0$, we obtain $\mathbb{E}(T_k) = k/(q - \delta)$. Choosing $k = \sqrt{n} \log \log n$ and following the steps of Lemma 16 by concentration — n.b., passage times from k to $k + 1$ are i.i.d. positive, integer-valued random variables and the first passage time from state 0 to state $\sqrt{n} \log \log n$ is the sum of $\sqrt{n} \log \log n$ independent random variables [31] — we obtain that for τ_n fixed as in Lemma 16, with high probability as $n \rightarrow \infty$, every activated interval gains at least $\sqrt{n} \log \log n$ new infected nodes over each of the first τ_n epochs of length $(2\sqrt{n}/(q - \delta)) \log \log n$.

Next, we follow the steps of Lemma 17 to establish the rate of the growth of the number of active intervals in Algorithm 3. In particular, (S.4) continues to hold as before. However, when lower-bounding p_τ in (S.5) we should account for the fact that each of the $X_{\tau-1} \sqrt{n} \log \log n$

infected nodes in the active interval could revert back to being susceptible; therefore, the $X_{\tau-1}\sqrt{n}\log\log n$ terms in (S.5) should be replaced by a binomial random variable with success probability $1 - \delta$ as follows:

$$\begin{aligned} p_\tau &\geq \mathbb{P}\left[\text{Bin}\left(L, \mathbb{P}\left[\text{Bin}\left(\text{Bin}(X_{\tau-1}\sqrt{n}\log\log n, 1 - \delta), \frac{2}{n}\right) \geq 2\right]\right) \geq 1\right] \\ &\geq 4L(1 - \delta)^2 X_{\tau-1}^2 \frac{(\log\log n)^2}{n}, \end{aligned}$$

where the last inequality holds with high probability as $n \rightarrow \infty$. Subsequently, (S.6) becomes:

$$X_\tau \geq (1 - \delta)^2 X_{\tau-1}^2 \left(\frac{\log\log n}{2}\right)^2.$$

Repeating the same steps as in Lemma 17 yields that for $\tau_n = \frac{\log\log n + t_n}{\log 2}$ and $t_n = t_n(C) = o(\log\log n)$, we have:

$$X_{\tau_n} \geq (1 - \delta)^{2\tau_n} \left(\frac{\log\log n}{2}\right)^{2\tau_n}$$

Finally, upon noting that $(1 - \delta)^{2\tau_n} \rightarrow 1$ for $\delta^2 \ll 1/n$, we obtain $X_{\tau_n} \geq Cn^{1/4}(\log n)^{1/2}$ for proper choice of t_n , with high probability as $n \rightarrow \infty$.

To complete the proof of Theorem 4 it only remains to verify the end regime, when enough nodes are infected so that any susceptible node will have an infected node in its \sqrt{n} -vicinity on \mathcal{C}_1 . Following the same steps as in the proof of Lemma 18, let T_n be the first time that at least $Cn^{3/4}\sqrt{\log n}$ nodes are infected, where $C > 1$ is a universal constant. We show that with high probability, the \sqrt{n} -neighborhoods of all nodes contain at least one infected node by time $T_n + 1$ and subsequently all nodes are going to be infected by time $T_n + 1 + 2\sqrt{n}/(q - \delta)$. The latter $2\sqrt{n}/(q - \delta)$ term can be derived as a bound on the random walk hitting time just as in (S.11). To finish the proof, we bound the probability that none of the nodes in an \sqrt{n} neighborhood of \mathcal{C}_1 has more than one neighbor among the more than $Cn^{3/4}\sqrt{\log n}$ nodes that are infected at time T_n . This probability can be upper-bounded as in (S.7) with the $Cn^{3/4}\sqrt{\log n}$ replaced by a binomial random variable of the same size and success probability $1 - \delta$ to account for the reversions:

$$\left(1 - \mathbb{P}\left[\text{Bin}\left(\text{Bin}(Cn^{3/4}\sqrt{\log n}, (1 - \delta)), \frac{2}{n}\right) = 2\right]\right)^{\sqrt{n}} \rightarrow n^{-2(1-\delta)^2 C^2},$$

which for $\delta \ll 1/\sqrt{n}$ can be upper-bounded by n^{-C^2} , and the proof is finished by a union bound over the n nodes around the cycle.

S8 Noisy complex contagions in higher dimensions

The circular lattices that we investigate in the previous sections only allow a single dimension for contagion to spread. In higher dimensions contagions can spread simultaneously in several directions and therefore progress faster. As an example consider the spread of 2-complex contagion on a 2D square lattice with closed diagonals (Figure S9A). This lattice structure is the two-dimensional equivalent of \mathcal{C}_2 — barring the boundary effects — and we denote it by \mathcal{Z}_4 , reserving the notation \mathcal{Z}_2 for the $\sqrt{n} \times \sqrt{n}$ square lattice without the diagonals: $\mathcal{Z}_2 := ([-\sqrt{n}/2, \sqrt{n}/2] \cap \mathbb{Z})^2$. Starting from two infected nodes at the center of \mathcal{Z}_4 , the area around them will grow at least quadratically in time — the infected area grows at least as fast as $2t^2$ with time t ; proportionally to the area of a sideways square (i.e., a diamond \diamond) with diagonals of length $2t$. Contagion slows down once we hit the boundaries but these boundary effects are asymptotically dominated (they only change the leading constant multiplier in our upper bounds).³ Therefore, the spread time on \mathcal{Z}_4 of size n can be upper bounded by $O(\sqrt{n})$. On the other hand, additional simple contagion infections can make the noisy 2-complex contagion spread faster than $2t^2$; however, starting from two nodes at the origin even 1-complex contagion that spreads immediately to any node with an infected neighbor will need at least $\Omega(\sqrt{n})$ time to spread (contagion in that case grows as $\lfloor \pi t^2 \rfloor$, proportionally to the area of a circle of radius t). This establishes our baseline for the spread time of noisy 2-complex contagion on \mathcal{Z}_4 as $\Theta(\sqrt{n})$.

We will compare this $\Theta(\sqrt{n})$ baseline with the spread time of noisy 2-complex contagion on the rewired lattice $\mathcal{Z}_{2,4/n}$, which is the \mathcal{Z}_4 -rewired equivalent of $\mathcal{C}_{1,2/n}$ in two dimensions. $\mathcal{Z}_{2,4/n}$ is constructed as the union of the $\sqrt{n} \times \sqrt{n}$ lattice (\mathcal{Z}_2) and random graph ($\mathcal{G}_{n,4/n}$), keeping the expected degrees off the boundaries of \mathcal{Z}_2 fixed at eight and preserving the minimal 2D structure of \mathcal{Z}_2 for the simple contagion spread, just as the \mathcal{C}_1 structure is preserved in $\mathcal{C}_{1,2/n}$. To upper-bound the spread time on $\mathcal{Z}_{2,4/n}$, we argue as in the one-dimensional case — recall our upper-bound on $T_{2,q}(\mathcal{C}_{1,2/n})$ in Section S4.2. We consider a more restrictive (hence, slower) infection process and derive an upper bound on the spread time of the slowed-down process. To this end, we divide the square \mathcal{Z}_2 into a grid of sub-squares, each of side length $n^{1/4} \sqrt{(\log \log n)^3}$. We consider a constrained process where the contagion (both simple and complex) along the \mathcal{Z}_2 edges is restricted within the sub-squares. Once this contagion reaches the boundaries of the sub-squares, it stops. Note that this process is by construction slower than the original process, and analyzing its spread time gives an upper-bound on $T_{2,q}(\mathcal{Z}_{2,4/n})$.

To demonstrate the spread mechanism resulting from the joint action of simple and complex contagion on $\mathcal{Z}_{2,4/n}$, consider any of the $n^{1/4} \sqrt{(\log \log n)^3} \times n^{1/4} \sqrt{(\log \log n)^3}$ sub-square on \mathcal{Z}_2 with an initially infected node inside. Call this node ν . Given simple adoption probability q and following the steps of Lemmas 16 and 19, the spread time of simple contagion along the horizontal and vertical axes of ν can be upper-bounded by a sum of i.i.d. geometric random variables that concentrate. Consider the largest square with side length at most $n^{1/4} \sqrt{\log \log n}$

³You can watch a video of a spread on a 100×100 \mathcal{Z}_4 lattice for better clarity: <https://www.youtube.com/watch?v=ijla5j21wfY>.

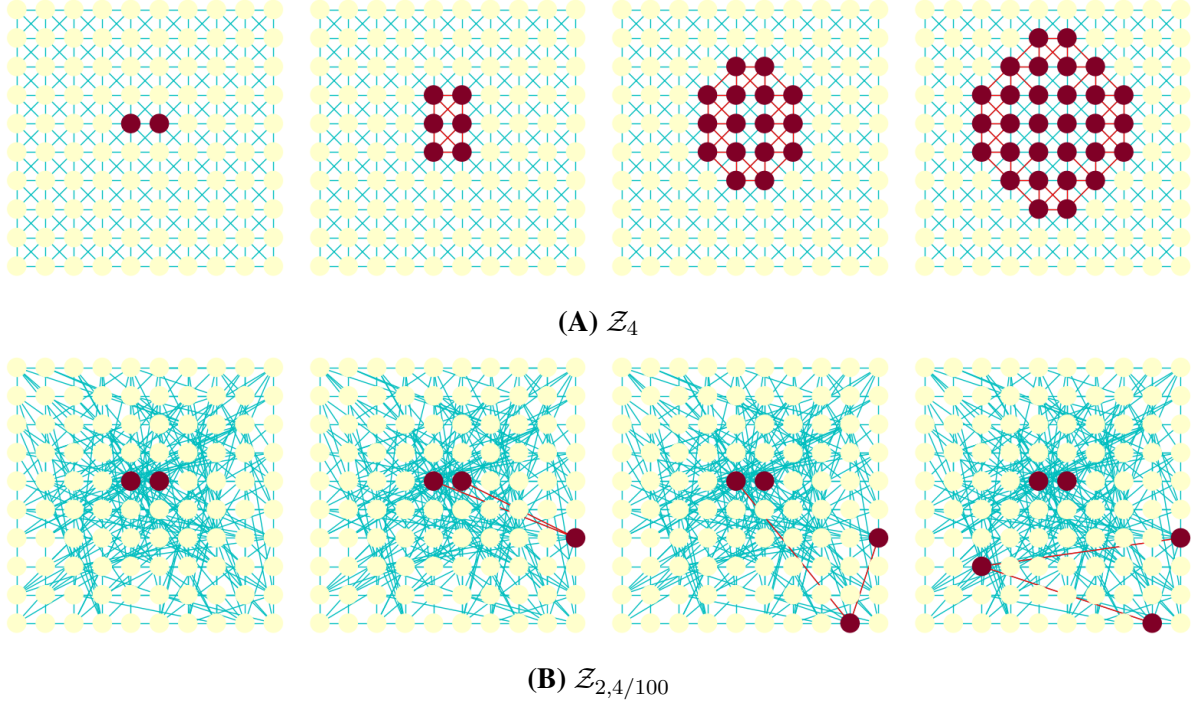


Figure S9: The first four steps of noisy 2-complex contagion on 10×10 , two-dimensional square lattices: (A) \mathcal{Z}_4 , a 10×10 square lattice with closed diagonals. Each node has eight neighbors (except at the boundary); and (B) $\mathcal{Z}_{2,4/n} = \mathcal{Z}_2 \cup \mathcal{G}_{n,4/n}$, $n = 100$, on average four edges are added to each node on the square lattice (10×10) to keep the overall average degrees fixed at eight.

that contains ν and is fully enclosed within the original $n^{1/4} \sqrt{(\log \log n)^3} \times n^{1/4} \sqrt{(\log \log n)^3}$ sub-square. Call this sub-sub-square \mathcal{S}_ν . Using the concentration bounds on the sum of i.i.d. geometric random variables we can claim that in less than $10(n^{1/4}/q) \sqrt{\log \log n}$ time with high probability all nodes on the same horizontal and vertical axis as the initially infected node in the sub-square will get infected ($\square \rightarrow \boxplus$). An additional $2n^{1/4} \sqrt{\log \log n}$ time is enough for the remaining off-axis nodes to get infected by complex contagion progression from the infected axes so that the entire \mathcal{S}_ν is infected ($\boxplus \rightarrow \blacksquare$), with high probability in $10(n^{1/4}/q) \sqrt{\log \log n} + 2n^{1/4} \sqrt{\log \log n} \ll 12(n^{1/4}/q) \sqrt{\log \log n}$ time for $q = o(1)$; the leading constant multiplier of 12 is chosen to be sufficiently large for our argument and can be reduced.

Our upper-bound proof for the constrained process proceeds similarly as our arguments in Sections S4.2 and S5 for the super-exponential activation growth by replacing intervals of length L_n on the cycle with sub-squares of area $n^{1/4} \sqrt{(\log \log n)^3} \times n^{1/4} \sqrt{(\log \log n)^3}$ on \mathcal{Z}_2 . We again proceed in epochs of length $12n^{1/4} \sqrt{\log \log n}/q$. Each square once it has an infected node acquires $\sqrt{n} \log \log n$ infected nodes through a combination of simple and complex contagion as described above with high probability in $12(n^{1/4}/q) \sqrt{\log \log n}$ time. The $\sqrt{n} \log \log n$ newly

infected nodes within each active sub-square will seed faraway nodes in other sub-squares by long-range, 2-complex contagion with high probability, and the “activated” sub-squares, in turn, grow and generate new activate sub-squares, sustaining the super-exponential growth in the number of active sub-squares over $2 \log \log n$ iterations of Algorithm 3 — established by the likes of Lemmas 17 and 20. At the last stage, we just wait for the *holes* within the sub-squares to be filled by a spread of simple and complex contagion within the square (similar to the end regimes characterized in Lemmas 18 and 21). Hence the total spread time of noisy 2-complex contagion on $\mathcal{Z}_{2,4/n}$ can be upper-bounded by $36n^{1/4}(\log \log n)^{3/2}/q$ and we have follows:

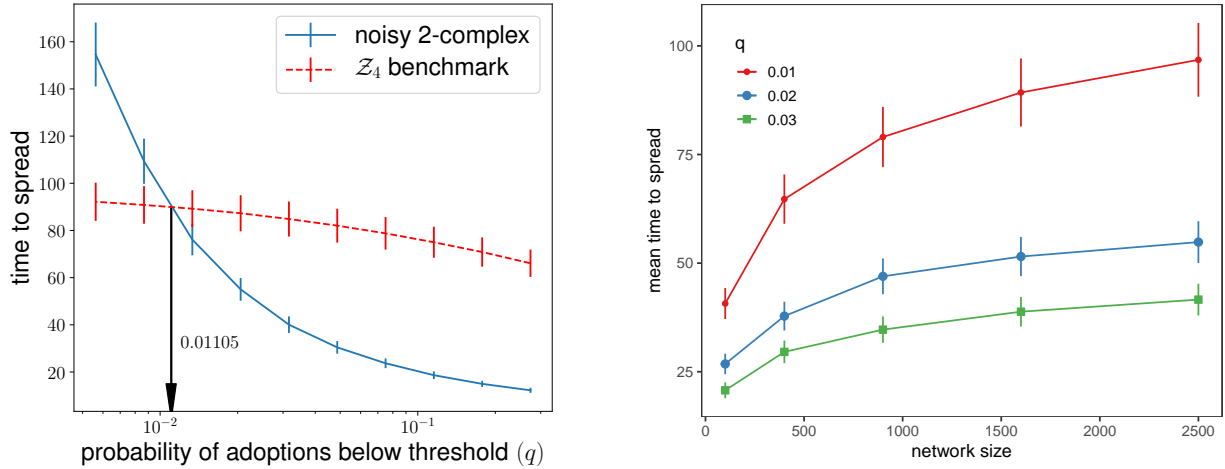
Proposition 30. *Consider the noisy 2-complex contagion with simple adoption probability q over $\mathcal{Z}_{2,4/n}$. With high probability as $n \rightarrow \infty$, $T_{2,q}(\mathcal{Z}_{2,4/n}) < \frac{36n^{1/4}}{q}(\log \log n)^{3/2}$.*

Although noisy complex contagions spread quadratically faster in two dimensions we can still establish a gap between the $\Theta(\sqrt{n})$ spread time on \mathcal{Z}_4 and the $O(\sqrt[4]{n}/q)(\log \log n)^{3/2}$ upper bound on the spread time over $\mathcal{Z}_{2,4/n}$ such that for $q \gg 1/\sqrt[4]{n}$ noisy 2-complex contagions spreads asymptotically, strictly faster on $\mathcal{Z}_{2,4/n}$ compared to \mathcal{Z}_4 . We note that this argument generalizes naturally to higher dimensions and will similarly illustrate the speeding up of the infection percolation due to the presence of long-range edges (with a combination of simple and complex contagion) for large enough q . In general, one can analyze the spread time in a similar manner in d dimensions. The side length of the sub-hypercubes in d dimensions should be $n^{1/2d}(\log \log n)^{3/d}$ and the contagion during the super-exponential activation phase should proceed in epochs of length $O((n^{1/2d}/q)(\log \log n)^{1/d})$. This ensures that the active sub-hypercubes will acquire $\sqrt{n} \log \log n$ new active vertices in each epoch by a combination of simple and complex contagion. Once these vertices are infected, the process spreads in a similar manner, by a combination of local infections and long-range complex contagion that activates other sub-hypercubes through long-range edges. Hence, the overall spread time on d -dimensional hypercube with random, long-range edges can be upper bounded by $O((n^{1/2d}/q)(\log \log n)^{1+1/d})$, which for $q \gg 1/n^{1/2d}$ is strictly faster than the $\Theta(n^{1/d})$ spread-time baseline on the d -dimensional hypercube with triad-closing instead of random, long-range edges.

Figure S10 shows the spread times of noisy 2-complex contagion by varying sub-threshold adoption probability q and network size n . We can see that the results of Figure S7 can be qualitatively reproduced but the value of q that leads to a faster spread on $\mathcal{Z}_{2,4/n}$ is higher in Figure S10A compared to Figure S7A.

S9 Simulations with empirical networks data

We expand on the results of simulations that we present in the main text (Figure 4) by providing additional statistics and measurements over these networks. Moreover, we provide simulations with variations of the original model to verify the robustness of our claims to changes in the model. We use five datasets that contain empirical social networks for:



(A) $T_{2,q}$ vs. q on \mathcal{Z}_4 and $\mathcal{Z}_{2,4/n}$, $n = 50 \times 50 = 2500$ (B) $T_{2,q}(\mathcal{Z}_{2,4/n})$ vs. n for $q = 0.01, 0.02, 0.03$.

Figure S10: Noisy 2-complex contagion spread times versus (A) sub-threshold adoption probabilities (q) on 50×50 square lattices (\mathcal{Z}_4 and $\mathcal{Z}_{2,4/n}$), and (B) network size (n).

- (i) 175 rural Chinese farm villages being encouraged to sign up for insurance [32],
- (ii) the friendship, and
- (iii) the health advice networks collected from 17 rural villages in Uganda [33],
- (iv) 77 village social networks collected in the study of participation in a microfinance program in South India [34],
- (v) the Facebook friendship social networks in the U.S. universities and colleges [35], from which we choose the 40 smallest networks.

The village networks in the first four datasets have as few as tens of nodes but have typically hundreds of nodes. A typical Facebook college network has thousands of nodes. Table S2 summarizes the network size statistics in all these datasets. For each social network in these datasets we are interested in how interventions that modify the network structure would affect the spread of contagion. We consider three intervention strategies:

- (i) random rewiring,
- (ii) adding new edges uniformly at random, and
- (iii) adding new edges at random with probability proportional to the number of open triads that each new edge would close.

Following the same conventions as in Figure 4 of the main text, we use black, orange, blue, and red colors to plot the values corresponding to the original network, as well as the modified networks under rewiring, triad-closing and random edge additions. The plots in Figure S11 are produced in the same way as Figure 4C of the main text. The latter is simulated over the 175 social networks in the Cai et al. [32] dataset, whereas in Figure S11 we use the other four datasets with fewer social networks — Chami et al. [33], Banerjee et al. [34], and Traud et al. [35].

Table S2: Size statistics for the empirical networks data

dataset	number of networks	min size	max size	median size	mean size
Cai et al. [32]	175	13	117	51.5	54.03
Chami et al. [33]	17	65	372	184	202.12
Banerjee et al. [34]	77	75	341	189	192.63
Traud et al. [35]	40	762	7677	3745	4153.82

In any given network, starting from two randomly chosen seeds (initially infected nodes) we measure the time until 90% of the nodes are infected. Under each intervention and model of contagion that we are considering, we draw 500 random spreading time samples over the original or modified networks and compare the spreading times in terms of their empirical cumulative distribution functions (ECDFs). On a few occasions we combine these samples for all the villages over the entire dataset and compare the overall ECDFs under each intervention: Figures S17, S18, as well as the bottom left insets in Figure S11, and the second and fourth rows in Figure S19 are generated this way. The intervention sizes are measured in terms of the percent of edges in the original networks, and unless otherwise specified, the intervention size is fixed at 10%: Figure 4 in the main text, as well as Figures S17 and S20, here, follow this convention. When varying the intervention size, we group the samples by their intervention size. The intervention size in each group is fixed at 5, 10, 15, 20 or 25%: Figures S18 and S19 are generated in this manner. In the first and third rows of Figure S19 we have overlaid the ECDFs of spreading times for each social network in the respective datasets (77 villages from the south Indian dataset [34] in the first row, and 17 villages from the Ugandan dataset [33] in the third row). In these two cases (the first and third rows of Figure S19) since different village sizes affect the time to 90% spread, we normalize the spreading times relative to the mean spread time in the original village (with no interventions); moreover, we put the x-axis in logarithmic scale to symmetrize the ratios below and above one.

To see how the spread times behave with the increasing size of real networks we plot the spread times versus network sizes for the 500 simulated spreads in each of the five network datasets for which we plotted the mean spread times in Figure 4A. Figure S12 shows a consistently slow increasing trend in all five datasets albeit subject to significant variability, because individual networks in each dataset vary on various factors (clustering, edge density, diameter, etc.) in addition to their size (cf. Figure S4B).

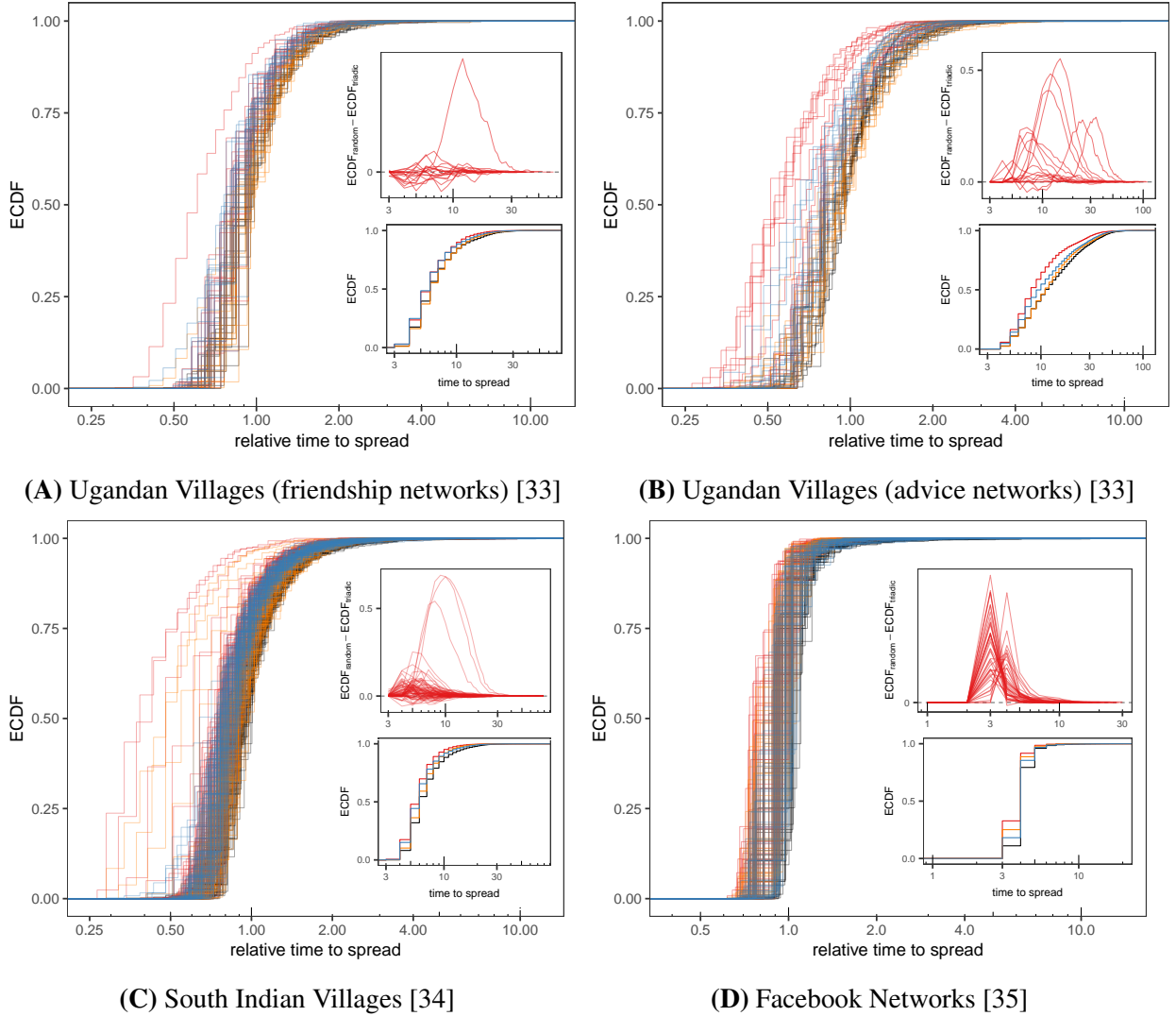


Figure S11: We replicate the plots in Figure 4C of the main text (that was simulated on social network data from Chinese farm villages [32]) for four other datasets.

Figure S13 shows the block diagram of the model that we have implemented for each agent in our simulations. The active and inactive infected states describe a situation where adopter agents may transition into a state where they are not effective in turning their neighboring non-adopters into adopters. We refer to this state as an inactive infected state and allow infected agents to transition back and forth between active and inactive states with probabilities α and γ as depicted in Figure S13. In the basic model that we study in the main text all infected agents are regarded as active; hence, $\alpha = 1$ and $\gamma = 0$. We also allow a probability δ for infected agents to transition back into the susceptible state. We discuss the robustness of our conclusions to increasing δ in Section S7; see also Theorem 4 and Figure 3B in the main text. Here we set $\delta = 0$, motivated by applications where infection connotes costly or hard-to-reverse

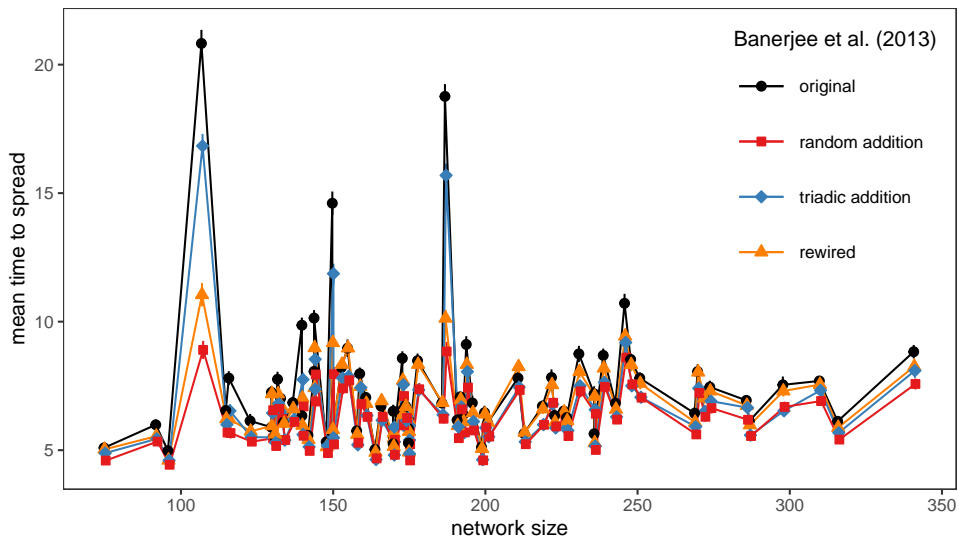
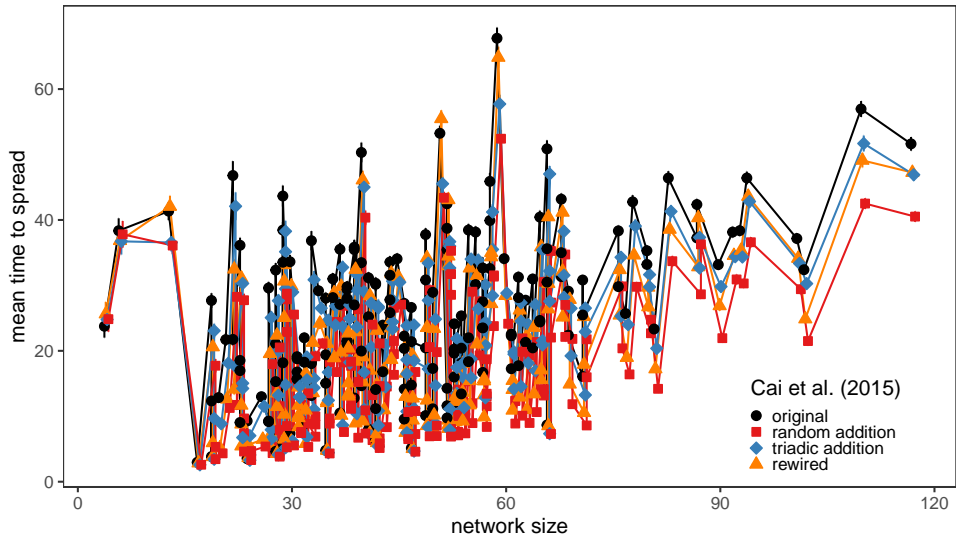


Figure S12: Mean spread times over individual networks in Chinese [32] and South Indian village [34] datasets. The means with their 95% CIs are calculated over the same 500 random samples that were used to plot the ECDFs in the Figures 4C and S11.

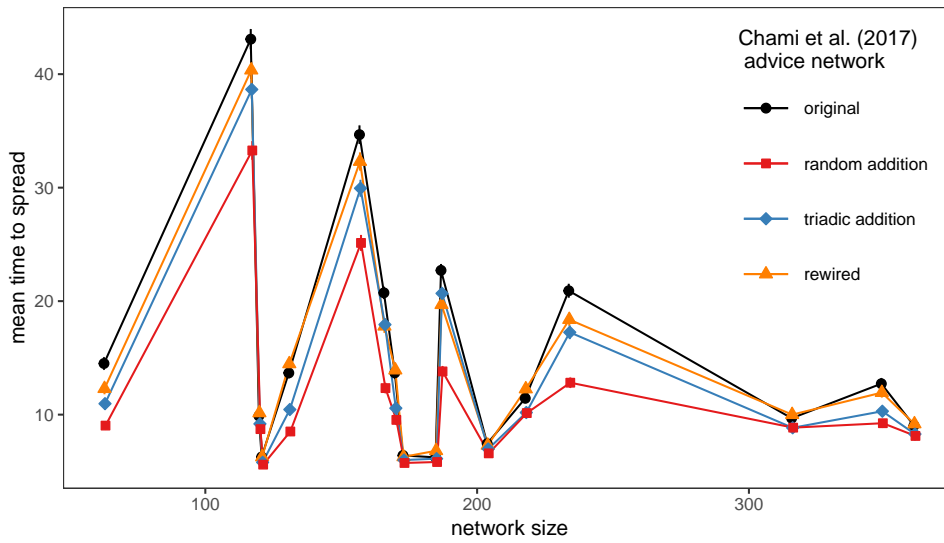
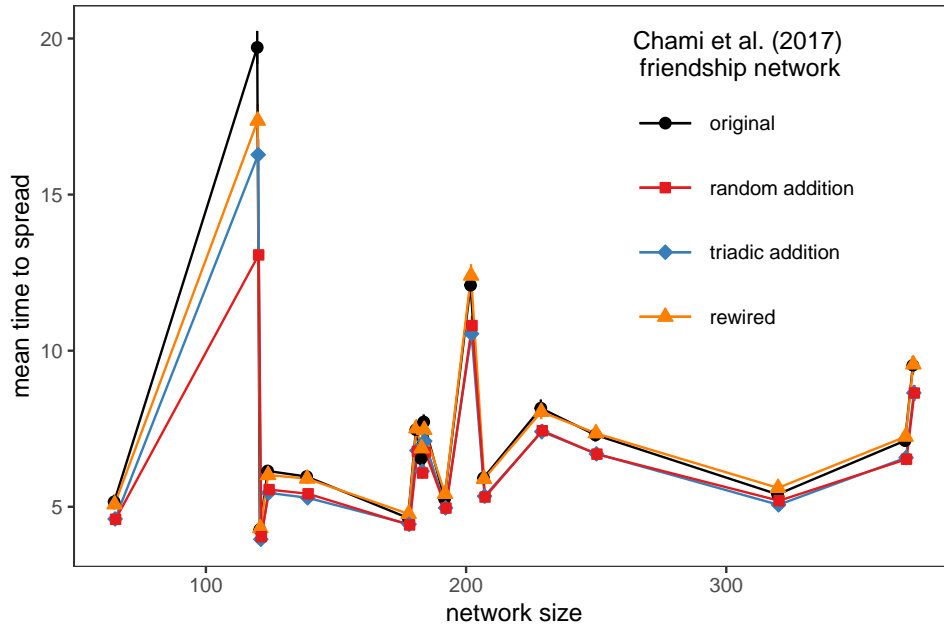


Figure S12: Mean spread times over individual networks in Ugandan village friendship (top) and advice (bottom) networks [33]. The means with their 95% CIs are calculated over the same 500 random samples that were used to plot the ECDFs in the Figures 4C and S11.

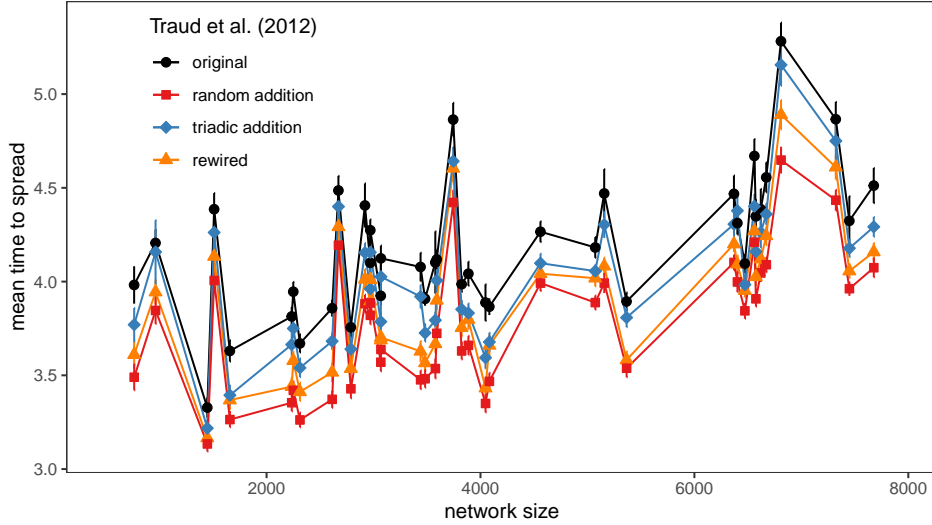


Figure S12: Mean spread times over individual networks in Facebook social networks [35]. The means with their 95% CIs are calculated over the same 500 random samples that were used to plot the ECDFs in the Figures 4C and S11.

actions such as product purchase.

The activation function block determines the type of contagion (simple or complex). Different models of contagion are characterized by different parameters. For example, the simple contagion activation functions shown in Figure 1 of the main text are parametrized by the independent transmission probabilities (β) along each edge. The probability of infection with x infected neighbors under this simple contagion activation function is given by $1 - (1 - \beta)^x$. On the other hand, the complex contagion activation function shown in Figure S13, on the right, is parametrized by a threshold value θ , adoption probability above threshold ρ , and adoption probability below threshold q . Similarly, logit and probit activation functions studied in Section S4S4.3 are characterized by a threshold θ and noise (or “rationality”) level σ . Unless otherwise specified, we compute the spreading time samples under the $(0.05, 1)$ model from Figure S17A ($\rho = 1, q = 0.05, \alpha = 1, \gamma = 0, \theta = 2$): the spreading time samples in Figures S19 and S20, here, as well as Figure 4 of the main text are all generated under the $(0.05, 1)$ model.

All the measurements on empirical networks are of the spread time until 90% of the total network sizes, except in Figure S14 where we plot the time until 25%, 50% and 75% of the total spread for comparison. Simple (sub-threshold) adoptions spread slowly as each adoption happens with small probability (q) and multiple discrete steps may pass before a simple adoption is realized. However, the benefits of random edge addition and rewiring are apparent even at low percentages (Figure S14D).

In special cases (Figure S17D, here, and Figure 3A in the main text) we make a distinction between what edges pass simple contagion adoptions (probability q) and what edges do not. Such models are not fully specified by the choice of activation functions and transition proba-

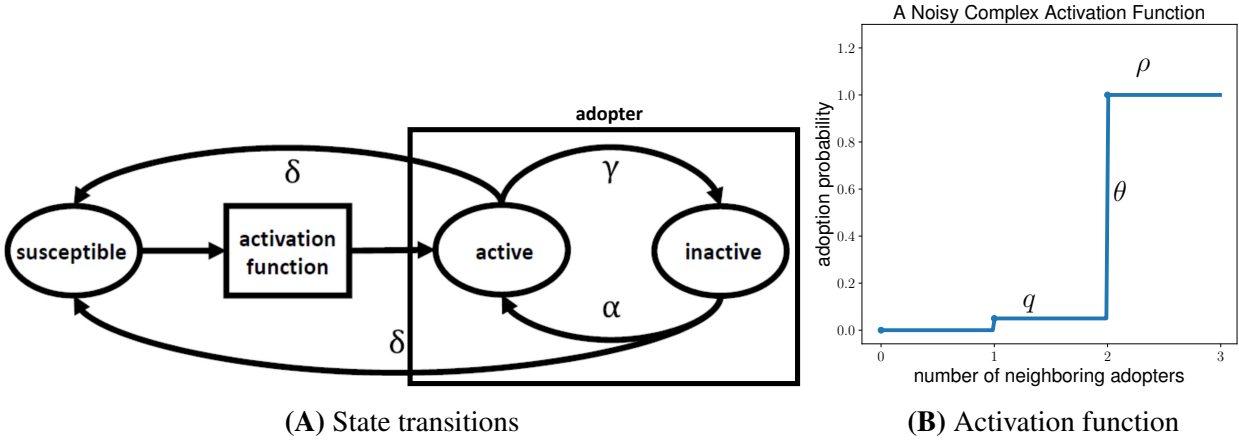


Figure S13: An agent-based simulation model. (A) Agents may be in susceptible, active or inactive states. Agents in active states influence others to become adopters, agents in an inactive state are adopters but do not influence others to become adopters. The arrows indicate the state transitions, labeled with their probabilities. The transition probabilities from a susceptible state to an active state depend on the states of the neighboring agents and is specified according to the agent’s activation function. (B) A noisy threshold-based action function is parametrized by the probability of adoptions above threshold, ρ , probability of adoptions below threshold, q , and threshold θ .

bilities α , γ , and δ , since we need to take into account the type of network edges along which transitions occur. In Figure S17D, we allow the simple contagion probability q only if the edge connecting the adopter and non-adopter agent is existent in the original network. Spreading time samples for this model are collected only under the edge addition interventions (random versus triad-closing). In Figure 3A of the main text we consider the spreading time over \mathcal{C}_2^n random graphs and allow for simple contagion probability q only along the \mathcal{C}_1 cycle edges.

Figures S15 and S16 show the overall ECDFs for the spread times of θ -complex contagion with probability $q = 0.05$ of adoptions below threshold. We present the results for the dataset of the Chinese farm village social networks [32]. In Figure S15, all nodes have the same θ and we vary $\theta = 2, 3, 4, 5$ in Figures S15A to S15D. In Figure S16, the value of θ for each node is set independently according to the same distribution. We test four distributions which all have the same support, $\theta = 2, 3, 4, 5$. We progressively shift the mode of the distributions from $\theta = 2$ in Figure S16A to $\theta = 5$ in Figure S16D. Working with distributions of thresholds allows us to test the robustness of our claims against heterogeneity in threshold values. In all cases the directions of the differences remain unchanged, even though their magnitudes become smaller with the increasing threshold values.

Figure S17 shows the overall ECDFs (combining all samples across all villages with 500 random samples per village) of the spreading times over the Chinese farm villages dataset

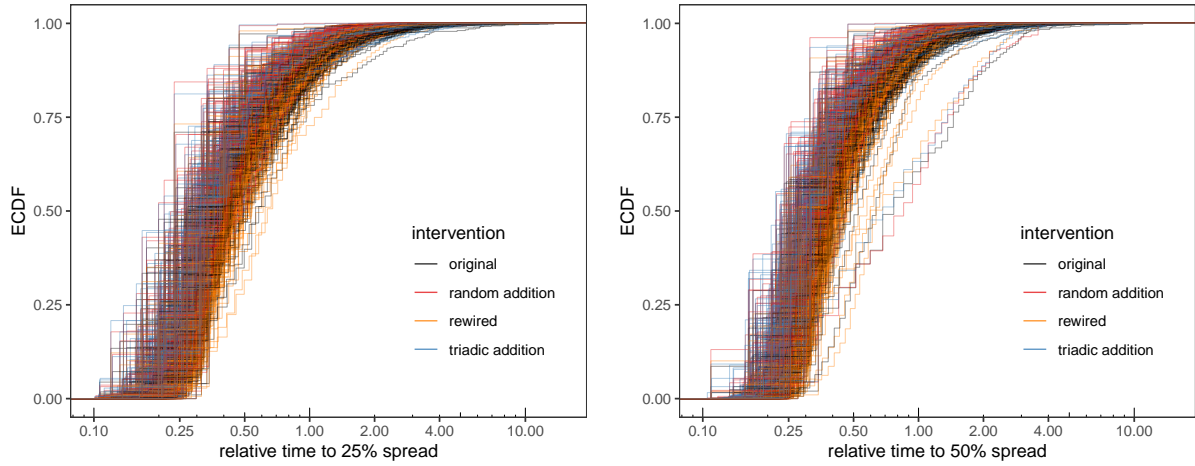
[32]. We present the results for six different models and activation function settings with 10% sized interventions. A more fine-grained version of this data where intervention sizes are varied between 5, 10, 15, 20, and 25% is presented in Figure S18. The two models labeled by $(0.05, 1(0.05, 0.5))$ and $(0.001, 1)$ in Figures S17C and S17F (see the Figure captions for the corresponding model parameters) are significantly slower. In their ECDFs, we can identify a fast and a slow regime which we attribute to complex and simple contagions, respectively. If the 90% spread is reliant on complex contagion, then the spreading time samples are visibly discrete and the total spread is achieved fast. If, on the other hand, a significant number of nodes are infected through simple contagion (coin flips with probability q), then contagion is slow and spreading time samples cover a wide range, resulting in a smooth section in the ECDF curve.

In contrast, the fractional threshold model that is labeled by $\text{REL}(0.05, 1)$ in Figure S17E is significantly faster; its ECDF is visibly discrete and does not contain a smooth, slow section. Under this fractional model a node is infected with high probability ($\rho = 1$) if the majority of its neighbors are adopters ($\theta^* = 0.5$); in particular, a leaf node with only one neighbor becomes an adopter as soon as its neighbor adopts. This is in contrast to the absolute threshold model $\theta = 2$ where a leaf node can only be infected through the slow simple contagion (coin flips) with probability q .

In Figure S19 we present the ECDFs of the spreading times over the south Indian [34] and Ugandan [33] villages for different intervention sizes (the intervention size in Figure S11 was fixed at 10%). To further demonstrate the stochastic dominance relation between the spreading times (as random variables) under various interventions, in Figure S20 we present the difference between the ECDFs with 10% interventions for all the social networks in our five datasets. The spreading samples in both Figures S19 and S20 are generated under the $(0.05, 1)$ model from Figure S17A ($\rho = 1, q = 0.05, \alpha = 1, \gamma = 0, \theta = 2$). If the positive difference persists throughout the entire support of two ECDFs, then we conclude the stochastic dominance relation between their respective random variables.

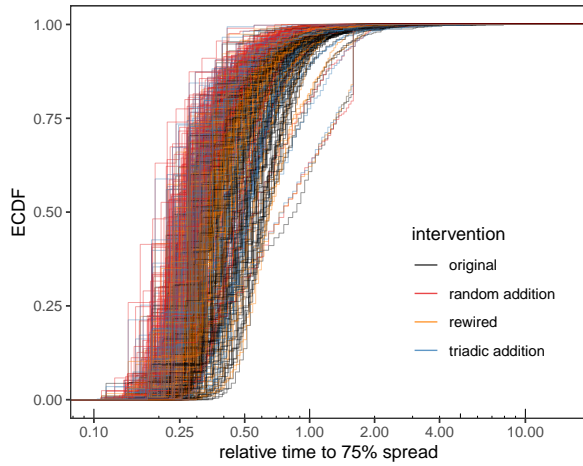
In Figure S21 we plot the mean time to spread versus the intervention size for random and triadic edge additions. We can thus answer how much larger does the intervention size for triadic addition have to be before it is faster than random addition in each set of empirical networks. For example, Figure S21A indicates that in the Cai et al. dataset even with 25% additional triad-closing ties the mean spread time is still slower than in the networks with 10% additional random ties.

In all these measurements, we observe the same direction (sign) for the effect of interventions on the spreading time: (i) rewiring speeds up the spread of contagion compared to the original networks, (ii) contagion spreads faster in the networks with added edges compared to the original networks, (iii) contagion spreads faster in the network with added random edges compared to the network with added triad-closing edges. The magnitude of differences are larger for larger interventions.

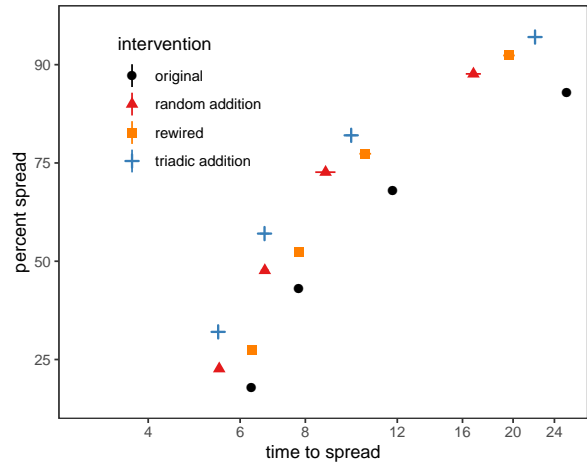


(A) 25% spread ECDFs overlaid for each village

(B) 50% spread ECDFs overlaid for each village



(C) 75% spread ECDFs overlaid for each village



(D) average overall

Figure S14: We measure the spread time of noisy 2-complex contagion ($q = 0.05$) to different percentages of the total in Chinese farm villages [32] with ECDFs overlaid for each village (A-C), as well as the overall average time to spread to different percentages (D) — compare with Figure 4C where percentage spread is 90%. The intervention sizes are fixed at 10%.

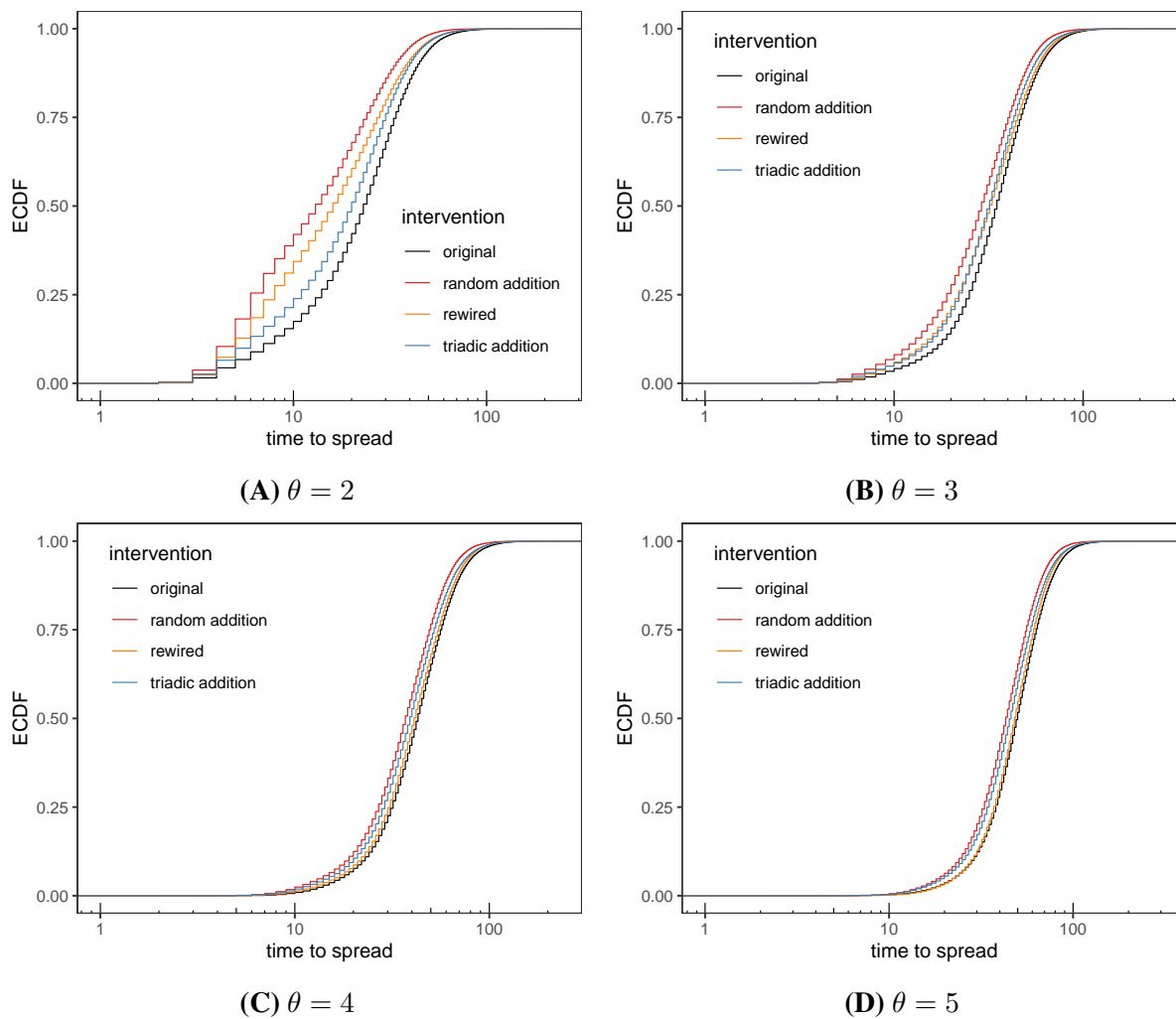


Figure S15: Spread time of θ -complex contagion with probability $q = 0.05$ of adoptions below threshold. We vary $\theta = 2, 3, 4, 5$ and plot the ECDFs over Chinese farm villages [32], under four different interventions with fixed size 10%.

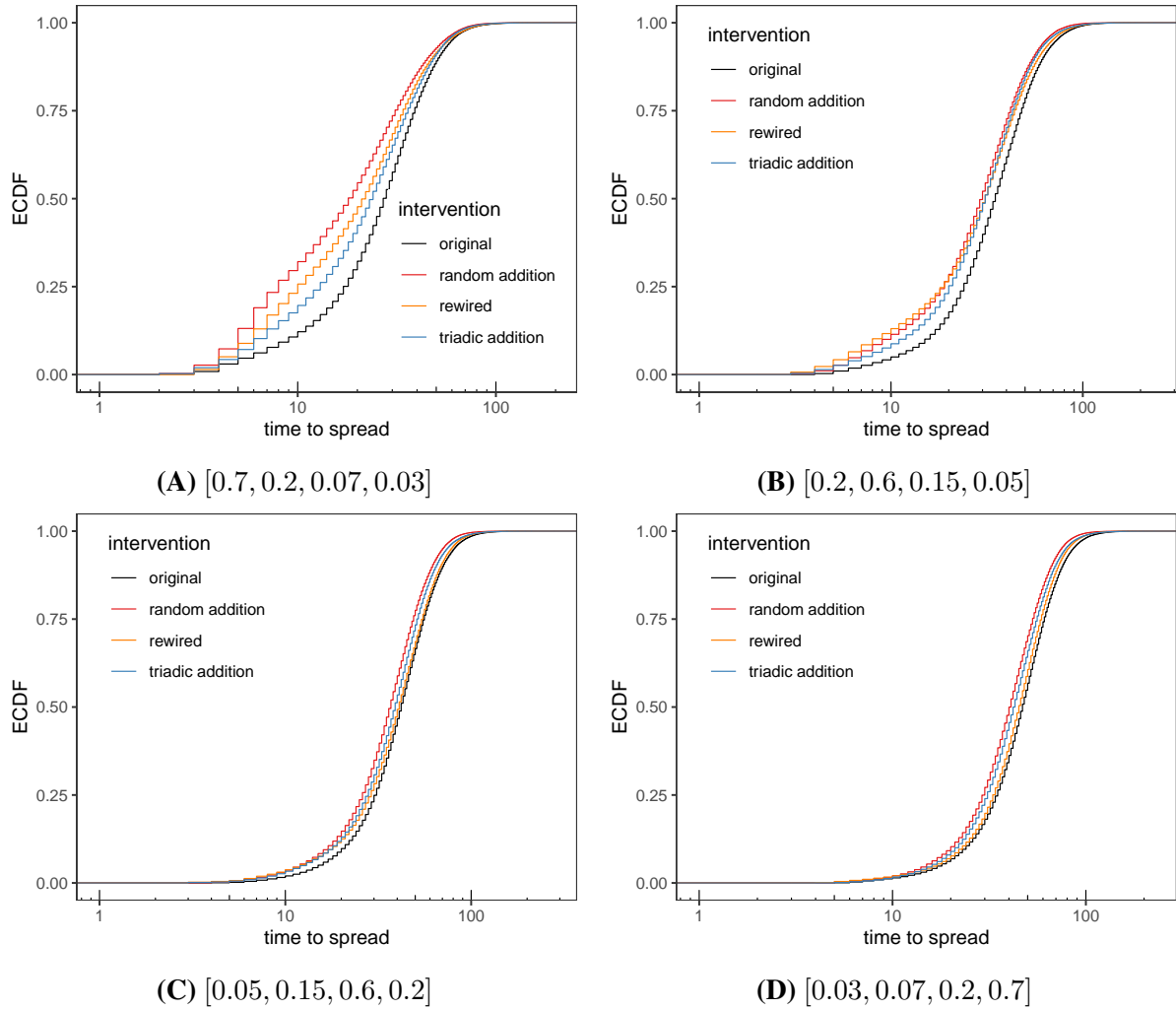


Figure S16: We plot the overall ECDFs under four conditions (with 10%-sized interventions) for the spread time of complex contagions over Chinese farming villages [32]. The probability of adoptions below threshold is set at $q = 0.05$. Each node's threshold is an independent random draw from the same distribution. We have plotted the results for four different distributions of thresholds. Each distribution is represented by its probability mass function with support over the four possible values $\theta = 2, 3, 4, 5$.

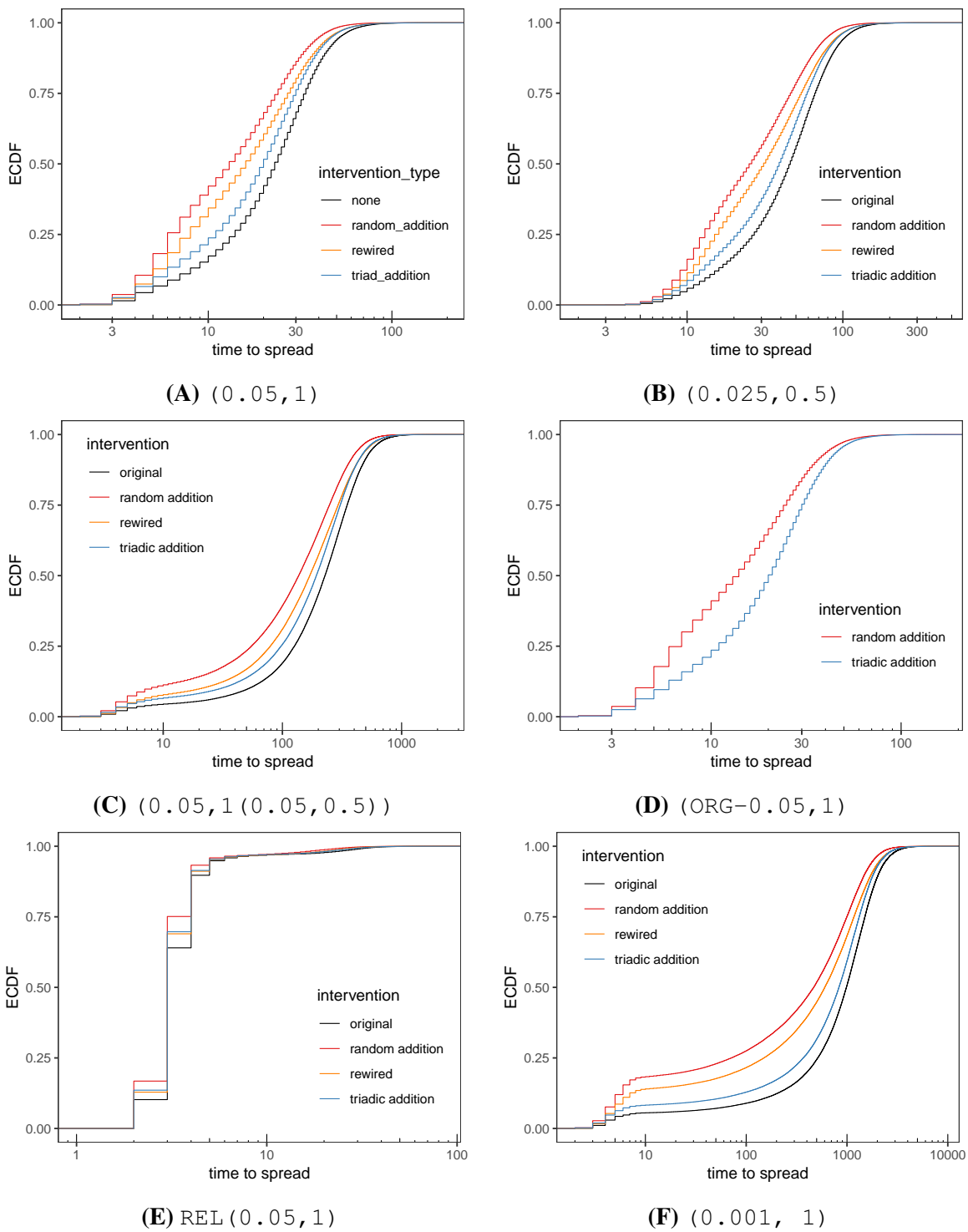


Figure S17: The overall ECDF for the spreading times over Chinese farm villages [32] under different contagion models and interventions with fixed size (10%): (A) $\rho = 1, q = 0.05, \alpha = 1, \gamma = 0, \theta = 2$, (B) $\rho = 0.5, q = 0.025, \alpha = 1, \gamma = 0, \theta = 2$, (C) $\rho = 1, q = 0.05, \alpha = 0.05, \gamma = 0.5, \theta = 2$, (D) $\rho = 1, q = 0.05, \alpha = 1, \gamma = 0, \theta = 2$, simple contagion adoptions happen only along the original edges and spreading time samples are collected only under edge addition interventions (triadic vs random), (E) $\rho = 1, q = 0.05, \alpha = 1, \gamma = 0, \theta^* = 0.5$, complex contagion with fixed common fractional threshold (θ^*), (F) $\rho = 1, q = 0.001, \alpha = 1, \gamma = 0, \theta = 2$.

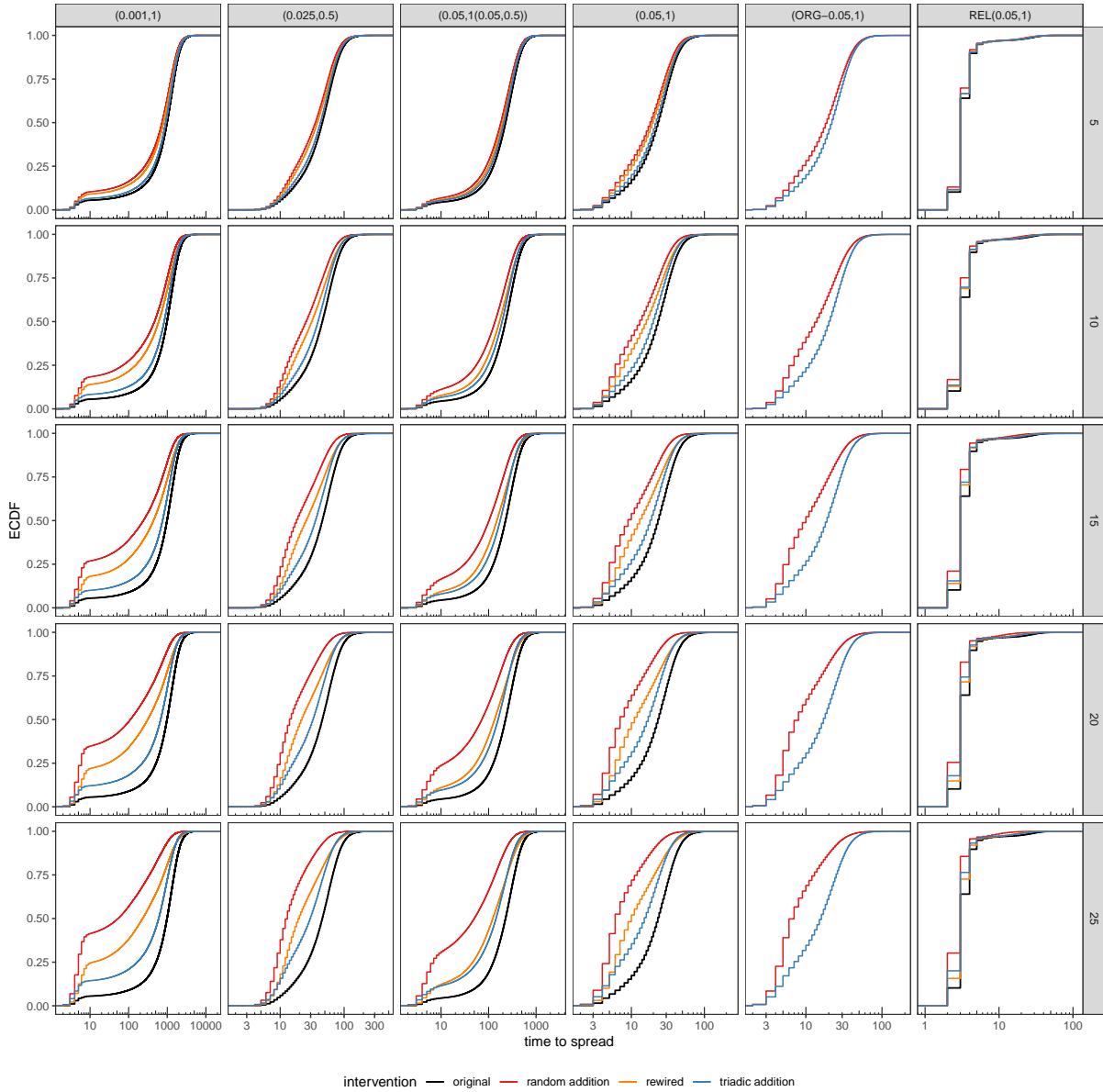


Figure S18: Overall ECDFs under various interventions grouped by the intervention sizes and contagion models for the Chinese farming villages [32]. The model labels at the top are as introduced in the captions of Fig. S17. The intervention sizes are shown on right side.

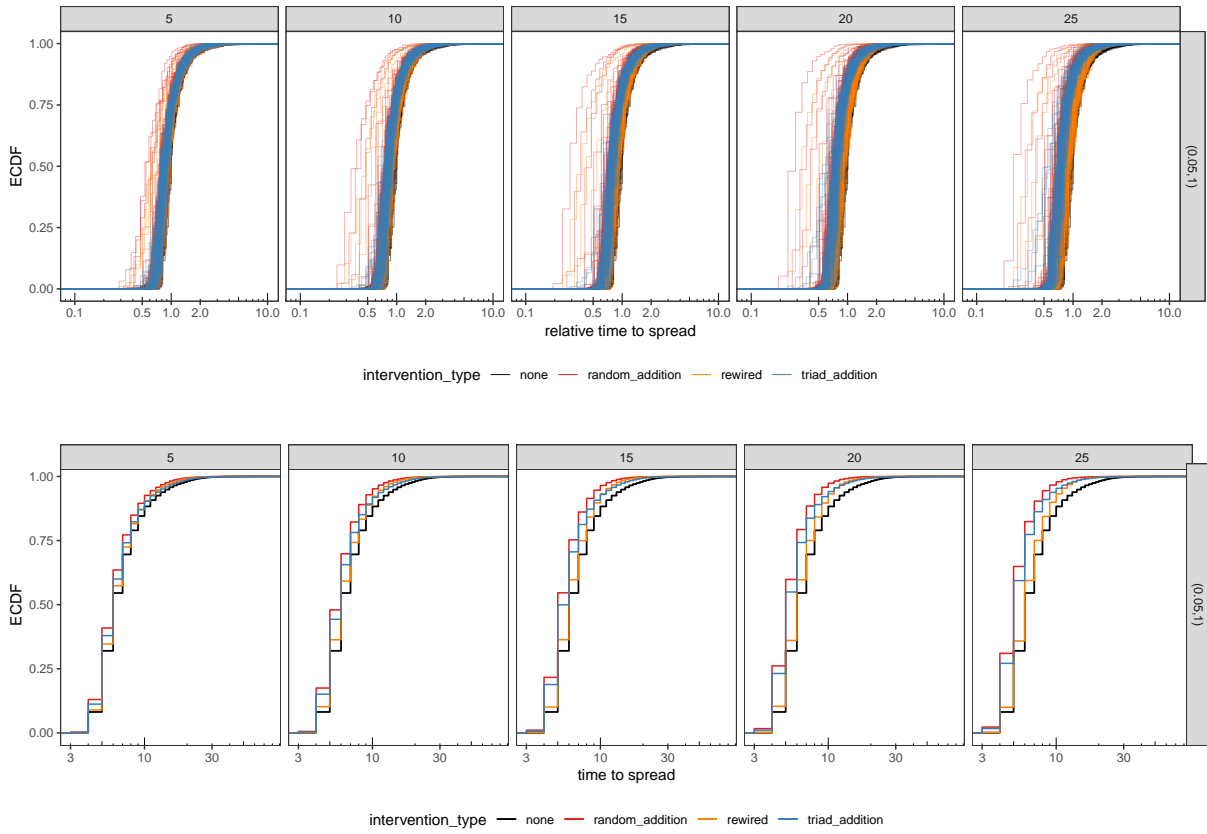


Figure S19: ECDFs under various interventions grouped by the intervention size for the South Indian villages[34]. The top figure shows the ECDFs for the individual villages (overlaid) and the bottom figure combines the random samples (spreading times) over the entire dataset. These figures follow the same conventions as Figure 4 of the main text.

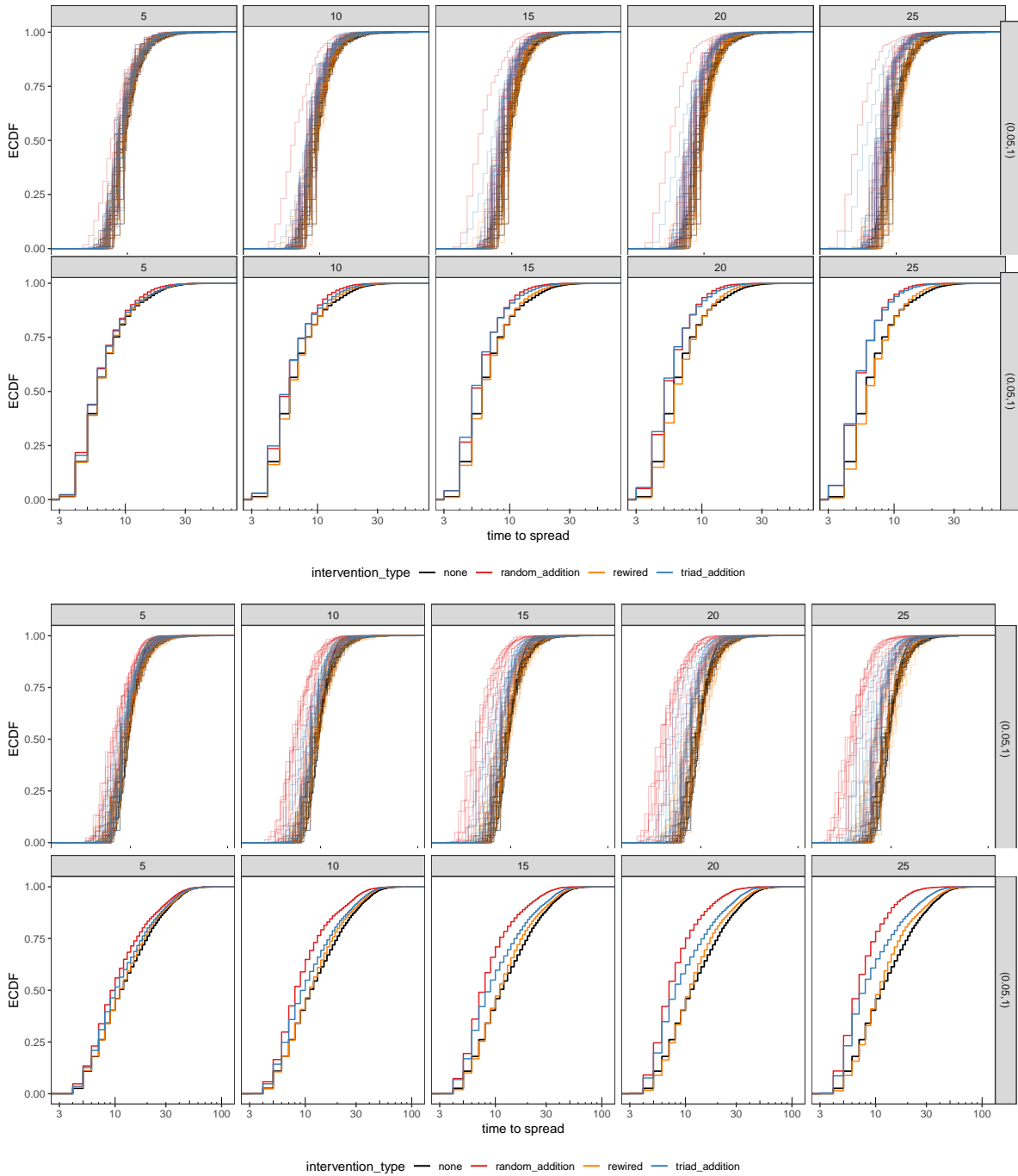


Figure S19: ECDFs under various interventions grouped by the intervention size for the Ugandan villages friendship networks, top two, and advice networks, bottom two [33]. The first and third rows show the ECDFs for the individual villages (overlaid). The second and fourth rows combine the random samples (spreading times) over the entire dataset, following the same conventions as Figure 4 of the main text.

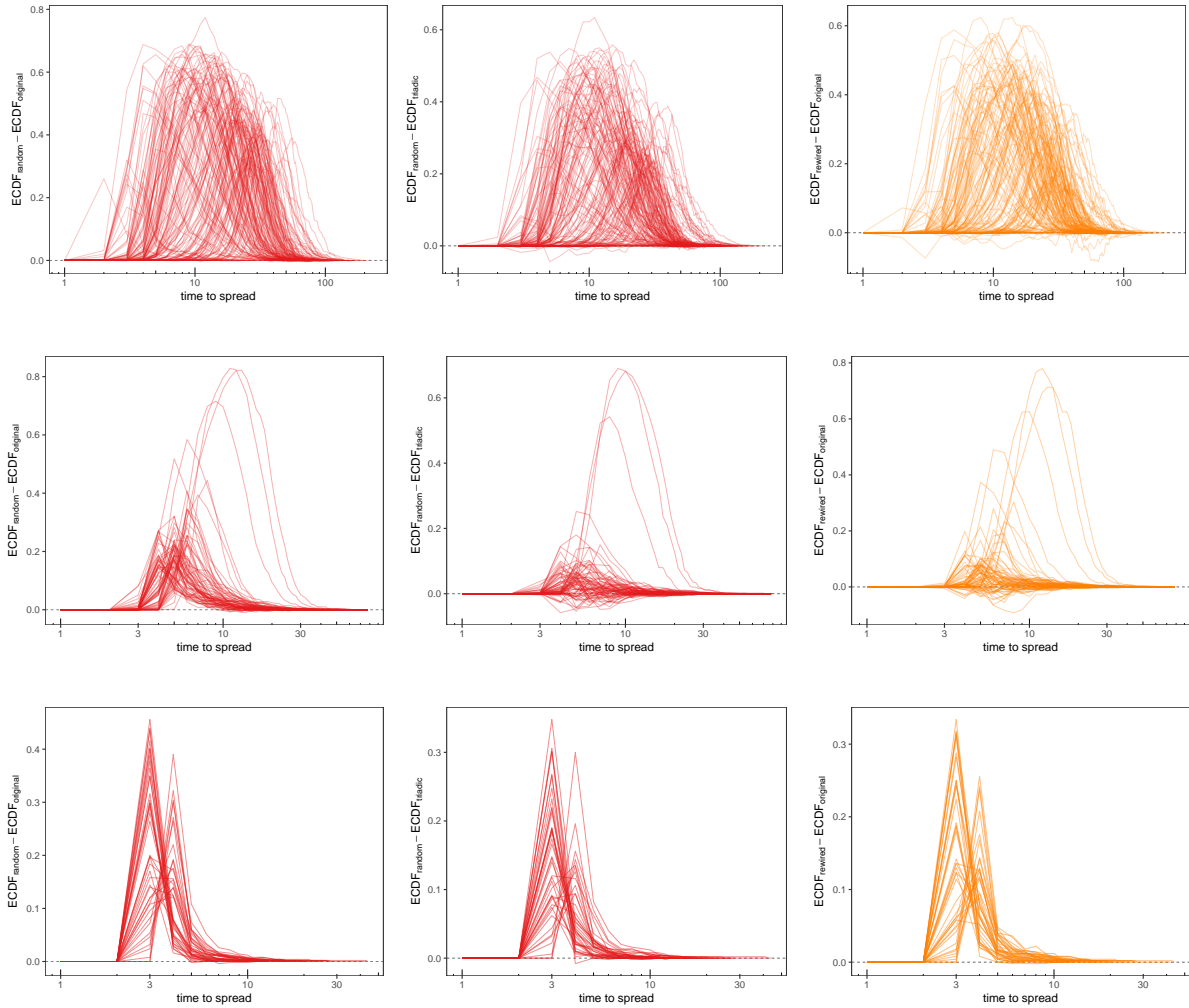


Figure S20: Difference between spreading time ECDFs in networks with 10% additional random edges and the original ones (leftmost column), between the networks with 10% additional random and triad closing edges (middle column), and between the 10% rewired and the original networks (rightmost column), for rural villages in China [32] (first row) and South India [34] (second row), as well as the Facebook social networks [35] (third row). The positive differences indicate the stochastic dominance relation between the spread times (as random variables) under one intervention over another. The spreading time samples are computed under the $(0.05, 1)$ model from Figure S17A with $q = 0.05$, $\alpha = 1$, $\gamma = 0$, and $\theta = 2$.

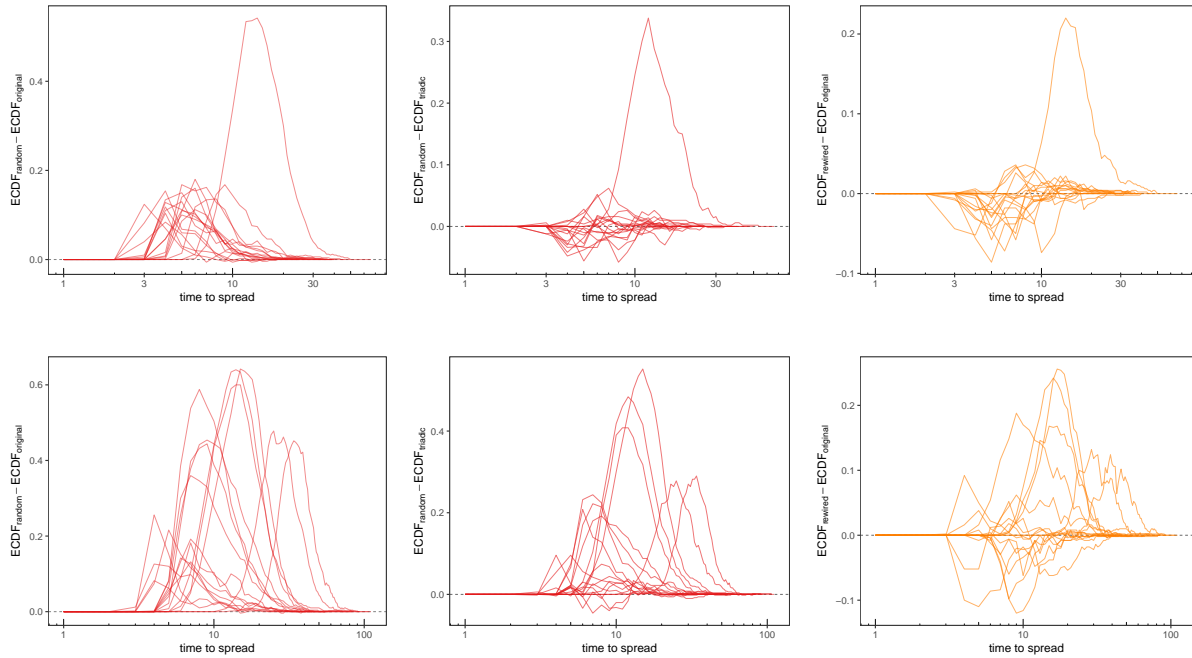


Figure S20: Difference between spreading time ECDFs in networks with 10% additional random edges and the original ones (leftmost column), between the networks with 10% additional random and triad closing edges (middle column), and between the 10% rewired and the original networks (rightmost column), for Ugandan villages [33], friendship networks (top row) and advice networks bottom row. The positive differences indicate the stochastic dominance relation between the spread times (as random variables) under one intervention over another. The spreading time samples are computed under the $(0.05, 1)$ model from Figure S17A with $q = 0.05$, $\alpha = 1$, $\gamma = 0$, and $\theta = 2$.

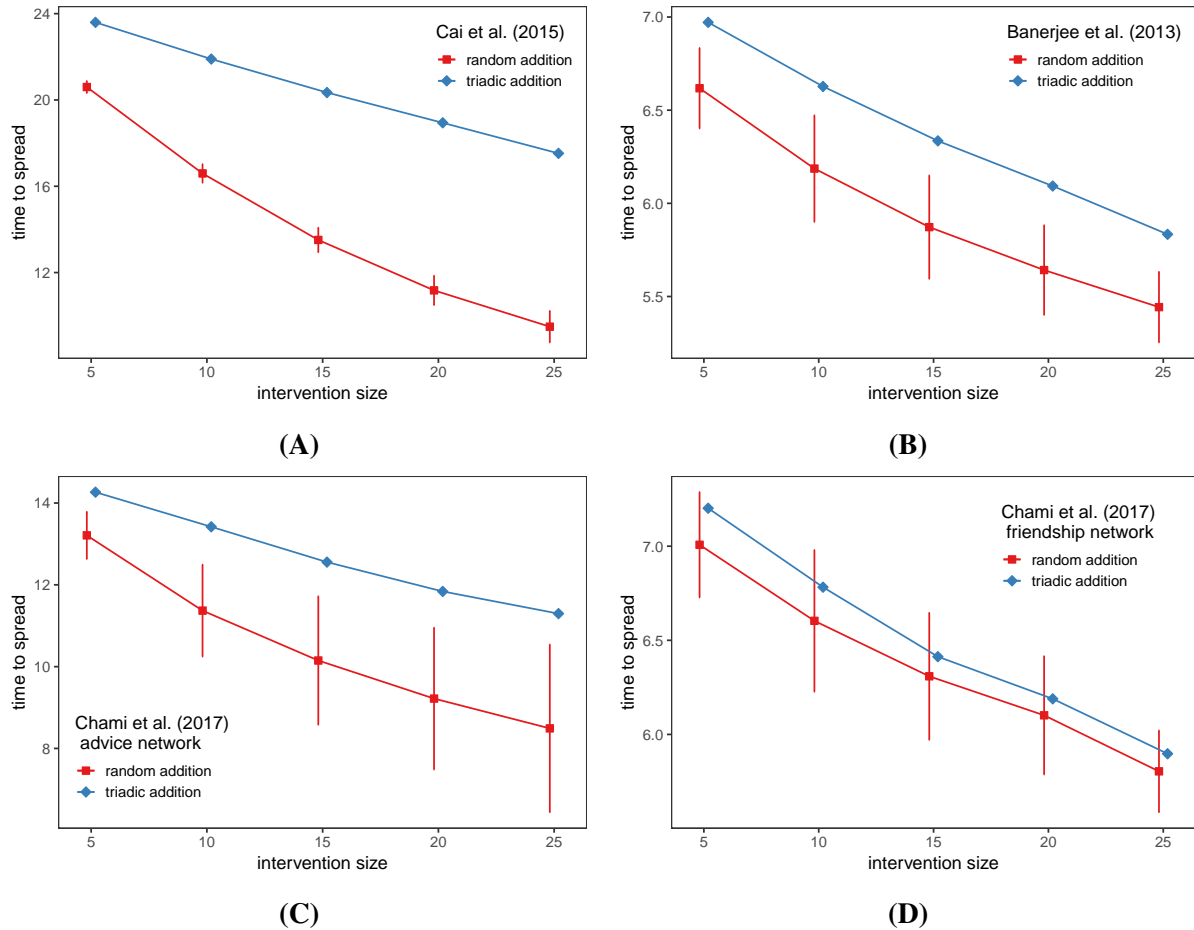


Figure S21: We plot the mean time to spread in four sets of empirical networks with added triad-closing or random ties. The x-axis indicates the number of added ties (intervention size) as percent of edges in the original networks. Each point averages over all networks in that set. Error bars are 95% confidence intervals for the difference from the spread times over the networks with added triad-closing ties. We compute the confidence intervals by treating each network as a single observation.

S10 References

- [1] H. P. Young, The dynamics of social innovation, *Proceedings of the National Academy of Sciences* **108**, 21285 (2011).
- [2] A. Montanari, A. Saberi, The spread of innovations in social networks, *Proceedings of the National Academy of Sciences* **107**, 20196 (2010).
- [3] J. Ugander, L. Backstrom, C. Marlow, J. Kleinberg, Structural diversity in social contagion, *Proceedings of the National Academy of Sciences* **109**, 5962 (2012).
- [4] S. Janson, R. Kozma, M. Ruzinkó, Y. Sokolov, Bootstrap percolation on a random graph coupled with a lattice, *Electronic Journal of Combinatorics* (2016).
- [5] R. Durrett, Some features of the spread of epidemics and information on a random graph, *Proceedings of the National Academy of Sciences* **107**, 4491 (2010).
- [6] G. Ghasemiesfeh, R. Ebrahimi, J. Gao, Complex contagion and the weakness of long ties in social networks: revisited, *Proceedings of the fourteenth ACM conference on Electronic Commerce* (ACM, 2013), pp. 507–524.
- [7] R. Ebrahimi, J. Gao, G. Ghasemiesfeh, G. Schoenebeck, Complex contagions in kleinberg’s small world model, *Proceedings of the 2015 Conference on Innovations in Theoretical Computer Science* (ACM, 2015), pp. 63–72.
- [8] R. Ebrahimi, J. Gao, G. Ghasemiesfeh, G. Schoenebeck, How complex contagions spread quickly in preferential attachment models and other time-evolving networks, *IEEE Transactions on Network Science and Engineering* **4**, 201 (2017).
- [9] G. Schoenebeck, F.-Y. Yu, Complex contagions on configuration model graphs with a power-law degree distribution, *International Conference on Web and Internet Economics* (Springer, 2016), pp. 459–472.
- [10] A. Nematzadeh, E. Ferrara, A. Flammini, Y.-Y. Ahn, Optimal network modularity for information diffusion, *Physical Review Letters* **113**, 088701 (2014).
- [11] M. O. Jackson, L. Yariv, Diffusion of behavior and equilibrium properties in network games, *American Economic Review* **97**, 92 (2007).
- [12] E. Abrahamson, L. Rosenkopf, Social network effects on the extent of innovation diffusion: A computer simulation, *Organization Science* **8**, 289 (1997).
- [13] D. Centola, M. Macy, Complex contagions and the weakness of long ties, *American journal of Sociology* **113**, 702 (2007).

- [14] D. J. Watts, S. H. Strogatz, Collective dynamics of ‘small-world’ networks, *Nature* **393**, 440 (1998).
- [15] M. E. Newman, D. J. Watts, Renormalization group analysis of the small-world network model, *Physics Letters A* **263**, 341 (1999).
- [16] J. Balogh, B. G. Pittel, Bootstrap percolation on the random regular graph, *Random Structures & Algorithms* **30**, 257 (2007).
- [17] H. Amini, N. Fountoulakis, Bootstrap percolation in power-law random graphs, *Journal of Statistical Physics* **155**, 72 (2014).
- [18] H. Amini, Bootstrap percolation and diffusion in random graphs with given vertex degrees, *The Electronic Journal of Combinatorics* **17**, 25 (2010).
- [19] S. Morris, Contagion, *The Review of Economic Studies* **67**, 57 (2000).
- [20] D. Acemoglu, A. Ozdaglar, E. Yildiz, Diffusion of innovations in social networks, *Decision and Control and European Control Conference (CDC-ECC), 2011 50th IEEE Conference on* (IEEE, 2011), pp. 2329–2334.
- [21] M. Granovetter, Threshold models of collective behavior, *American Journal of Sociology* **83**, 1420 (1978).
- [22] S. Aral, L. Muchnik, A. Sundararajan, Distinguishing influence-based contagion from homophily-driven diffusion in dynamic networks, *Proceedings of the National Academy of Sciences* **106**, 21544 (2009).
- [23] E. Bakshy, I. Rosenn, C. Marlow, L. Adamic, The role of social networks in information diffusion, *Proceedings of the 21st international conference on World Wide Web* (ACM, 2012), pp. 519–528.
- [24] D. Centola, The spread of behavior in an online social network experiment, *science* **329**, 1194 (2010).
- [25] B. Mørsted, P. Sapiezynski, E. Ferrara, S. Lehmann, Evidence of complex contagion of information in social media: An experiment using twitter bots, *PloS one* **12**, e0184148 (2017).
- [26] J. Ugander, L. Backstrom, C. Marlow, J. Kleinberg, Structural diversity in social contagion, *Proceedings of the National Academy of Sciences* **109**, 5962 (2012).
- [27] J. Lee, D. Lazer, C. Riedl, Complex contagion in viral marketing: Causal evidence and embeddedness effects from a country-scale field experiment, *Available at SSRN 4092057* (2022).

- [28] M. E. Newman, D. J. Watts, Scaling and percolation in the small-world network model, *Physical Review E* **60**, 7332 (1999).
- [29] B. Doerr, *Theory of Randomized Search Heuristics: Foundations and Recent Developments* (World Scientific, 2011), pp. 1–20.
- [30] S. Janson, Tail bounds for sums of geometric and exponential variables, *Statistics & Probability letters* **135**, 1 (2018).
- [31] D. Cox, H. Miller, The theory of stochastic processes, Chapman and Hall, New York **398** (1965).
- [32] J. Cai, A. De Janvry, E. Sadoulet, Social networks and the decision to insure, *American Economic Journal: Applied Economics* **7**, 81 (2015).
- [33] G. F. Chami, S. E. Ahnert, N. B. Kabatereine, E. M. Tukahebwa, Social network fragmentation and community health, *Proceedings of the National Academy of Sciences* **114**, E7425 (2017).
- [34] A. Banerjee, A. G. Chandrasekhar, E. Duflo, M. O. Jackson, The diffusion of microfinance, *Science* **341**, 1236498 (2013).
- [35] A. L. Traud, P. J. Mucha, M. A. Porter, Social structure of facebook networks, *Physica A: Statistical Mechanics and its Applications* **391**, 4165 (2012).